FORMULATION OF MODEL-BASED OPTIMAL CONTROL FOR PRACTICAL APPLICATIONS

NGUYEN HOANG TUAN MINH

(BEng with Honors)

A THESIS SUBMITTED FOR THE DEGREEE OF

DOCTOR OF PHILOSOPHY

DEPARTMENT OF ELECTRICAL & COMPUTER ENGINEERING

NATIONAL UNIVERSITY OF SINGAPORE

2013

Declaration

I hereby declare that this thesis is my original work and it
has been written by me in its entirety.
I have duly acknowledged all the sources of information
which have been used in the thesis.

This thesis has also not been submitted for any degree in any
university previously.

_____

Nguyen Hoang Tuan Minh
National University of Singapore
Singapore
02 August 2013

Summary

Model predictive control has come out of its main field - chemical process control in terms of successful industrial applications and as a focus of academic research. More and more components have been designed as add-ins of this well-known framework. Coming along with its new form is a long standing feature of offset-free control through disturbance model estimation and compensation. This feature produced controllers that perform very well for certain processes, but not adequately address others such as robust control and fast implementation. It stresses disturbance rejection workload to the system state estimator, thus prevents robust control to integrate. These limitations have become apparent when a wider range of applications for model predictive control is under consideration.

In this thesis, it is shown that by reformulating the encountered problems into solvable forms, model predictive control can actually solve much more practical problems than it is expected.

This study first presents a new framework of tracking model predictive control that resolves these issues. By exploiting the control philosophy of the propositional-integral-differential (PID) controller, offset-free features and robust designs for MPC can be integrated in a seamless manner. A design of offset-free MPC is presented, amenable to readily accept robust feedback control as an integral core. Through PID-state augmentation, a PID mapping from outputs to optimal inputs is constructed. Parametric programming further provides a fast implementation of these distributed PIDs through gain scheduling design. These techniques provide increased flexibility in the design of model predictive control for industrial applications.

Further exploration on PID control optimization in some real-world problems is examined by applying the above framework. As the first example, control on the movement of a high precision ultrasonic motor is used. By separating the usual linear motion model and the nonlinear effects of friction, the framework has been applied to robustly compensate the friction uncertainties which could not be modeled easily through experiment data. The second example shows the competitive strength of this MPC method when integrated with advanced techniques such as sliding mode observer. It provides an elegant solution to temperature optimization in in-vitro fertilization process. The last example demonstrates that for process systems such as chemical reaction, control of blending ratio can also benefit from flexible problem analyzing and reformulating. Such applications prove the effectiveness of the proposed method, and at the same time promote it to a larger scale of applications.

The result of this thesis is the creation of a framework for the development of an industrially implementable controller that improves the current technology. Furthermore, its performance in several applications is rigorously analyzed by appropriate formulation of the problems. This framework provides a flexible basis that retains and enhances the necessary features to handle industrial control applications.

Acknowledgements

This thesis is the product of my interaction with a number of people, with whom I have had the pleasure to discuss a wide range of topics in control, engineering and science.

I would first like to thank my supervisor, Dr Tan Kok Kiong, for listening to my sometimes very scattered thoughts and helping me channel them in the right direction. Throughout my studies he took an active interest in my work and encouraged me to keep at it when I could not see the light at the end of the tunnel.

The Mechatronics and Automation Lab in NUS has been my home for the last for years and everybody who has passed through has contributed to my understanding. I personally thank Dr Huang Sunan for valuable ideas during our discussion in both control theory and application. Thank Su Yang, my senior, who has recognized the contribution of my work in MPC and encouraged me to continue until this end. Thank Yuan Jian, Yang Rui, as they have been so supportive in my hardware implementation problems. Thank Liang Wenyu for the collaboration and Yu Shuang for good, entertaining conversations in machine learning. There are other members of the lab who has helped me in some way or another.

I take this opportunity to thank the NUS-SIMTech Joint Lab in Precision Control for providing me with generous financial support to attend conference. I also have had the chance to explore industrial mechatronics systems in this lab thanks to Dr Chen Silu and Dr Teo Chek Sing.

Finally, I give my special thanks to my family, my friends Nguyen Thi Tram Anh, Huynh Hoai Nguyen and Tran Chieu Minh. They have supported and inspired me during this whole study time.

Contents

List of Tables

List of Figures

Chapter 1

Introduction

Originating from linear quadratic regulator (LQR) theory, the original model predictive control (MPC) has speedily reached out to process industries and become a platform of its own. First, it picks up the internal model control structure, as shown in Fig. 1.1. This leads to two facts: 1) The performance of *unconstrained* MPC is not inherently better than that of classic control, 2) From an optimal control point of view, optimizing the MPC controller for a certain performance criteria is affine, much simpler than a nonlinear function of the traditional feedback controllers (such as PID) [Garcia et al., 1989]. The former fact is easy to understand, since without constraints a MPC only results in a linear feedback gain that can be tuned using other methods. However, the latter demonstrates that optimal control, especially with constraints involved, is more advantageous for MPC. Hence, when mathematical tools such as linear/quadratic programming comes in the field, MPC advances along this direction. This new approach, as practical as PID, was adopted widely for multivariable systems in the industry.

MPC has accounted for a vast spectrum of applications, and there are reasons for its versatility. First, MPC is based on modeling and optimization, the two factors that help engineers to understand an arbitrary system and manipulate it to follow certain criteria. Secondly, it is the ability to handle constraints which brings MPC, but not LQR, a big step closer to real-world optimization. Chemical process plants have actuator constraints; facility layout and location design are subject to space and time limitation; even designs in transformation optics, the study of bending light by material transformations, must satisfy a predetermined refractive index range for the sake of feasible choice of materials. One

can say MPC is a representation of direct optimization in the control area, beside other hysteretic methods like genetic algorithm or neural network.

MPC, certainly, has its unique features to stand out from the big optimization world. Often applied on large dynamical systems with constraints, MPC optimizing over a finite-time horizon is less expensive and more suitable for control purposes. Using the current dynamic state of a system, MPC calculates a sequence of future optimal inputs to operate it. At this point, only the first input is sent to the system. The idea is that disturbance sources (model uncertainties, disrupting noises) may render other future inputs useless. In the next sampling time, the optimization window moves one step forward, and the procedure is repeated. In other words, MPC operates on a feedback manner instead of one-time optimal design. This feature is named *receding horizon control*. This finite-time optimal control does not guarantee the overall system stability, so other features of MPC have been added: terminal cost and terminal region [Mayne et al., 2000] for classical convergence analysis. In summary, MPC is customized for system control.

1.1 Motivation

In this part the origination of interest that brought up this research work is presented. It starts from the current practice of MPC in the industry, describes the two big issues of control problems and how people addressed them separately in MPC, and finally shows a framework to unify these solutions - the goal to be achieved.

1.1.1 Industrial Model Predictive Control

As mentioned, MPC is referred as a general framework in the industry rather than a specific control technique, due to much interest arising to develop it. The first description of MPC, IDCOM, was developed in industry and reported in Richalet et al. [1978]. The impulse response model is used to describe the system response, so it is only applicable to linear stable plants. The report points out significant benefits of a multilevel control structure: MPC, with better dynamic control quality, drives the optimal setpoint nearer to the constraints to minimize costs (Fig. 1.2).

(a)

(b)
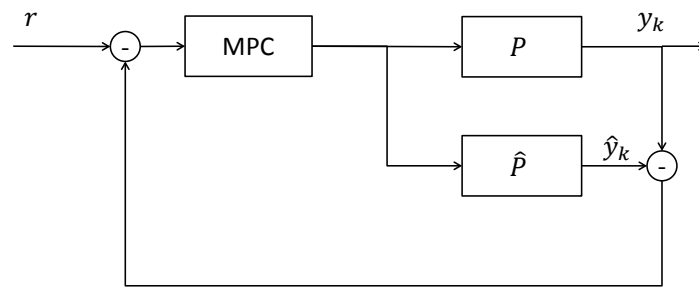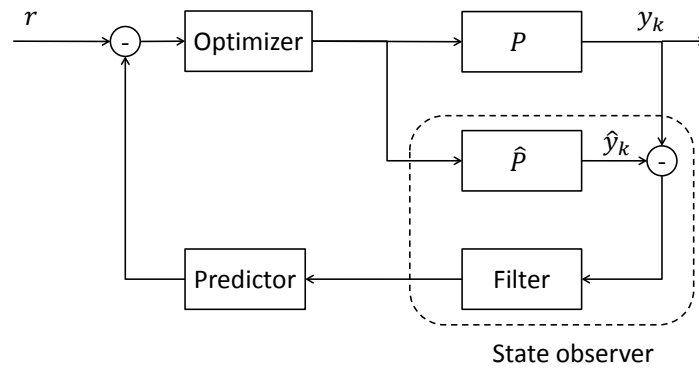
Figure 1.1: MPC structure under internal model view.

This structure is now followed by many practitioners and researchers [Froisy, 2006; Maeder and Morari, 2010; Pannocchia et al., 2007]. Later progress expands the flexibility of MPC framework. Not until in Cutler et al. [1983]; Garcia and Morshedi [1986] that quadratic programming is systematically introduced to solve the constrained optimization. Efforts by engineers at Shell Research [Marquis and Broustail, 1998; Yousfi and Tournier, 1991] combine MPC with state space system description and Kalman filter, which are used in most of the current research literatures. Other practical solutions to system identification, control block, removal of ill-conditioning, constraint violation recovery are also mounted on this framework, creating different MPC strategies for both linear and nonlinear plants [Qin and Badgwell, 2003]. A recent generation of MPC (DMCplus, RMPCT) offers multi-objective optimization, direction consideration of model uncertainty.

Among the practical extensions of MPC, the two properties, *offset-free*
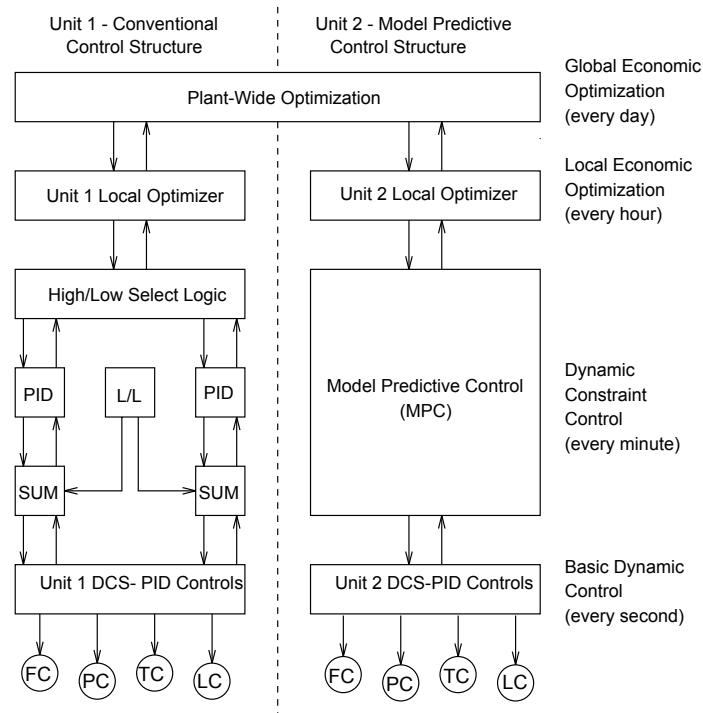
Figure 1.2: Comparison of traditional control structure and MPC structure [Qin and Badgwell, 2003]

.

tracking and *robust control*, are the most critical features that concern MPC implementation, whether it is in the original process industry, economics (slow process) or new areas such as automotive (fast process). They are essentially related to the types of disturbances/uncertainties contained inside the controlled systems: modeling mismatch, input and output disturbances, etc. In the next subsections, a review of techniques developed to deal with these problems is discussed.

1.1.2 Offset Free Tracking

Offset-free tracking in MPC refers to an essential group of techniques which estimate the disturbance infiltrating the model by measuring the outputs and compensating the offset due to the disturbance via the adjustment of the MPC target generation. This approach has been predominantly used since the first generation DMC, IDCOM-M (dealing with constant step disturbances) and now in the modern MPC solutions SMOC, RMPCT and DMCplus (dealing with integrating output disturbances).

Much research effort has embraced this disturbance estimation and

compensation method. In the first class of disturbance models, step disturbance, a constant disturbance vector is assumed to enter input/output channels. The authors in Muske and Badgwell [2002]; Muske and Rawlings [1993] suggested to integrate this information into the observer model and exploit Kalman filter to estimate the disturbance. The estimated constant disturbances are reflected back to the target design, which proves to be quite effective and sets an example for industrial MPCs at that time. As disturbance models evolve to be more complex, sufficient conditions for offset-free tracking were first presented in Pannocchia and Rawlings [2003]. Minimal presentation of disturbance models was discussed in Maeder et al. [2009]. A recent research work departed from linear model and proved the results for nonlinear cases [Morari and Maeder, 2012]. On the application sides, this method was used in a project to enhance MPC-based softwares, developed by AspenTech [Froisy, 2006]. Performance improvement was reported in applications for wind turbines [Dang et al., 2012], vapor compression cycle [Wallace et al., 2012] and wastewater treatment process [Martin et al., 2012].

On the other hand, the disturbance estimation and compensation approach needs more breakthroughs on several aspects. The feasibility conditions depends of the detectability of the overall system, and the control performance depends on the disturbance model. Hence, the selection of disturbance model becomes critical [Froisy, 2006]. It is pointed out that disturbance model combined with a Kalman filter has several performance limitations [Bageshwar and Borrelli, 2009].

1.1.3 Robust Formulation

A natural question about MPC is its robustness to model uncertainty and noise. The original open-loop model predictive control is about determining the current control action by solving an optimal problem with only the information of current state. This method cannot restrain the spread of predicted trajectories resulting from disturbances, so feedback policies including disturbances along the controlled horizon have been researched [Magni et al., 2003; Scokaert and Mayne, 1998]. It implies that for a specified range of model variations/ noises, the system stability is maintained and the performance specifications are met. To design MPC with this consideration in mind, there is a trade-off between the accuracy

of the uncertainty description and the computational complexity of the controller synthesis. There are two popular ways to model the uncertainty: stochastic model and bounded model.

As mentioned, a common formulation for robust model predictive control is based on the assumption that model uncertainty (whether multiplicative or additive) can be described in terms of bounded compact sets. In most of these cases, the asymptotic stability of the origin cannot be established, but only of a set in its neighborhood. A Lyapunov function must be zero within this set and non-zero otherwise [Kerrigan and Maciejowski, 2003; Scokaert and Mayne, 1998]. An improved approach is proposed in Mayne et al. [2005], following Lee II and Kouvaritakis [2000] to construct a stage cost related to the suboptimal control, but the *nominal* initial state is additionally taken as decision variable. The minimal robust positively invariant set required for these approaches can be obtained efficiently in Rakovic et al. [2005]. Another name for this framework is *tubed* MPC [Langson et al., 2004].

With the assumption that stochastic model gives a more informative description on disturbances, advocating researchers think it is less conservative than the "worst-case" control. Indeed, this plays a key role in soft constraints of a probabilistic nature. Recent results in Nagy and Braatz [2003]; van Hessem and Bosgra [2002] deal with purely stochastic noise and Mark et al. [2011]; Primbs and Sung [2009] deal with stochastic tubes.

1.1.4 Research Goals

The goal of this thesis is to establish a link between the offset-free MPC and the robust formulation. Replacing the disturbance model by the integrating augmentation, a new framework is created to guarantee offset-free tracking and facilitate the robust control techniques to be integrated. The following points will be shown:

- The advantages of using integrating state over the dynamic disturbance compensation.
- The seamless integration of robust control into the new framework.
- Applications of the new framework.

1.2   Organization and Highlights

This dissertation is organized as follows. Chapter 2 and 3 establish the new framework for robust tracking model predictive control. Chapter 4, 5 and 6 practice the framework in different scenarios of real applications.

Chapter 2: Offset-free and Robustness in Model Predictive Control - A New Bridge

This chapter builds a unified framework for the design of an offset-free model predictive control (MPC) which facilitates a robust control design to be incorporated at the core. Integral and differential state variables are introduced to the original state space representation as a natural extension to derive a tracking MPC without the need for disturbance compensation via target adaptation. The simple augmentation enables a MPC controller to steer, under input and state constraints, the system states towards a terminal set containing the origin. Therein the terminal set, the control gains can be flexibly designed using any robust control synthesis which has a mature literature. Thus, a bridge is inherently built into the framework to allow robust feedback control designs to be incorporated under an offset-free MPC formulation. This bridge fills a long standing gap separating MPC and robust control, allowing them to be designed as modular yet seamlessly linked and be complementary components under the framework. From a theoretical perspective, the framework allows a clean and seamless analysis of the MPC and robust control in unison. From an application perspective, the framework enables a clear and systematic design flow which incorporates both the control components under one unified setting.

Chapter 3: Adaptive PID Network Using Local Robust Optimization

In chemical process applications, model predictive control (MPC) effectively deals with input and state constraints during transient operations. However, industrial PID controllers directly manipulates the actuators, so they play the key role in small perturbation robustness. This chapter considers the problem of augmenting the commonplace PID with the constraint handling and optimization functionalities of MPC. First, we review the MPC framework, which employs a linear feedback gain in

its unconstrained region. This linear gain can be any preexisting multi-loop PID design, or based on the two stabilizing PI/PID designs for multivariable systems proposed in the chapter. The resulting controller is a feedforward PID mapping, a straightforward form without the need of tuning PID to fit an optimal input. The parametrized solution of MPC under constraints further leverages a familiar PID gain scheduling structure. Steady state robustness is achieved along with the PID design so that additional robustness analysis is avoided.

Chapter 4: Robust Control of an Linear Ultrasonic Drive with Large Friction

Ultrasonic motors used in high-precision mechatronics are characterized by strong frictional effects, which are among the main problems in precision motion control. The traditional methods apply model-based nonlinear feedforward to compensate the friction, thus requiring closed-loop stability and safety constraint considerations. This chapter introduces a systematic approach using piecewise affine models to emulate the friction effect of the motor motion. The established model predictive control framework can be employed to deal with piecewise affine models. The increased complexity of the model offers a higher tracking precision through a gain-scheduling optimal input.

Chapter 5: Intelligent Control of In-vitro Fertilization Medical Systems

In-vitro fertilization (IVF) and related technologies are arguably the most challenging of all cell culture applications. This chapter introduces an integrated mechatronic solution for oocyte retrieval procedure before the oocytes are further put into laboratory processing during IVF treatment. It facilitates the surgery operation and addresses the temperature inaccuracy of follicular fluid during the transfer to the patients body. The mechanical design is implemented into a medical-standard conforming platform. An accurate temperature estimation and optimization scheme are proposed. Comparison before and after the introduction of the new prototype under various operating conditions reveals a significant improvement in performance. This yields a potential application for the medical/healthcare industry.

Chapter 6: Ratio Control in Interacting Processes

Ratio control for two interacting processes is proposed with a PID feed-forward design based on model predictive control scheme. At each sampling instant, the MPC control action minimizes a state-dependent performance index associated with a PID-type state vector, thus yielding a PID-type control structure. Compared to the standard MPC formulations with separated single-variable control, such a control action allows one to take into account the non-uniformity of the two process outputs. After reformulating the MPC control law as a PID control law, we provide conditions for prediction horizon and weighting matrices so that the closed-loop control is asymptotically stable, and show the effectiveness of the approach with simulation and experiment results.

Chapter 7: Concluding Remarks

This chapter summarizes the contributions made by this thesis and outlines directions for future research.

Chapter 2

An Unified Framework for Robust and Offset-free Model Predictive Control

2.1 Introduction

Offset-free model predictive control (MPC) refers to an essential group of techniques which estimate the disturbance infiltrating the model by measuring the outputs and compensating the disturbance via the adjustment of the MPC target tracking formulation. This approach has been predominantly used since the first generation of MPC: DMC, IDCOMM (dealing with constant step disturbances) and now in the modern MPC solutions SMOC, RMPCT and DMC-plus (dealing with integrating output disturbances) [Qin and Badgwell, 2003]. The disturbance compensation approach is commonly adopted in the industry with the advantages it offers. Disturbance sources are observed from the process data and the disturbance model is determined. With the model, the disturbance rejection workload is mainly entrusted to a state estimator which leverages on Kalman filters to derive smooth and optimal estimation of the disturbances. The state and input target (x_s, u_s) are updated based on the estimated bias so that MPC regulation subject to constraints can be realized without increased complexity. This has remained for long as the basic framework to achieve target tracking MPC. Over the last two decades, efforts were devoted to refine and expand the validity of the disturbance model for MPC. In process control, the hallmark paper Muske and Rawlings [1993] provided an analytical base for MPC

with different disturbance models: zero-mean, output and input step disturbances. The authors in Muske and Badgwell [2002]; Pannocchia and Rawlings [2003] independently introduced a dynamical disturbance model which can be rendered into a state-space representation. They discussed crucial conditions under which offset-free control can be guaranteed. These conditions require that the augmented system model is detectable and the number of unmeasured disturbances is *equal* to the number of measured outputs (see a proof in Rawlings and Mayne [2009], Chapter 1). The second requirement was subsequently relaxed to be *less than or equal* [Maeder et al., 2009]. The disturbance estimation approach has been extended to deal with servo disturbance [Maeder and Morari, 2010] and it is recently explored on nonlinear systems [Morari and Maeder, 2012].

However, there are clear and outstanding *constraints* associated with this conventional framework. First, from an application and industrial perspective, the improved margin of performance from disturbance estimation is achieved by passing on the complexities of configuring and tuning an accurate dynamical disturbance model to the control engineers. Inaccuracy in the modeling effort will directly incur inadequate cancellation and offsets. Thus, these complex yet crucial responsibilities are not readily assimilated by practitioners, and therefore the framework cannot be effectively rooted into place in the industry. Secondly, a general, systematic and practically amenable way to yield an accurate disturbance estimation without undue burden on the practitioners has not appeared to-date, largely due to the non-general restrictions to be overcome. These restrictions include conditions of the augmented model (plant + disturbance) on detectability and conditions on the rank of the state-to-output matrix [Froisy, 2006] which have remained a tall order to generalize in a straightforward manner. For theorists, the co-existence of the disturbance compensation scheme and the MPC controller in the augmented system have long impeded closed-loop analysis to be done in the same rigorous and comprehensive manner when they are separated. The specific choice of a disturbance model has direct implications on the performance of the MPC. Besides, a class of systems will always incur performance limitation, as proven in Bageshwar and Borrelli [2009]. Thirdly, established robust control techniques which are mature in their own rights, have been unable to flourish under this

framework of tracking MPC mainly due to the target adjustment mode. To-date, there have not been many results on offset-free robust predictive control. Attempts to impose robust control with an output disturbance model [Lovaas et al., 2010] or to extend the control to a nonlinear system with a dynamical disturbance model [Morari and Maeder, 2012] have faced challenging implementation issues. The disturbance estimation framework has long remained as the springboard for tracking MPC designs, but equally long and persistent have been the constraints inherited under the framework.

This chapter thus seeks to present a new and unified framework for the design of offset-free MPC which is amenable to readily accept robust feedback control as an integral core. Departing from the disturbance compensation framework, it preserves the offset-free property using simply the integration of the output error, tantamount to the integral control action of the PID controller. This approach is adopted as it is arguably the easiest-to-understand method in offset-free control and one which can be more readily accepted by practitioners. State integration is commonplace in robust tracking control of linear systems [Zhou and Doyle, 1998] (Sec. 14.8), [Zhang et al., 2004] and nonlinear systems [Fujioka et al., 2009; Jiang and Marcels, 2001; Seshagiri and Khalil, 2005] and they are not sensitive to modeling errors. However, this simple concept has not found its way to tracking MPC, though integrated states have been mentioned, not in depth, in various MPC contexts [Angeli et al., 2000; Grancharova et al., 2004; Sakizlis et al., 2004; Tan et al., 2000]. To the best of our knowledge, the augmentation of PID states to facilitate a unified framework to allow tracking MPC and robust feedback control to co-exist in a natural and complementary manner has not been proposed or observed before.

Under this framework, an opening is created and launched for a clean and straightforward flow of robust control into the core of the offset-free MPC. Disturbances which render active constraints at steady state and drive offset-free MPC tracking infeasible [Pannocchia and Rawlings, 2003; Rawlings and Mayne, 2009] are now a done deal using established robust control (H_∞). Inaccuracy in the disturbance model used in the robust control is in turn mitigated by the offset-free property of the tracking MPC. Extensions to nonlinear systems is more easily facilitated too, since a disturbance model is no longer necessary and the system state

can be predicted through an augmented model [Raffo et al., 2010], although no constraint was considered in that work. This PID-augmented model is the simple yet crucial key under the proposed framework to bridge offset-free MPC to robust and nonlinear system research/application fields.

The chapter is limited in discussions to linear constrained systems, and it will aim to highlight the potential to exploit the framework based on a PID-state augmentation to open up new and exciting possibilities in MPC both in theory and in applications. We will show a design flow instance that can apply robust control on offset-free MPC for linear systems. The result is a flexibly configurable and unified MPC design framework which can accommodate existing MPC implementations (*online*- or *offline*-optimization) and robust feedback designs for linear systems (e.g. H_2/H_∞). The problem of output overshooting in integral MPC is addressed. It accordingly ignites exciting possibilities in performance enhancement and scope of applications of the control under the new framework. The inherent bridge between two large research areas: robust control and offset-free MPC will be detailed. Some of the discussion points can be extended to nonlinear systems. Future possible work under this framework will be discussed.

2.2 Robust Offset-free Linear Feedback for Unconstrained Systems

In this section, a robust linear feedback is designed by using the PID structure. This gain will be used to design the core components of model predictive control presented in Section 2.3.

2.2.1 Building PID Model

Suppose the discrete system to be controlled has the state-space formulation in Eq. (2.2) where $x \in \mathbb{R}^n$ is the vector of state, $u \in \mathbb{R}^m$ is the inputs, $y \in \mathbb{R}^p$ is the measured outputs and $v \in \mathbb{R}^q$ is the controlled outputs.

$$x_{k+1} = f(x_k, u_k)$$
$$y_k = C_y x_k$$
$$v_k = C_v y_k, \tag{2.1}$$

subject to the linear set of constraints

$$Ex_k + Fu_k \leq G \qquad (2.2)$$

in which E, F, G define the input and output constraints. Assume that a
full-state estimation from the measured outputs y is available. The main
objective here is to calculate the optimal system input u_k so that v_k tracks
a piecewise constant reference v_s.

By linearizing the system around the required operating point, the
system in Eq. (2.1) becomes

$$x_{k+1} = Ax_k + Bu_k + Ew_k$$
$$v_k = Cx_k. \qquad (2.3)$$

with $C = C_v C_y$. Calculation of steady-state target (x_s, u_s) from the track-
ing reference (not dependent on disturbance) was provided in Muske
and Rawlings [1993]. Denote the deviations $\tilde{x}_k = x_k - x_s$, $\tilde{u}_k = u_k - u_s$
and the tracking error $\tilde{v}_k = C\tilde{x}_k$, the deviation model from the steady-
state target is exactly similar to Eq. (2.3).

The deviation model can be augmented with integral and differential
terms of the tracking error to ensure tracking performance on v_k.

$$\begin{bmatrix} \tilde{x}_{k+1} \\ \sum \tilde{v}_{k+1} \\ \Delta \tilde{v}_{k+1} \end{bmatrix} = \begin{bmatrix} A & 0 & 0 \\ C & I_q & 0 \\ C(A - I_n) & 0 & 0 \end{bmatrix} \begin{bmatrix} \tilde{x}_k \\ \sum \tilde{v}_k \\ \Delta \tilde{v}_k \end{bmatrix} + \begin{bmatrix} B \\ 0 \\ B \end{bmatrix} \tilde{u}_k + \begin{bmatrix} W \\ 0 \\ 0 \end{bmatrix} w_k \quad (2.4)$$

Because v_k is a measurable vector from y_k, the observability of the
system in Eq. (2.4) is implied from the observability of the original
system in Eq. (2.1). Following a Hautus test, the integral term is con-
trollable, while the differential term is only stabilizable (it can not be
controlled to any arbitrary value but 0 when $\tilde{x}(k)$ is regulated to 0).

2.2.2   Robust Offset-free Feedback with PID

It is recommended in [Shinskey, 1994] that PID controllers can be tuned
to reject disturbances more effectively than MPC that uses bias updates.
In fact, when a sudden change in disturbance occurs, the observer takes
time to correctly estimate the new disturbance before effectively adjust-
ing the setpoint. Having said that, PID also requires good tuning to

gain a better performance than bias updates. Hence, robust control approaches are suggested to be the best way to tune PID gain here. It is also interesting that the differential term D, with the benefit of disturbance rejection in PID, can implement the purpose of robust control designs.

Using this philosophy, established H_2/H_∞ robust control methods can be designed for the following system

$$z_{k+1} = \bar{A}z_k + \bar{B}\tilde{u}_k + \bar{W}w$$
$$v_k = \bar{C}z_k + \bar{D}\tilde{u}_k. \tag{2.5}$$

where z, v denote the complete state and output error of system (2.4); $\bar{A}, \bar{B}, \bar{C}, \bar{D}$ are the system matrices accordingly. The disturbance model W information is needed to design a state feedback $u = Kz$ negating the disturbance effect. However, note that an inaccurate choice of W here will not affect the tracking performance as severely as in the bias update case where it easily results in biased setpoint adjustment.

Robust control ensures the norm of the transfer function T_{wv} from the disturbance w to the interested variables v minimized so that

$$\left\| T_{wv}(s) \right\|_{2/\infty} = \left\| (\bar{C} + \bar{D}K)(sI - A - BK)W \right\|_{2/\infty} \leq \gamma, \tag{2.6}$$

where γ is a measure of robustness. As in [Chen, 2000; Doyle et al., 1989], solution to a regular H_2/H_∞ problem has been well established in the literature.

The resulting robust control gain is actually a tuning for PID control. This is resulted from the PID-state formulation in (2.4).

Theorem 1 *A control law $\tilde{u}(k) = K\tilde{z}(k)$ implements PID control on the system state $x(k)$ which ensures robust tracking for $v(k)$.*

Proof 1 *Because $\tilde{z}$ is the augmented state error, the control law is written as*

$$\tilde{u}(k) = K\tilde{z}(k)$$
$$= K_1\tilde{x}(k) + K_2 \sum \tilde{v}(k) + K_3\Delta\tilde{v}(k)$$
$$= K_1\tilde{x}(k) + K_2 C_v \sum \tilde{x}(k) + K_3 C_v \Delta\tilde{x}(k). \tag{2.7}$$

Since $rank(C_v) = q \leq n$, there are $m \times (n - q)$ P controllers and $m \times q$ PID controllers. In particular, PID control is applied to the state variables which influence the tracked output $v(k)$, so they are robust against disturbances.

2.3 MPC Solution for Constrained Systems

2.3.1 Design of integral MPC components

Having designed a robust linear state feedback as the terminal gain for MPC, we are now ready to derive a complete MPC formulation. This receding horizon regulator is based on minimizing a finite horizon quadratic objective function at each time k.

$$
V_N^o(z_k) = \min_{u^N}. \ \frac{1}{2}z_{k+N}^T P z_{k+N} + \sum_{j=0}^{N-1}(z_{k+j}{}^T C_0^T Q C_0 z_{k+j} + \tilde{u}_{k+j}^T R \tilde{u}_{k+j}) \tag{2.8}
$$

$$
subj.\ to \quad \bar{E}z_{k+j} + \bar{F}u_{k+j} \leq \bar{G}. \quad \forall j \in 0, ..., N-1
$$

$$
z_{k+N} \in X_f \tag{2.9}
$$

where $u^N = \{\tilde{u}_0, ..., \tilde{u}_{N-1}\}$ and only $\tilde{u}_0$ is applied to the plant due to the receding horizon policy. Q, R are symmetric positive definite penalty matrices on state and inputs (Q can be semidefinite). $P \geq 0$ is the terminal penalty matrix, which is also positive definite. $\bar{E}, \bar{F}, \bar{G}$ represent the constraints translated from Eq. (2.2). X_f is the terminal constraint.

As observed in Eq. (2.4), the future $\Delta v(k+j)$ is not dependent on the current $\Delta v(k)$ but on the prediction $x(k+j)$, thus a differential weighting on the diagonals of Q does not lead to a non-zero gain K_3 for $\Delta v(k)$. The differential gain only appears implicitly through the state feedback robust gain K designed for the terminal region. In other words, it is robust control designs that bring the differential term into the PI control in MPC. This feature differentiates this work with other MPC-related works in the literature [Raffo et al., 2010; Sakizlis et al., 2004].

There are a few options to choose which state variables are penalized by adopting different structures for C_0. In this note, we use $C_0 = \begin{bmatrix} \bar{C} & I_q & I_q \end{bmatrix}$ because penalizing $\sum \tilde{v}$ ensures offset-free results and regulating $\Delta\tilde{v}$ improves stability.

The problem in Eq. (2.8)-(2.9) is solvable by quadratic programming techniques, or more advanced methods with dynamic programming [Saffer-II and Doyle-III, 2004]. Here MPC component design is a more interesting problem. Two important properties: feasibility and stability are discussed to give a tuning guide for MPC parameters.

Feasibility Assume the feasibility of the optimization problem is given at $k = 0$. Persistent feasibility of the receding horizon control is guaranteed if X_f is control invariant.

Stability Complied to the MPC stability criteria in Mayne et al. [2000], the value function $V_N^o(z)$ should approach the infinite horizon unconstrained optimal value $V_\infty^{uc}(z)$. The following sufficient conditions are useful to obtain K, X_f and P.

1. The terminal gain K is a stabilizing gain so that the closed loop matrix $A_K = \bar{A} + \bar{B}K$ is stable.
2. The terminal constraint set X_f is the constraint invariant admissible polyhedron of the system $z_{k+1} = A_K z_k$ with respect to the state and input constraint $\bar{E}z_k + \bar{F}u_k \leq \bar{G}$.
3. $V_f(z) = \frac{1}{2}z^T P z$ is a Lyapunov control function inside X_f, e.g.

$$
\begin{aligned}
V_f(z_{k+1}, Kz_k) - V_f(z_k) &= z_k^T A_K^T P A_K z_k - z_k^T P z_k \\
&\leq -z_k^T C_0 Q C_0 z_k - z_k^T K^T R K z_k, \ \forall z_k \in X_f,
\end{aligned}
\tag{2.10}
$$

Hence K can be computed as the robust gain from Section 2.2. X_f can be calculated analytically using the methods detailed in Alessio et al. [2006]; Blanchini [1999]; Gilbert and Tan [1991]. P can simply be chosen as the solution of the equality in (2.10), the unique positive-definite solution of a discrete Lyapunov equation

$$
A_K^T P A_K - P = -(C_0 Q C_0 + K^T R K)
\tag{2.11}
$$

once K is known [Grieder et al., 2005]. When the state reaches the terminal region, the input gain is switched to the local robust gain K.

Remark 1 *For linear stable systems, the constraint $z_{k+N} \in X_f$ in Eq. (2.9) could be omitted. For linear unstable or nonlinear systems, it must be added as a relaxation of the terminal equality constraint in Muske and Rawlings [1993]. In this case, N should be chosen large enough so that z_k can be steered to the terminal constraint set X_f within N steps ($0 \in X_f$); an alternative solution for small N with cheaper computation is proposed in Rawlings et al. [2008].*
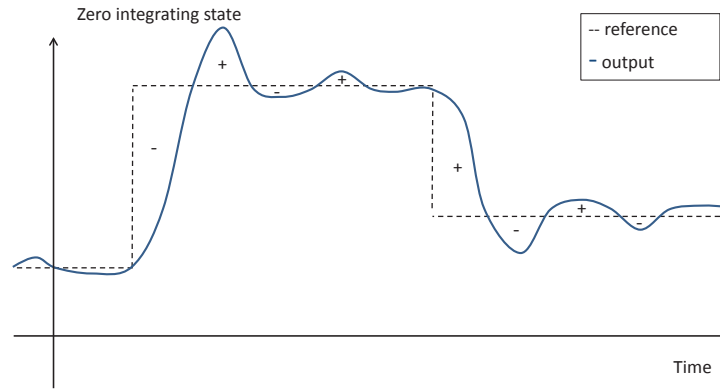
(a)
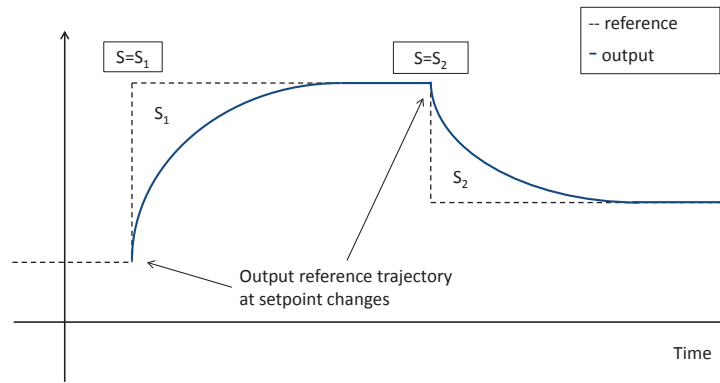
(b)

Figure 2.1: (a) The output overshoot caused by $s = 0$; (b) A simple solution to update the integrating reference at setpoint change events.

2.3.2 Overshoot Problem in Integral MPC

Integrating state of output errors in MPC induces large overshoots for output tracking, repeatedly reported in Maeder and Morari [2010]; Muske and Badgwell [2002]. This problem is particularly of interest to MPC controllers. It raises an interesting question to discuss about this phenomenon.

To address this question, one first needs to differentiate the two causes of output overshoot: the windup problem resulted from active input constraints, and the penalization of integrating state variables in the performance cost. Often, the input constraints are active during first stage of MPC, but the windup problem will not happen. It is worth mentioning that in MPC the model 2.4 is used only in the time window from the current point to N future steps, so the integrating state variables
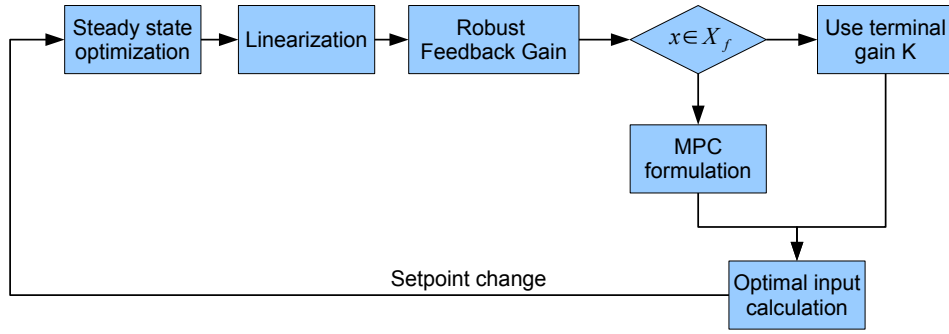
Figure 2.2: Design flow for the robust tracking MPC.

are reset to 0 at every sampling time. The second problem, however, is usually encountered. By minimizing the sum of square $(\sum \tilde{v}_{k+1})^2 + ... + (\sum \tilde{v}_{k+N})^2$ in the performance cost, the integrating state is regulated to 0, which causes a overshoot to make up for the initial transient stage (Fig. 2.1a).

In standard MPC controllers, the overshoot phenomenon has been addressed with a reference trajectory in most of the commercial products [Qin and Badgwell, 2003]. This reference trajectory is often a first- or second-order trajectory with user-defined time constants. Based on this technique, a non-zero constant reference s for the integrating state can be proposed in Fig. 2.1b. This proposed approach can determined efficiently in the computation of steady-state target (x_s, u_s).

2.4 Bridging Robust Linear Feedback and Integral Model Predictive Control

The design of the robust control at the core of the framework can leverage on a whole variety of well known robust control designs such as H_∞, feedback Lyapunov function or min-max minimization [Bara and Boutayeb, 2005; Bemporad et al., 2003; Garcia et al., 2003] to derive the terminal gain of MPC as in Section 2.2.2. The terminal cost and terminal region are formed subsequently. The MPC synthesis under this approach will thus possess a robust stability property i.e., the convergence to the origin under the presence of a disturbance is guaranteed when the state reaches the terminal region.

Robust performance along the nominal trajectory, which is a stronger
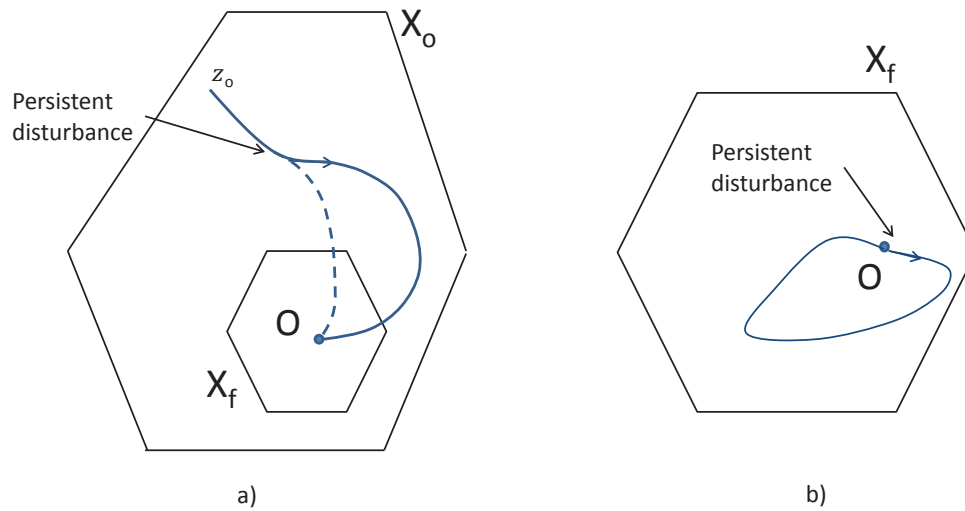
Figure 2.3: Addictive disturbance happening at (a) Active-constraint region, thus offset-free property is required to drive x to X_f; (b) Neighborhood of the setpoint, thus robust control helps to maintain x within X_f so that offset-free control is ensured.

property, will require more analysis on the disturbance structure. For this problem, techniques such as tube-based MPCs [Mark et al., 2011] can be applied directly on the PID-augmented state. The inherent PID form in Eq. (2.5) still ensures the offset-free property. Hence, compared to the disturbance estimation and compensation approach, this framework can incorporate robust control directly. At the same time, it enables direct analysis of robustness and closed loop performance.

By itself, robust control aims at reducing but not removing the effect of possible sources disturbances. The tracking MPC steps in to fill this gap. In most cases, offset-free control helps to negate the persistent disturbances and drives the state to the unconstrained region so that a robust input gain can be employed (provided that the target is inside this region). Hence, offset-free control reinforces robust stability when disturbance seeps in from outside the terminal region, as illustrated in Fig. 2.3a.

Robust control also helps to realize a steady-state assumption which offset-free MPC hinges on. According to Rawlings and Mayne [2009], in constrained systems, offset-free tracking under disturbance can be categorized into three outcome cases: there is zero steady state offset; the system trajectory is unbounded; the system constraints are active at

21

steady states. An important assumption to ensure offset-free control is that the steady-state is contained in the unconstrained region. However, a large disturbance may change the outcome from the first case to the last case and render offset-free tracking infeasible [Muske and Badgwell, 2002; Pannocchia and Rawlings, 2003]. Under this situation when tracking MPC fails, robust control methods, in particular H_∞, can minimize such effects and guarantee zero tracking error in the steady state as in Eq. (2.6) (Fig. 2.3b). This connection can be used in further analysis on robust sensitivity inside the terminal region.

2.5 Example

This example shows that the approach can actively seek a steady state solution that is output offset-free, provided that a feasible steady state conforming to the system constraints. Furthermore, steady state PI gains that follows some robust specification of H_2/H_∞ can be derived in the terminal set.

Consider the following coupled tank system

$$
\begin{aligned}
x_{k+1} &= Ax_k + Bu_k + d_k \\
v_k &= Cx_k,
\end{aligned}
\tag{2.12}
$$

in which

$$
A = \begin{bmatrix} 0.9034 & 0.0140 \\ 0.0461 & 0.9674 \end{bmatrix}, B = \begin{bmatrix} 0.2087 & -0.0239 \\ -0.0215 & 0.3428 \end{bmatrix}, C = \begin{bmatrix} 1 & 0 \end{bmatrix}. \tag{2.13}
$$

The system state is augmented as $z = \begin{bmatrix} \tilde{x} & \sum \tilde{x}_1 \end{bmatrix}$ so that

$$
z_{k+1} = \begin{bmatrix} A & 0 \\ C & I_q \end{bmatrix} z_k + \begin{bmatrix} B \\ 0 \end{bmatrix} \tilde{u}_k. \tag{2.14}
$$

LQR is first used to design the terminal gain, and that is compared with other H_∞ solutions which minimizes the disturbance effect on $v_k = Q_1[\tilde{x}_1 \ \sum \tilde{x}_1 \ \Delta \tilde{x}_1 \ \tilde{u}_1 \ \tilde{u}_2]^T$ with $Q_1 = diag(q_p, q_i, q_d, q_1, q_2)$. Following the terminal gain design, the terminal weighting matrix P and the terminal set X_f are constructed as in Section 2.3.

The offset-free properties of the proposed MPC approach with the
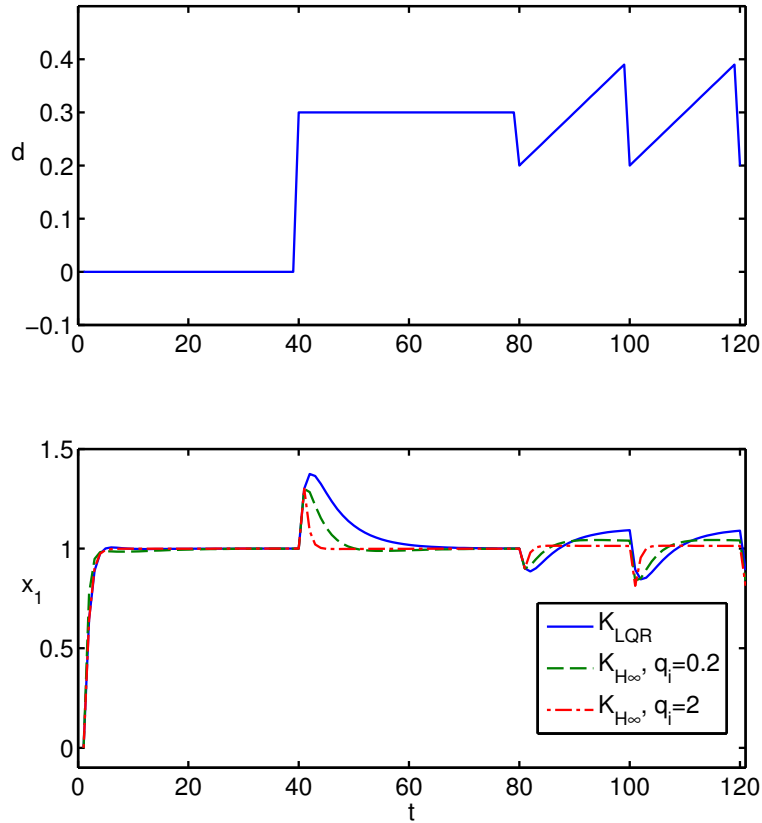
Figure 2.4: Tracking ability of MPC robust integral control under disturbance effect. (a) Disturbance (b) Output response.

different terminal gain designs are analyzed in Fig. 2.4. Under persistent disturbance (e.g. model uncertainty, step disturbance), all the designs meet the target tracking requirement, although restricting the disturbance effect on the integrating output error improves the disturbance rejection. The benefit of H_∞ tuning is further shown through a ramp disturbance, where a higher integral term yields a much smaller output offset. Thus MPC with H_∞ is very effective in disturbance rejection.

As seen in Fig. 2.5, the disturbance rejection is translated between the input channels. Evident in the system model, the input channel u_1 is mainly responsible for disturbance rejection on x_1. Thus the performance would be clearly affected, for example, if there was an input constraint $u_1 \geq -0.2$. In the case of H_∞ design, this can be mitigated by translating the load from u_1 to u_2 (certainly in the case the lower constraint of u_2 is not active). At the same time, by minimizing the output error, the proposed approach can further reduce its upper bound. In conclusion, the robust control design at the equilibrium will be greatly beneficial if operating near the constraint is required.
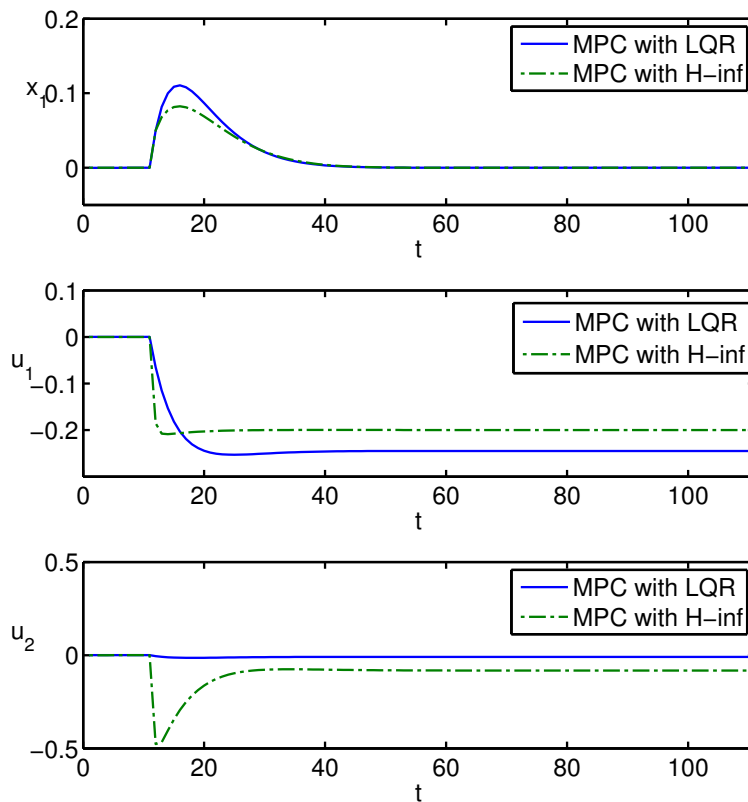
Figure 2.5: Disturbance effect minimized on u_1 and translated to u_2

The problem with this approach is that the robust design uses a high gain, thus corresponding to a small terminal region X_f for MPC. With a small disturbance, the state is inside the positively invariant set X_f of the closed-loop system $z_{k+1} = Az_k + B\tilde{u}(k)$, and the constraints are kept. However, if the disturbance is large enough to drive the states outside of X_f (since X_f small), the state reaches its steady value without the help of the $K_{H\infty}$ gain, but the gain of the offset-free MPC in the unconstrained region. Thus though the performance is still offset-free, the desired characteristics of H_∞ is not fully imposed.

2.6 Conclusion

Robust and offset-free control are two important and desirable properties to be implanted in an industrial controller such as MPC. This chapter elaborated a unified MPC framework under which these characteristics can be efficiently delivered in the control performance. The key to the union of these two mature fields is the use of a PID-augmented

model which removes the need for a disturbance estimation approach and facilitates the role of established robust control in the core terminal region of the MPC. The framework opens the access of offset-free MPC to robust and nonlinear control, and contributes to both analysis and applications of MPC. A systematic design flow for practical application of the proposed methodology has been formulated, and potential areas which can benefit from the framework are discussed in the chapter.

Chapter 3

Gain-scheduling PID Network Using Model Predictive Control

In chemical process applications, model predictive control (MPC) effectively deals with input and state constraints during transient operations. However, industrial PID controllers directly manipulates the actuators, so they play the key role in small perturbation robustness. This chapter considers the problem of augmenting the commonplace PID with the constraint handling and optimization functionalities of MPC. First, we review the MPC framework, which employs a linear feedback gain in its unconstrained region. This linear gain can be any preexisting multiloop PID design, or based on the two stabilizing PI/PID designs for multivariable systems proposed in the chapter. The resulting controller is a feedforward PID mapping, a straightforward form without the need of tuning PID to fit an optimal input. The parametrized solution of MPC under constraints further leverages a familiar PID gain scheduling structure. Steady state robustness is achieved along with the PID design so that additional robustness analysis is avoided.

3.1 Introduction

Multilevel control attracts intensive research as a systematic tool for control of real plants with respect to high-level target while adhering to the local constraints [Tatjewski, 2008]. The upper levels are usually concerned with plant-wide steady state objectives with slow sampling rate. The lower levels address fast dynamic control. There is a mature trend of applying advanced optimization packages to fill the gap between these

two layers. Well-known industrial examples such as AspenOne and
RHMPC use MPC as the core optimizer to deal with constraints [Froisy,
2006; Qin and Badgwell, 2003]. MPC is a constraint-handling optimiza-
tion method where the core idea is based on the receding horizon con-
trol. At each sampling time, the current plant output/state is measured,
and an optimal input is derived to minimize a performance index sub-
ject to state and input constraints. This desired input is sent to PID
controllers to directly manipulate the actuators. These PIDs must be
tuned to minimize the mismatch with the updated optimal input at each
sampling step. The first objective of the chapter aims to bypass this
two-phase complication through direct optimization of the PID gains.

Currently, there are two approaches of MPC, using either *online* im-
plementation [Mayne et al., 2000] for slow processes or *offline* implemen-
tation [Bemporad et al., 2002] for fast processes. The former control
approach solves in real-time an optimization problem, thus it is more
flexible to system design changes. The latter approach solves the same
problem offline for all feasible states, and obtains the optimal control
law in real-time by searching the current state over feasible regions. This
scheme, named parametric MPC, can effectively facilitate a PID gain
scheduling implementation. The resulting PID controller will deal with
constraints by changing gains upon the transition of active constraint
regions, not at each time step. This is the second and main objective:
to develop a practical implementation of parametric MPC in process
control.

The PID realization of MPC can be achieved with its robustness prop-
erty intact. In fact, a great number of research methods have carefully
addressed the robustness of MPC for perturbations both along the tra-
jectory (robust performance) and at steady state (robust stability). Poly-
topic uncertainty model is discussed in Grieder and Morari [2003] with
LMI and in Bemporad et al. [2003]; Nagy and Braatz [2004] where min-
max solutions are formed; bounded disturbances addressed by tube-
based MPC is proposed in Alvarado et al. [2008]; Mark et al. [2011]. The
tradeoff lies in the complexity of the solutions. In this note, we are keen
on observing the robust stability provided by the simple PID form of the
proposed solution.

In the literature, many finite-horizon optimal PID designs for con-
strained multivariable systems have been attempted to deliver a system-

atic PID tuning. In Moradi [2003], the velocity form of PID prohibited the variable gain structure, thus a fixed PID gain must be used across the prediction horizon. In Arousi et al. [2008]; Camacho et al. [2003]; Sato [2012] the GPC-based PID design approximated the plants by a first or second order model, thus limiting their applications to multivariable plants. The solution in Di Cairano and Bemporad [2010] partially solved the problem, but the two controllers MPC and PID must operate in parallel. Hence a flexible framework for optimal PIDs is still under on-going research.

Collectively through the two mentioned objectives, this chapter seeks to improve the MPC-based PID scheme to further close the gap between MPC optimization and PID controllers. In Section 3.2, we formulate the tracking problem and analyze the controllability and observability of the augmented system. In Section 3.3, we describe the MPC formula and show that either a new or existing multi-loop unconstrained PID designs can be adopted into the framework. For convenience, two methods are provided to calculate the PI/PID gains at the operating point so that the closed loop system is stable. The first method applies LQR on the PI state while the latter leads to linear matrix inequalities (LMI) with the size proportional to the number of tracked outputs. Section 3.4 applies this PID design on the piecewise affine (PWA) solution of MPC, which suggests a distributed PID gain scheduling framework to deal with constraints.

Notation

The operators $\sum, \Delta$ are the integral and differential terms. The notation $Q \succ 0$ denotes positive definiteness. x, $\hat{x}$ and $\tilde{x}$ denote the state, estimated state and state error; u and $\tilde{u}$ denote the input for tracking and regulating problems, respectively. Subscript i indicates matrix/vector component and k is the prediction step; superscript i is the critical region index. I_m is an identity matrix of order m.

3.2 Preliminaries

To obtain a linear feedback involving proportional-integral-differential gains, it is necessary to form a system state that contains the correspond-
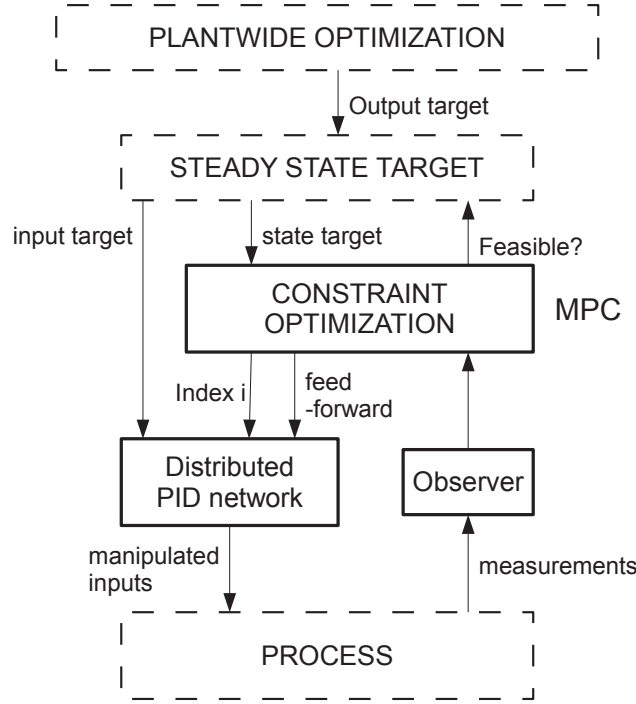
Figure 3.1: Optimization control with multi-layers.

ing variables. Provided that is the case, an optimal linear feedback gain is also an optimal PID gain. This section introduces the augmented PI/PID-state systems and covers the analysis of their controllability and observability.

3.2.1 Plant Model

Consider a linear time-invariant system

$$
\begin{aligned}
x(k+1) &= Ax(k) + Bu(k) \\
v(k) &= C_v x(k) \\
y(k) &= Cx(k).
\end{aligned}
$$
(3.1)

subject to the constraint

$$
Ex(k) + Fu(k) \leq G.
$$
(3.2)

In (3.1), $x(k) \in \mathbb{R}^n, u(k) \in \mathbb{R}^m, v(k) \in \mathbb{R}^q \, (q \leq n)$, and $y(k) \in \mathbb{R}^p$ are the state, input, tracked output and measured output. Assume (A, B) is controllable and (A, C) is observable; C, C_v having full row rank; E, F, G

are appropriate matrices defining the state and input constraints.

The plant model (3.1) is augmented with an integral of the tracked output $\sum v(k)$ to ensure zero offset during the steady state. The following PI-state model is used

$$
\begin{bmatrix} x(k+1) \\ \sum v(k+1) \end{bmatrix} = \begin{bmatrix} A & 0 \\ C_v & I_q \end{bmatrix} \begin{bmatrix} x(k) \\ \sum v(k) \end{bmatrix} + \begin{bmatrix} B \\ 0 \end{bmatrix} u(k)
$$
$$
y(k) = Cx(k). \tag{3.3}
$$

In special cases, $C_v = I$ requires a full-state tracking while $C_v = C$ expects only output tracking.

Proposition 2 *The PI-augmented system* (3.3) *is detectable. Furthermore, it is controllable if and only if (A,B) is controllable and*

$$
rank \begin{bmatrix} A - I_n & B \\ C_v & 0 \end{bmatrix} = n + q \tag{3.4}
$$

Proof 2 *The Hautus condition for observability is*

$$
rank \begin{bmatrix} A^T - \lambda I_n & C_v^T & C^T \\ 0 & I_q - \lambda I_q & 0 \end{bmatrix} = n + q \quad \text{for all } \lambda \in \mathbb{C}. \tag{3.5}
$$

The condition (3.5) *holds everywhere except at* $\lambda = (1, 0)$*, but the unobservable integrating state can be controlled to decay to a constant so the system is detectable.*

Similarly, (3.4) *follows directly from Hautus controllability where only the case of* $\lambda = (1, 0)$ *is to be checked.*

By addition of the differential term, the PID-state system presents as

$$
\begin{bmatrix} x(k+1) \\ \sum v(k+1) \\ \Delta v(k+1) \end{bmatrix} = \begin{bmatrix} A & 0 & 0 \\ C_v & I_q & 0 \\ C_v(A - I_n) & 0 & 0 \end{bmatrix} \begin{bmatrix} x(k) \\ \sum v(k) \\ \Delta v(k) \end{bmatrix} + \begin{bmatrix} B \\ 0 \\ C_v B \end{bmatrix} u(k)
$$
$$
y(k) = Cx(k). \tag{3.6}
$$

This PID-augmented system is detectable and stabilizable. The proof is similar to Proposition 3.4.

Remark 2 *The number of tracked variables is presumed less than or equal to the number of manipulated variables ($q \leq m$ for PI case and $q \leq m/2$ for PID case); the other case was well treated in* Maeder et al. [2009].

The objective is to design a finite-horizon optimal control based on the augmented system (3.3) or (3.6) so that $v(k)$ tracks a piece-wise constant reference.

3.2.2 Observer Design

From the system detectability, an observer can make use of the system (3.1) to estimate the current state, and simply calculate the integral and differential state through a sum of the estimated $\hat{v}(k) = C_v \hat{x}(k)$ and its difference.

Since (A, C) is observable, the observer is designed as

$$
\begin{aligned}
\hat{x}(k) &= A\hat{x}(k-1) + Bu(k-1) \\
&\quad + L_x[-y(k-1) + C\hat{x}(k-1)] \\
\sum \hat{v}(k) &= \sum \hat{v}(k-1) + C_v\hat{x}(k-1) \\
&\quad + C_v L_x[-y(k-1) + C\hat{x}(k-1)] \\
\Delta\hat{v}(k) &= C_v(\hat{x}(k) - \hat{x}(k-1))
\end{aligned}
\tag{3.7}
$$

It is only necessary to design the observer gain L_x as $eig(A + L_xC) < 1$ so that $\hat{x}(k) - x(k) \to 0$. This automatically leads to $\Delta\hat{v}(k)$ being stable. The integral estimation error is not required to decay to zero, but a steady state because $\sum \hat{v}(k) - \sum v(k) \to const$ means $\hat{v}(k) - v(k) \to 0$.

3.3 Controller Design

3.3.1 MPC Tracking

This section will outline the general MPC controller design for a state space model that results in PI/PID control implementation fulfilling the constraints.

Consider the linear system with constraints $z(k+1) = A_m z(k) + B_m u(k)$. Define the operating points (z_s, u_s) and the deviation variables

$$
\begin{aligned}
\tilde{z}(k) &= z_s - z(k) \\
\tilde{u}(k) &= u_s - u(k),
\end{aligned}
\tag{3.8}
$$

$$\text{then} \quad \tilde{z}(k+1) = A_m \tilde{z}(k) + B_m \tilde{u}(k)$$

$$\tilde{y}(k) = C_m \tilde{z}(k). \tag{3.9}$$

The finite-horizon quadratic optimal control problem is posed as

$$V_N^o(\tilde{z}_0, \tilde{U}) = \min_{\tilde{U}} . \, \tilde{z}_N^T P \tilde{z}_N + \sum_{k=0}^{N-1} (\tilde{z}_k^T C_m^T Q C_m \tilde{z}_k + \tilde{u}_k^T R \tilde{u}_k) \tag{3.10}$$

$$subj. \, to \quad \tilde{z}_k \in X, \tilde{u}_k \in U \quad \forall k \in 0, ..., N-1,$$

$$\tilde{z}_0 \in X_0, \tilde{z}_N \in X_f,$$

$$\tilde{z}_{k+1} = A_m \tilde{z}_k + B_m \tilde{u}_k,$$

where $\tilde{U} = \{\tilde{u}_0, ..., \tilde{u}_{N-1}\}$. Here $Q \geq 0, R \succ 0$ are the weighting matrices, $(Q^{1/2}, A_m)$ is detectable; $P \geq 0$ is the terminal penalty matrix. X_0, X_f are the initial feasible set and the terminal constraint set. Note that X, U are translated constraints from (3.2) through the transformation in (3.8). By the receding horizon policy, only $\tilde{u}_0$ is applied to the plant.

Assumption 1 *The state and input constraints are not active for $k \geq N$. Also, X_f contains the origin.*

The optimizer $\tilde{U}$ stabilizes (3.9) if the value function $V_N^o(\tilde{z})$ corresponds to a local Lyapunov function V_f within the terminal set X_f. In addition, the decay rate of that Lyapunov function must be larger than the stage cost [Mayne et al., 2000]. Under this setup, any admissible $\tilde{z}_0$ is steered to a level set of V_f (and so X_f) within N steps, after which convergence and stability of the origin follow. In other words, z_k is stable at z_s for $k \geq N$.

Therefore, given the state and input weighting matrices Q, R, one would want to first compute an unconstrained stabilizing feedback $\tilde{u} = K\tilde{z}$ and its Lyapunov function $V(\tilde{z})$ that satisfy

$$V_f(\tilde{z}) = \tilde{z}^T P \tilde{z} \geq 0,$$

$$\Delta V_f(\tilde{z}) = \tilde{z}^T A_K^T P A_K \tilde{z} - \tilde{z}^T P \tilde{z}$$

$$\leq -\tilde{z}^T Q \tilde{z} - \tilde{z}^T K^T R K \tilde{z}, \, \forall \tilde{z} \in X_f, \tag{3.11}$$

where $A_K = A_m + B_m K$. The other ingredients of MPC formula are then determined as follows.

- X_f is the maximal positively invariant polyhedron of $\tilde{z}_{k+1} = A_m \tilde{z}_k + B \tilde{u}_k$ with respect to $\tilde{z}_k \in X, \tilde{u}_k \in U$. As commented in Rawlings

and Mayne [2009], if X_f is ellipsoidal, the problem is no longer a quadratic program but a convex program but can be solved with available softwares.

- X_0 is the N-step stabilizable set of the system (3.10) with respect to X_f. N is a trade-off value between the complexity of MPC problem and a larger set X_0 (i.e. larger initial error $\tilde{z}_0$).

- P is chosen as the solution of the equality in (3.11), the unique positive-definite solution of a discrete Lyapunov equation once K is known [Grieder et al., 2005].

X_0, X_f can be calculated analytically using the method detailed in Alessio et al. [2006]; Blanchini [1999].

A popular choice for K is obtained from the LQR gain with weighting matrices Q, R [Chmielewski and Manousiouthakis, 1996; Scokaert and Rawlings, 1998]. However, in this note, it is left as a general stabilizing gain K that will be computed in the next section.

3.3.2 Computation of Stabilizing PI/PID

This session describes a method to compute an unconstrained feedback gain K that is used to reconstruct the MPC formula (3.10). It is because this gain would result in PI/PID controllers, as shown in the following theorem. For the general case, let $z = \begin{bmatrix} x^T & \sum v^T & \Delta v^T \end{bmatrix}^T$.

Let $(\bar{A}, \bar{B}, \bar{x})$ be the augmented model and state of (3.3). We show how to obtain the gain K as either PI or PID gains.

PI Controller ($K_3 = 0$)

For this case, it is essential to obtain the feedback gain for $z = \bar{x} = \begin{bmatrix} x^T & \sum v^T \end{bmatrix}^T$. The PI control can be formulated by applying LQR to the error model of (3.3) to produce a PI control law $u(k) = K_{PI} z(k)$. From here simply take $(A_m, B_m, C_m) = (\bar{A}, \bar{B}, \bar{C})$, $K = K_{PI}$ and use (3.11) to apply the MPC formula.

PID Controller ($K_3 \neq 0$)

To get a non-trivial differential gain K_3, one can treat the differential term as an output feedback of the system (3.3) [Zheng et al., 2002]. Define $\phi = \begin{bmatrix} x^T & \sum v^T & \phi_3^T \end{bmatrix}^T$ where $\phi_3 = \Delta v - C_v B u = C_v (Ax + Bu - x) - C_v B u =$

$C_v(A - I_n)x$. Then

$$\bar{x}(k+1) = \bar{A}\bar{x}(k) + \bar{B}u(k)$$

$$\phi(k) = \bar{C}\bar{x}(k) = \begin{bmatrix} I_n & 0 \\ 0 & I_q \\ C_v(A - I_n) & 0 \end{bmatrix} \bar{x}(k). \tag{3.12}$$

Design of static output feedback (SOF) $u(k) = F\phi(k)$ for the discrete time system above has been investigated in Bara and Boutayeb [2005]; Dong and Yang [2007]; Garcia et al. [2003]; He et al. [2008] which use LMI conditions. There exists more outputs than inputs in this case, so we present a simple solution to determine F in Theorem 3 [Bara and Boutayeb, 2005]. In that work, the solution can be extended to the H_∞ design, but the details are omitted here for simplicity (refer to Remark 4).

Theorem 3 *System* (3.12) *is stabilizable by a static output feedback if there exist a symmetric positive definite matrix* $P_0 \in \mathbb{R}^{(n+q)\times(n+q)}$ *and a positive scalar* $\sigma \in \mathbb{R}$ *such that*

$$\bar{A}^T P_0 \bar{A} - P_0 + \sigma \bar{B}\bar{B}^T \prec 0 \tag{3.13}$$

is satisfied. Furthermore, the SOF gain F can be obtained by solving

$$(\bar{A} + \bar{B}F)^T P_0 (\bar{A} + \bar{B}F) - P_0 \prec 0. \tag{3.14}$$

Conditions (3.13), (3.14) can be solved as two LMI problems. Once we have found a stabilizing output feedback $u(k) = F\phi(k)$ or equivalently $\tilde{u}(k) = F\tilde{\phi}(k)$, it can be rewritten in the PID form as

$$\tilde{u}(k) = F_1 \tilde{x}^T + F_2 \sum \tilde{v}^T + F_3 \Delta\tilde{v} + F_3 C_v B\tilde{u}(k) \tag{3.15}$$

$$\text{so } \tilde{u}(k) = (I_n + F_3 C_v B)^{-1}[F_1 \tilde{x}(k)^T + F_2 \sum \tilde{v}(k) + F_3 \Delta\tilde{v}(k)]$$

$$= K_{PID}\tilde{z}(k), \tag{3.16}$$

where $\tilde{z} = \begin{bmatrix} \tilde{x}^T & \sum \tilde{v}^T & \Delta\tilde{v}^T \end{bmatrix}^T$. The invertibility of matrix $(I_n + F_3 C_v B)$ is a necessary condition to render K_{PID}.

The MPC formula takes $\tilde{z}(k+1) = A_m \tilde{z}(k) + B_m \tilde{u}(k)$,

$$A_m = \begin{bmatrix} A & 0 & 0 \\ C_v & I_n & 0 \\ C_v(A - I_n) & 0 & 0 \end{bmatrix}, B_m = \begin{bmatrix} B \\ 0 \\ C_v B \end{bmatrix} u(k) \qquad (3.17)$$

and $K = K_{PID}$ to apply into (3.11).

Remark 3 *Applying LQR directly to PID state for system (3.17) will not result in a PID controller. In fact, since A_m is no longer full rank, the optimal input $\tilde{u}(k) = (R + B_m^T Q B_m)^{-1} B_m^T Q A_m \tilde{z}(k)$ depends only on the first two components of $\tilde{z}(k)$, so it is not a full PID but a PI gain. However, we realize that increasing the weight on Δv of Q does reduce the overshoot and enhance the disturbance response of $v(k)$.*

Remark 4 *The PID design for multivariable systems used in this chapter is not unique. It is possible to use other techniques such as Dickinson and Shenton [2009]; Soylemez et al. [2003]; Toscano and Lyonnet [2009] to derive a robust PID gain before applying it into MPC.*

3.4 From Parametric MPC to PID Gain Scheduling

The result from Section 3.3 holds when it is applied to either an *online* or *offline* MPC formulation. In this section, we particularly use parametric MPC (offline) to demonstrate the PID gain scheduling realization.

3.4.1 Parametric MPC

Observe that the problem (3.10) minimizes a convex value function subject to a convex constraint set. We have the following definition

Definition 1 (Critical Region) *A critical region is defined as the set of parameters $\tilde{z}$ for which the same set of constraints is active at the optimum $(\tilde{z}, \bar{U}^0(\tilde{z}))$.*

In other words, if the constraints in (3.10) are presented as $G\bar{U} \leq S\tilde{z} + W$ and A is an associated set of row index,

$$CR_A = \{\tilde{z} \in X_0 \mid G_i \bar{U}^0 = S_i \tilde{z} + W_i \text{ for all } i \in A\} \qquad (3.18)$$
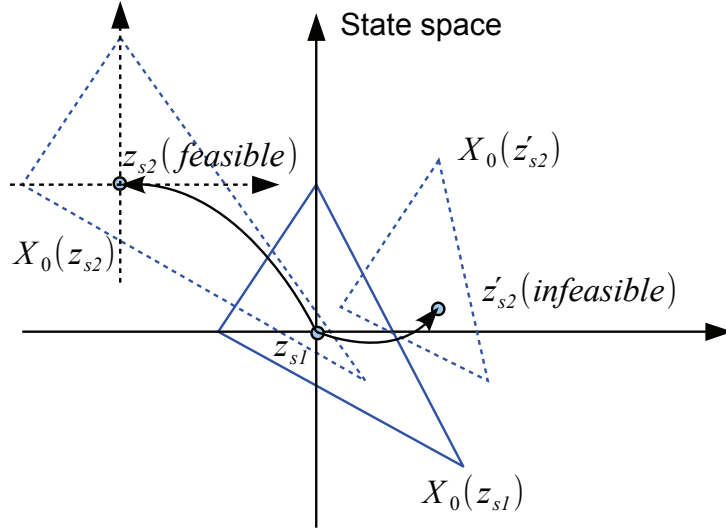
Figure 3.2: Feasibility check of new setpoint z_{s2}.

In Baotic [2002]; Tondel et al. [2003], it is shown that these critical regions are a finite number of closed, non-overlapped polyhedra and they cover completely X_0. Since $\tilde{U} = \{\tilde{u}_0, ..., \tilde{u}_{N-1}\}$, the same properties apply for $\tilde{u}_0^0$. Theorem 4 states the key result (see Bemporad et al. [2002]).

Theorem 4 (Parametric solution of MPC) *The optimal control law $\tilde{u}_0^0 = f(\tilde{z}_0)$, $f : X_0 \mapsto U$, obtained as a solution of (3.10) is continuous and piecewise affine on the polyhedra*

$$f(\tilde{z}) = F^i\tilde{z} + g^i \quad if\ \tilde{z} \in CR^i, i = 1, ..., N^r, \tag{3.19}$$

where the polyhedral sets $CR^i \triangleq \{H^i\tilde{z} \leq k^i\}$, $i = 1, ..., N^r$ are a partition of the feasible set X_0.

Tracking for piecewise constant setpoint

Recall the admissible set X_0 the MPC controller can stabilize depends on the linearized model $x(k+1) = f(x(t))|_{x=x_s}$ and control horizon N. Tracking of a new setpoint can be done by increasing N_2 based on the new model so that a jump in reference $z_{s1} \rightarrow z_{s2}$ is feasible within N_2 steps.

In the case of fixed N, Corollary 5 states the necessary and sufficient condition for a new feasible setpoint.
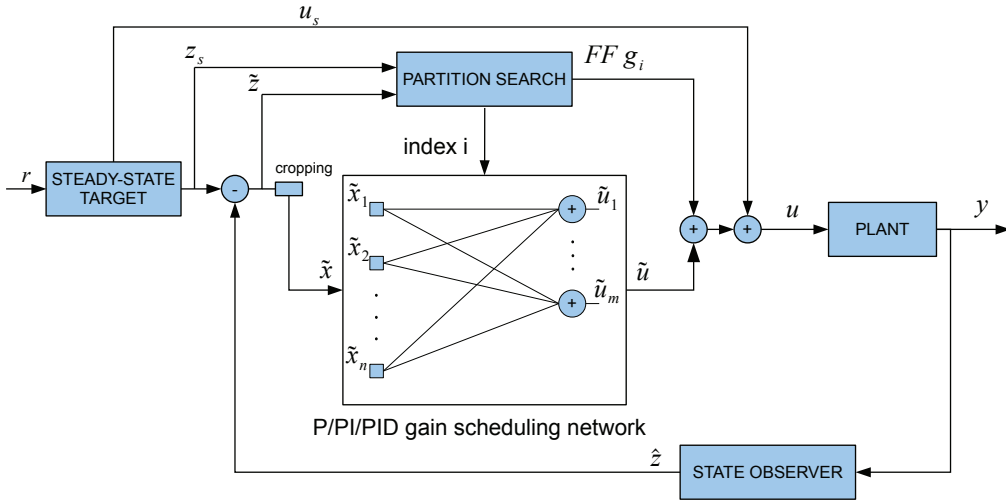
Figure 3.3: Proposed PID gain scheduling structure.

Corollary 5 *With a fixed-horizon proposed controller, a change in setpoint $z_{s1} \rightarrow z_{s2}$ is feasible if and only if $z_{s1} - z_{s2} \in X_0(z_{s2})$.*

Proof 3 *The proof can be inferred from Fig 3.2. If z_{s1} is out of the maximal admissible region $X_0(z_{s2})$ constructed around z_{s2}, it is impossible to drive the current error $\tilde{z} = z_{s1} - z_{s2}$ to zero with the existing controller.*

Corollary 5 suggests a way to detect if a new setpoint is feasible so that the local optimization for steady state target can recalculate z_s early before the infeasibility happens. One can use a single model and treat the model mismatch at a different operating point as disturbance, but generally X_0 still needs to be rebuilt through (3.8) because the constraints change with setpoint relocation.

3.4.2 PID Gain Scheduling Design

The optimal input of MPC is applied for regions outside X_f. When $\tilde{z}(k)$ reaches X_f, the system will be stabilized by the pure gain $F^0 = K$. Therefore, one practical way to design PID for constrained systems is designing a PID gain for its unconstrained region, which has been accomplished in Section 3.3, and applying these settings on the MPC formulation (3.10).

Fig. 3.3 shows a series of PIDs plus a single feedforward vector where the controller gains are determined from (3.19). Each of the PIDs is fully
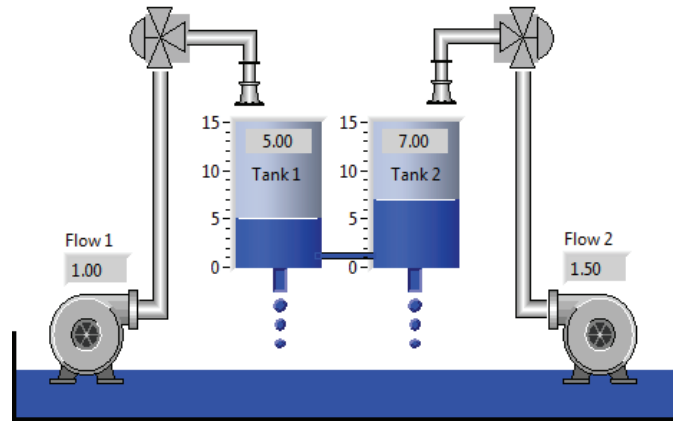
Figure 3.4: Two coupled tanks for chemical processing

flexible (might contain only P or PI components) and has its own gain-scheduling table for different partition indexes. At each time step, the proposed scheme would look for the region in which the augmented error $\tilde{z}(k)$ lies in. This search engine would broadcast the region index i to the PID network. The feedforward term associated with region i is added to compensate the active constraints. Non-zero tracking accounts for the addition of steady state input and recovers the input delivered to the plant.

Remark 5 *As seen from Fig. 3.3, the PID network consists of one-to-one mappings between each state variable error of the original state x and an input. This fact results from equation (2.7).*

3.5 Example

The proposed control design is illustrated in the following example, generalized from Bemporad et al. [2002] with two inputs. Consider a con-

tinuous stirred-tank reactor model in Fig. 3.4

$$A = \begin{bmatrix} 0.7326 & -0.0861 \\ 0.1722 & 0.9909 \end{bmatrix}, B = \begin{bmatrix} 0.0609 & 0 \\ 0 & 0.0064 \end{bmatrix},$$

$$C = \begin{bmatrix} 1 & 0 \\ 0 & 1 \end{bmatrix}, X = \left\{ x \in \mathbb{R}^2 | \begin{bmatrix} -0.5 \\ -0.5 \end{bmatrix} \le x \le \begin{bmatrix} 1.5 \\ 2.5 \end{bmatrix} \right\},$$

$$U = \left\{ u \in \mathbb{R} | \begin{bmatrix} -2 \\ -2 \end{bmatrix} \le u \le \begin{bmatrix} 2 \\ 2 \end{bmatrix} \right\}. \tag{3.20}$$

The task is to track the level 1 x_1 with the reference x_{1s} = 1. To observe the robustness of tested controllers, the disturbances d_1 = [1; −0.5] (impulse), d_1' = [0.01; −0.01] (additive) within an active constrained region at k = 3 and d_2 = [−0.15; 0] (additive) at steady state k = 100 are introduced.

The three following controllers are compared: simple parametric MPC (I), the whole state tracking with full PI (II) and x_1-tracking with partial PID (III). The prediction horizon (also control horizon in this case) is chosen as N = 2.

Tuning weighting matrices for PID control had been discussed in Nguyen et al. [2011]. For PI, $z = \begin{bmatrix} x_1^T & x_2^T & \sum x_1^T & \sum x_2^T \end{bmatrix}^T$ and $Q = diag(1, 1, 0.001, 0.001)$, $R = 0.01I_2$; for PID $z = \begin{bmatrix} x_1^T & x_2^T & \sum x_1^T & \Delta x_1^T \end{bmatrix}^T$, $Q = diag(1, 1, 0.001, 0.1)$, $R = 0.01I_2$. MATLAB LMI solver is used to obtain the unconstrained PID gain for case III, and Multiparametric toolbox [Kvasnica et al., 2004] is applied to obtain the gains under critical regions.

The unconstrained gain K in the three cases are

$$K_I = \begin{bmatrix} 4.501 & 3.792 \\ 0.711 & 2.160 \end{bmatrix},$$

$$K_{II} = \begin{bmatrix} 5.792 & 6.353 & 0.289 & 0.469 \\ 1.103 & 7.094 & -0.579 & 0.326 \end{bmatrix},$$

$$K_{III} = \begin{bmatrix} 0.493 & 1.399 & 0.139 & -0.392 \\ 3.014 & 18.545 & 1.765 & -0.766 \end{bmatrix}, \tag{3.21}$$

and they resulted in control laws with 8, 14, 12 critical regions, respectively.

From the state response in Fig. 3.5, it is observed that the scheme I can not negate the additive disturbance happened either at an active

constraint region or at steady state. It results in offset $\tilde{x} = \begin{bmatrix} 0.06 & -0.06 \end{bmatrix}^T$ and $\tilde{x} = \begin{bmatrix} -0.05 & -0.45 \end{bmatrix}^T$, respectively. The scheme II can track both the state variables but with significant overshoot due to the regulation of $\sum \tilde{v}$ back to 0. That effect can be removed by tracking it to a constant (as a tuning parameter), but ignored in this example for simplicity. The scheme III tracks x_1 as required, and successfully forces the disturbance effect into x_2. The tracking under setpoint change and disturbance rejection also happens faster than scheme II. It should be emphasized that all the three schemes are able to deal with the state and input constraints $x_1 \leq 1.5$, $u \leq 3$ during transient stage because of the feedforward term g^i in the parametric MPC law.

Fig. 3.6 gave another perspective of the result. Provided that the impulse disturbance did not excite the current state out of the feasible region X_0, it is feasible to find an optimal input for all the three schemes. Secondly, scheme II hit on the outer constraint $\tilde{x}_1 = -0.5$ ($x_1 = 1.5$) and took a long time to recover. Indeed, an integral windup happened at this upper output bound. The scheme III showed the full PID potential. It is known that the proportional-integral deals with the present and past behavior of the plant. The differential term predicts the plant behavior and can be used to stabilize the plant faster. This is in line with Remark 3. The trajectory quickly returned to the origin in both cases of setpoint change and additive disturbance. Lastly, while scheme II regulated the state error back to the origin, scheme III only drove it to the axis $\tilde{x}_1 = 0$ as expected. It meant only $m \times q$ PIDs and $m \times (n - q)$ Ps are needed to track q outputs.

In conclusion, it is observed that as long as the disturbance does not drive the equilibrium outside of the unconstrained region, output tracking using the integral state variables remains feasible. The robust stability during transient stage is inherent through the PID form. The robust stability around setpoint only concerns the PID control design described in Section 3.3.2, which can be improved further by H_∞ approaches as stated in Remark 4. Overall, extension to integral and differential terms is the natural to perform tracking control.

3.6   Conclusion and Future Work

As it was never emphasized enough, the link between MPC and a robust linear controller at equilibrium is revisited in this chapter. We modify the linear controller to be capable of offset-free tracking. The resultant control architecture is a PID gain scheduling network with a feedforward part to deal with state and input constraints. A simple test for setpoint tracking feasibility is also discussed. Finally, the example results show that the robustness stability of the proposed method is inherent within the PI/PID structure when disturbances arrives.

Future works will involve designing the unconstrained PID gain which enlarges the terminal region of MPC. In addition, the overall PID state space can be decoupled into smaller subspaces so that the partition searching operation is more efficient. Distributed MPC has the potential to apply this technique, where similarities in gain scheduling control can be found at Blanchini [2000]; Blanchini and Pellegrino [2007].
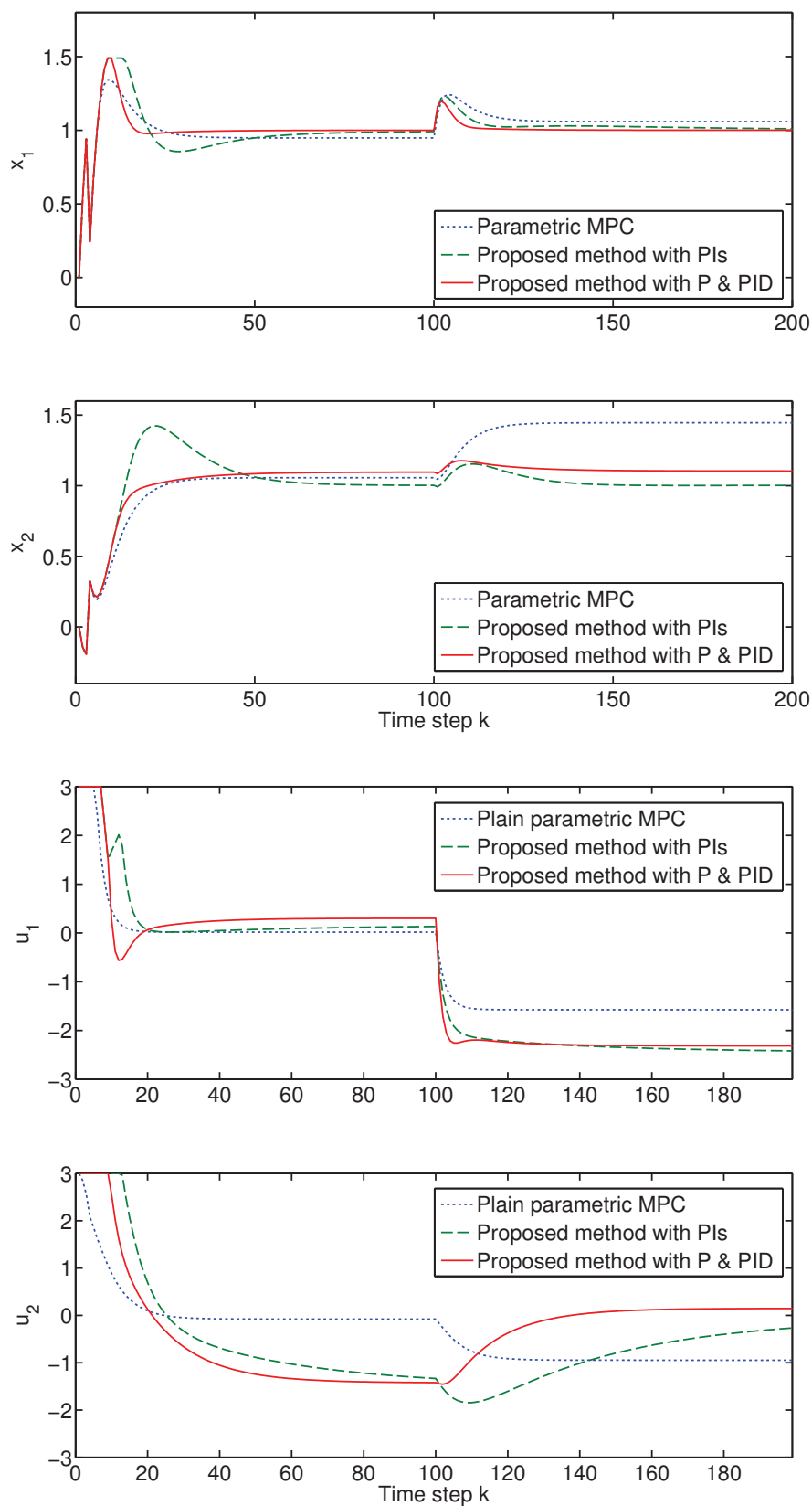
Figure 3.5: State responses and control inputs under disturbances at transient and steady-state.
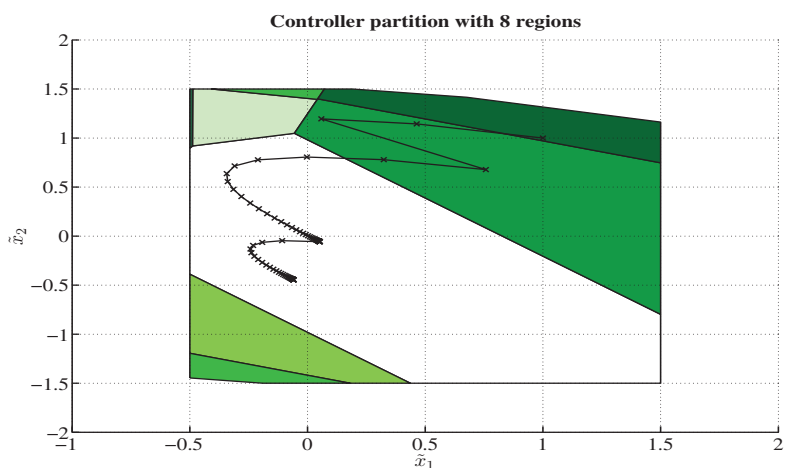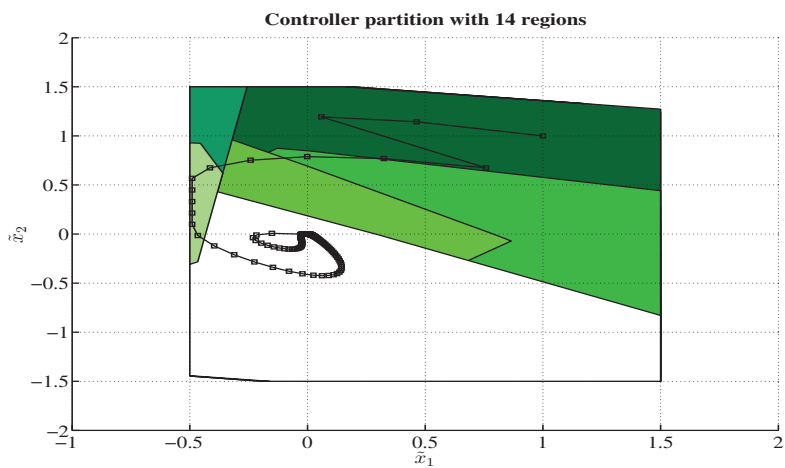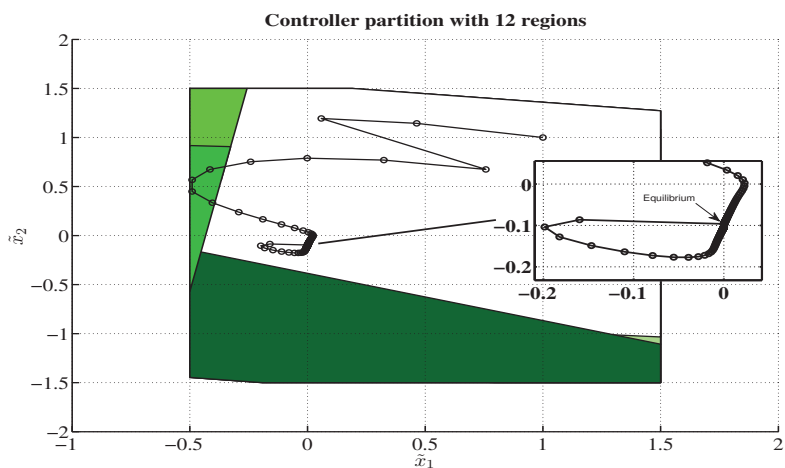
Figure 3.6: Controller partitions projected on subspace $[\tilde{x}_1, \tilde{x}_2]$ and the state trajectory with (a) Scheme I, (b) Scheme II (cut at $\sum \tilde{x}_1 = \sum \tilde{x}_2 = 0$) and (c) Scheme III (cut at $\sum \tilde{x}_1 = \Delta \tilde{x}_1 = 0$).

Chapter 4

Robust Control of a Linear Ultrasonic Drive

Ultrasonic actuators used in high-precision mechatronics are character-ized by strong frictional affects, which are among the main problems in precision motion control. The traditional methods apply model-based nonlinear feedforward to compensate the friction, thus requiring closed loop stability and safety constraint considerations. In this chapter model-based parametric controllers are derived to obtain an optimal position-ing control for these motors. A systematic approach which uses piece-wise affine models greatly simplifies the friction model choice in the traditional methods. Issues about the nonlinear affects of the friction are addressed by designing a robust control law near zero speed. These developments result in a gain-scheduling optimal input, which is sim-ple to carry out in real-time applications. The controller is expected to improve the constraint safety and the tracking performance for actuator operation.

4.1 Introduction

The ultrasonic motor (USM) is a type of piezoelectric actuators which use some form of piezoelectric material and rely on the piezoelectric effect. The USM offers advantages of high resolution and speed to ensure the precision and repeatability, so it is widely used in precision engineering, robots and medical and surgical instruments where high accuracy is required. While a typical piezoelectric actuator (PA) is driven directly by the deformation of the piezoelectric material, the USM provides motions

by the friction between the piezoelectric material on the stator and the rotor. Thus, the USM offers another advantage of theoretically unlimited travel distance in comparison with the typical piezoelectric actuators.

This chapter examines the USM M-663 made by *Physik Instrumente (PI)* as a testbed. Fig. 4.1 shows its internal structure and working principle. The rotor motion is based on a alumina tip attached to the piezo-ceramic plate (the stator). This plate is segmented on one side by two electrodes. Depending on the desired direction of motion, either the left or right electrode of the piezo-ceramic plate is excited with a standing wave to produce high-frequency vibration. Because of the asymmetric characteristic of the standing wave, the tip moves along an inclined linear path with respect to the friction bar surface and drives the rotor forward or backward. Each oscillatory cycle of the tip can transfer a 0.3 μm linear movement to the friction bar. With the high-frequency oscillation, it will result in a smooth and continuous rotor motion. An external drive is used to convert analog input signals into the required high-frequency drive signals. The motor is employed in a semi-automated device for medical operation on human ear membrane. The operating conditions defined by the manufacturer are: travel range $\pm 9.5\,mm$, maximum speed $400\,mm/s$ and input voltage $\pm 10\,V$. Because of the strict constraints in medical operation, additional control constraints arise: tracking overshoot less than 5 %, settling time within $0.1\,s$, maximum steady state error $0.02\,mm$. Controlling the actuator under such constraints and performance requirements requires specific consideration.

For control applications involving small displacement and velocities, friction modeling and compensation can be very important, especially around velocity reversal. Because the friction presents a nonlinear switch which is dependent on the motion direction, using a single linear model to design a linear controller results in inaccuracy especially at low-speed control Armstrong and Amin [1996]. Additionally, a practical controller should respect the physical limitation of the motor input and safety constraints on the system variables (e.g., position range, speed).

To overcome friction, the traditional control algorithms reported in the literature decouples the friction model from the linear motion system and mitigates it separately. Beside a linear regulator such as PID, the input contains a nonlinear feedforward component. These meth-

ods differ from one another in the nonlinear friction models as well as the techniques to compensate for it. Along this perspective, much research efforts have been focusing on building accurate friction models Dupont et al. [2002]; Hayward et al. [2009]; Parlitz et al. [2004]. The compensation, usually of bang-bang type in practice, resolves the friction problem and leaves PID with other unmeasured disturbances including the friction model mismatch. The approaches are simple to implement and if properly tuned, they provide fast transient response, good static accuracy and robustness to the motor parameter variations Peng and Lin [2007]. However, the nonlinear compensation is contingent on asymptotic stability, which relies on the specified friction model. The frictional affects can also depend on rotor position and system degeneration, so a fixed friction model may require more computing time to compute. Finally, such control tactics do not deal systematically with constraints on the control input and variables, so manual safety considerations have to be taken care.

To address the mentioned limits, the hybrid model predictive control (MPC) approach which is easy to implement and has all the advantages of model-based control has been proposed. The flexibility of MPC framework is that it can use mathematical programming to solve systematically constrained optimization. A recent rising approach to deal with friction in electrical drive is based on piecewise affine (PWA) modeling of the nonlinear frictional affects. Theoretically, the idea of MPC for PWA systems was developed nicely by Lazar et al. [2006]. In the context of Herceg et al. [2009]; Vasak et al. [2007], the authors applied this method to design time-optimal control strategies for industrial actuators. Although the method still depends on the choice of friction models and considers no robustness, the tracking performance is promising.

In this chapter, a robust optimal design is adapted via the familiar quadratic programming for a tractable solution. The commonly used friction models are approximated by several linear segments so MPC is aware of this impeding force at low speed. A constrained optimal control problem for PWA systems is then formulated to provide stability-guaranteed input. Specially, an integral MPC design imposes the robustness on model-plant mismatch near zero-speed. Implementation of the real-time control is handled by a gain-scheduling table so that the complexity is comparable to the traditional feedforward PID. Section 4.2
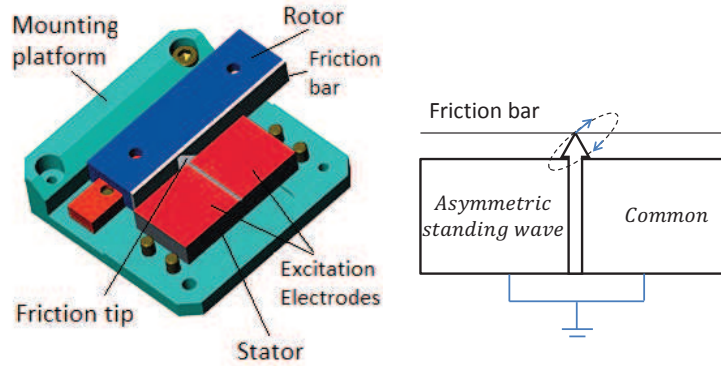
Figure 4.1: Linear ultrasonic motor structure and motion description.

describes how the piecewise affine model can fit in the shape of friction forces. Section 4.3 describes model predictive control concepts in the motion tracking context. Integral MPC with robustness design is also presented. In Section 4.4 simulation studies are described before final implementation on the experiment setup is reported. The chapter is concluded in Section 4.5.

Notations

y, v denote position and velocity of the motor. F, f are the general friction and its components. A, B, C, D are matrices of a state space dynamics. The indices i, j are for different system dynamics and gain-scheduling regions, respectively. All sets mentioned in this context are polyhedral sets.

4.2 Piecewise Affine Model of Motion

Consider a classical linear motion model which takes the form

$$\begin{bmatrix} \dot{y} \\ \dot{v} \end{bmatrix} = \begin{bmatrix} 0 & 1 \\ a & b \end{bmatrix} \begin{bmatrix} y \\ v \end{bmatrix} + \begin{bmatrix} 0 \\ c \end{bmatrix} (u - F(v)) \tag{4.1}$$

where y, v is the rotor position and velocity; $F(v)$, the friction as shown in Fig. 4.3, consists of the constant Coulomb friction f_c, viscous friction $F_l = kv$ and Stribeck effect F_{nl} which shows the friction continuously decreases when the motor starts accelerating Hayward et al. [2009].

From there, the motion system of ultrasonic motor can be represented
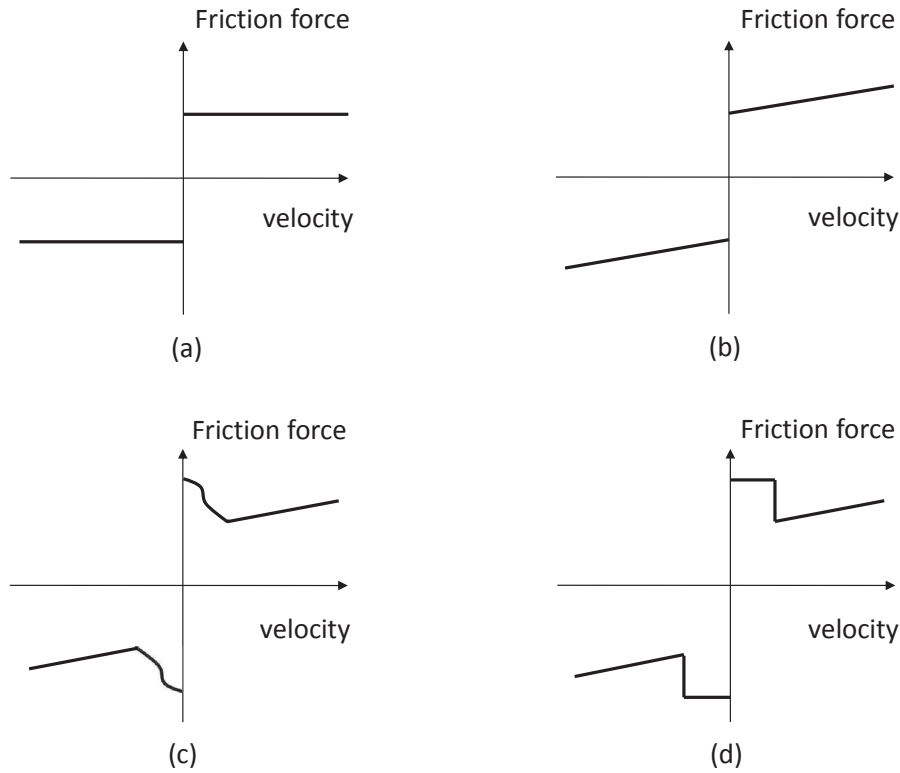
Figure 4.2: Various friction models. (a) Coulomb. (b) Coulomb + viscous. (c) negative viscous + Coulomb + viscous: Form A. (d) negative viscous + Coulomb + viscous: Form B.

in four regions A-D, as in Fig. 4.3. Because the viscosity is linear in v, models in regions A and D can be represented by (4.1). In regions B and C, the same structure can be employed to approximate the system, but with different linear dynamics; the complexity in the pre-sliding regime will be addressed by the robust design in Section 3.3.

Firstly, the asymmetric static friction values at which the motor starts moving, determined by injecting a sine wave function with low frequency and amplitude $3\,V$, are $f_{cp} = 2.5V, f_{cn} = -2.9\,V$ as seen from Fig. 4.4.

Secondly, the effective relationship from input to rotor position is identified at two operating ranges: very low speed and normal speed. Test inputs with bi-frequency square waves and magnitude $u = \pm 5\,V$ and $u = \pm 3\,V$ (prior to adding the mean $\frac{f_{cn}+f_{cp}}{2}$) are used to stimulate the position response. The defining planes between the regions A and B, C and D are taken at the velocity v_n, v_p obtained by applying $u = \pm 3\,V$ so the regions B and C encompasses the nonlinear friction F_{nl}. The correlation between the effective inputs, which are obtained by modulating the

Figure 4.3: Motion friction (solid) described by linear segments (dashed) over four regions A - D. The outer regions A, D are depicted by the linear model $\{A_1, B_1\}$ while the inner regions B, C are characterized by $\{A_2, B_2\}$.

test inputs with the static friction forces as

$$
u = \begin{cases} u - f_{cp} & \text{if } u > 0 \\ u - f_{cn} & \text{if } u < 0, \end{cases} \tag{4.2}
$$

and the output are examined. The dynamic models $\{A_1, B_1\}$, $\{A_2, B_2\}$ for the two velocity ragnes are obtained from MATLAB System Identification toolbox (subspace method) and validated in Fig. 4.5.

Denote the state $x = \begin{bmatrix} y & v \end{bmatrix}^T$. The piecewise affine model, after being transformed to discrete time, can be formally defined in the four convex subspaces

$$
x_{k+1} = \begin{cases} A_1 x_k + B_1(u_k - f_{cp}) & \text{if } v \geq v_p \ (\Omega_1) \\ A_1 x_k + B_1(u_k - f_{cn}) & \text{if } v \leq v_n \ (\Omega_2) \\ A_2 x_k + B_2(u_k - f_{cp}) & \text{if } 0 \leq v \leq v_p \ (\Omega_3) \\ A_2 x_k + B_2(u_k - f_{cn}) & \text{if } v_n \leq v \leq 0 \ (\Omega_4) \end{cases} \tag{4.3}
$$

Let $f_c = f_{cp}$ or f_{cn}. Because regions A, D and B, C share the same linear dynamics, the control design only needs to consider two cases $\{A_i, B_i\}$ for $i = 1, 2$. We have the following compact system depending on the

Figure 4.4: Measurement of static friction using sine wave input.

sign and magnitude of the velocity v

$$x_{k+1} = A_i x_k + B_i(u_k - f_c) \text{ for } i = 1, 2. \tag{4.4}$$

Remark 6 *The choice of $u = 3\,V$ is just large enough to bypass f_c so that it can stimulate the motion at a very low speed. This choice results in the velocity range $[v_n, \, v_p] = [-9, 9]\,mm/s$ which safely contains the nonlinear part of the friction.*

Fig. 4.5(b) shows that a linear model could not fit well on the inner region which contains a nonlinear part of the friction. In Section 4.3, this model mismatch will be addressed by implanting robust control within the MPC terminal set.

4.3 Model Predictive Control for PWA Model

This section presents the integral model predictive design, including of state augmentation, MPC tracking formulation and robust design.

Since the position tracking is emphasized, the new augmented inte-

gral system $(\bar{x}_k, \bar{u}_k, \bar{y}_k)$ is

$$
\begin{bmatrix} x_{k+1} \\ r_{k+1} \\ \theta_{k+1} \end{bmatrix} = \begin{bmatrix} A_i & B_i & 0 \\ 0 & 1 & 0 \\ C_i & -1 & 1 \end{bmatrix} \begin{bmatrix} x_k \\ r_k \\ \theta_k \end{bmatrix} + \begin{bmatrix} B_i \\ 1 \\ 0 \end{bmatrix} \bar{u}_k
$$

$$
\bar{h}_k = \begin{bmatrix} C & -1 & 0 \\ 0 & 0 & 1 \end{bmatrix} \bar{x}_k, \quad i = 1, 2, \tag{4.5}
$$

where r is the reference position and $\bar{u}_k = u_k - f_c$. For convenience, denote the system matrices for these augmented systems as $(\bar{A}_i, \bar{B}_i, \bar{C}_i)$ and $(i = 1, 2)$. Due to the motion system characteristics, this model description already contains an integrator and it is not necessary to use Δu-tracking formula here. Instead, the integrating state θ_k guarantees tracking property.

A MPC optimal control scheme uses the system (4.5) to predict the output error ahead in time and uses current feedback errors to compensate any disturbance. The particular form of MPC is stated as follows

$$
V_N^o(\bar{x}_0, \bar{U}) = \min_{\bar{U}} \bar{x}_N^T P \bar{x}_N + \sum_{k=0}^{N-1} (\bar{x}_k^T \bar{C}^T Q \bar{C} \bar{x}_k + \bar{u}_k^T R \bar{u}_k) \tag{4.6}
$$

$$
subj.\,to \quad \bar{x}_N \in X_f, \bar{u}_N = K\bar{x}_k,
$$

$$
\bar{x}_k \in \mathbb{X}, \bar{u}_k \in \mathbb{U} \quad k = 0, ..., N-1, \tag{4.7}
$$

where different prediction models ($i = 1, 2$) in (4.5) are used for respective regions. $\mathbb{X}, \mathbb{U}$ are the state and input constraint set.

In the MPC literature, the terminal cost P, the terminal set X_f and the terminal gain K are key components Rawlings [2000]. After at most N control steps, the MPC scheme expects the state $\bar{x}_k$ to reside inside the terminal set X_f, which is a control invariant set maintained by a linear state feedback $\bar{u} = K_i \bar{x}$. This goal is enforced by the decreasing Lyapunov function $V_N^0(x_k) = x_k^T P x_k$ within X_f. Here, it is essential to consider the design of components for all dynamics within the PWA systems.

Stability analysis for piecewise-affine systems using MPC has been analyzed before in Cuzzola and Morari [2002]; Lazar et al. [2006] with the design of the pair P, K and associated X_f. We are more focusing on the robustness aspect in this chapter. Equivalently, it is desirable to keep the system state to stay within a terminal constraint invariant set inside the regions B and C (near the switching surface of the friction) by
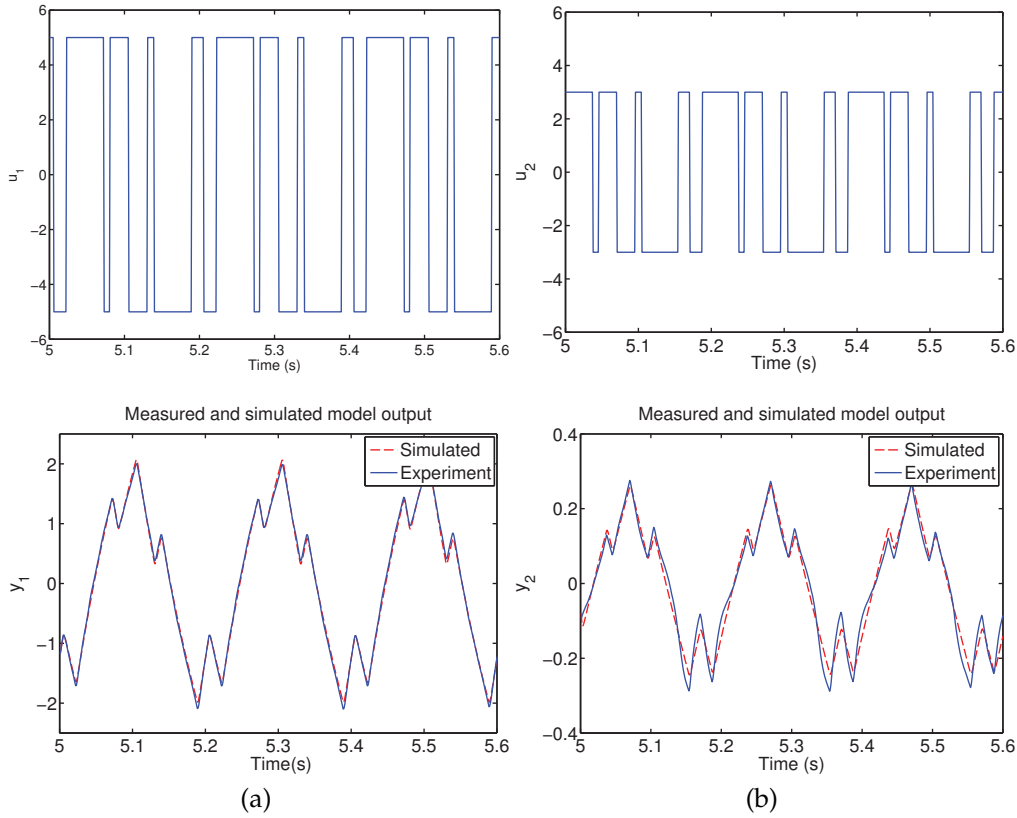
Figure 4.5: Model validation at two input ranges (a) around $u_1 = 5$ and (b) $u_2 = 3$.

a robust gain K, even with modeling errors. Such a gain can be designed specifically for the dynamic $\{A_2, B_2\}$ with robust control techniques. The rest of Section 4.3 describes a method to design of MPC components based on this goal.

Terminal gain

Consider again the augmented dynamics from (4.4). Given Q, R as desirable weighting matrices, design the feedback input $\bar{u}^{fb} = K\bar{x}$ such that the system

$$\bar{x}_{k+1} = \bar{A}_2 \bar{x}_k + \bar{B}_2(\bar{u}_k^{fb} + w_k)$$
$$\bar{y}_k = \bar{x}_k$$
$$\bar{h}_k = \bar{C}_2 \bar{x}_k \tag{4.8}$$

is robust against the friction model mismatch $w_k \in \mathbb{R}$ ($|w_k| \leq w^*$). This design can use one of many existing techniques in the literature to deal

with input disturbance. For this application, the rotor position and speed are measured directly, so full information on $\bar{x}_k$ of (4.5) is available, except the disturbance w_k. H_∞ design for *regular, state* feedback systems Oliveira et al. [2002], [Chen, 2000, Ch. 11] can be applied to solve the related discrete-time Riccati equations. The robust gain K must guarantee

$$\left\| T_{wy} \right\|_\infty < \gamma \tag{4.9}$$

where T_{wh} is the transfer function from w_k to h_k and γ is the infima of the H_2/H_∞ design.

Terminal cost

To guarantee the monotonous decreasing of the cost function V_N^o inside the terminal set, the terminal cost P should satisfy

$$(\bar{A}_2 + \bar{B}_2 K)^T P (\bar{A}_2 + \bar{B}_2 K) - P \leq -Q - K^T R K \tag{4.10}$$

A feasible pair (K, P) must satisfy H_∞ condition (4.9) and Lyapunov condition (4.10) together. These conditions can be addressed in Lemma 6.

Lemma 6 *Let $Z = P^{-1}$ and transform $Y = KG$ where G is invertible and denote $\Psi = \bar{A}_2 G + \bar{B}_2 Y$. The conditions (4.9), (4.10) can be satisfied simultaneously if there exists a solution (Z, Y, G) to the following LMI*

$$\begin{bmatrix} Z & \Psi & \bar{B}_2 & 0 \\ \Psi^T & G + G^T - Z & 0 & G^T \bar{C}_2^T \\ \bar{B}_2^T & 0 & I & 0 \\ 0 & \bar{C}_2 G & 0 & \gamma I \end{bmatrix} > 0, \tag{4.11}$$

$$\begin{bmatrix} G + G^T - Z & G^T & Y^T & \Psi^T \\ G & Q^{-1} & 0 & 0 \\ Y & 0 & R^{-1} & 0 \\ \Psi & 0 & 0 & Z \end{bmatrix} > 0. \tag{4.12}$$

After solving this LMI, the terminal weight P and the feedback K are simply recovered as $P = Z^{-1}$ and $K = YG^{-1}$.

Proof 4 *Assume (4.11) feasible, we have $G + G^T > Z > 0$ and G non-singular. Since Z is positive definite, $(Z - G)^T Z^{-1} (Z - G) \geq 0$, so $G^T Z^{-1} G \geq G +$*

*$G^T - Z$. From here we can replace $G + G^T - Z$ by $G^T Z^{-1} G$ and $\Psi = \bar{A}_2 G +$
$\bar{B}_2 Y$ in (4.11). Pre- and post- multiply the inequality with $T := diag\,[I, G^{-1}Z, I, I]$
and T^T we recover*

$$
\begin{bmatrix}
Z & (\bar{A}_2 + \bar{B}_2 K)Z & \bar{B}_2 & 0 \\
Z(\bar{A}_2 + \bar{B}_2 K)^T & Z & 0 & Z\bar{C}_2^T \\
\bar{B}_2^T & 0 & I & 0 \\
0 & \bar{C}_2 Z & 0 & \gamma I
\end{bmatrix} > 0,
\qquad (4.13)
$$

*which is a standard LMI condition for $\left\| T_{wy} \right\|_\infty < \gamma$ of the system (4.8) (see
Oliveira et al. [2002]).*

*Similarly, the matrix inequality $G^T Z^{-1} G \geq G + G^T - Z$ can be used in
(4.12). After applying Schur complement, the inequality (4.10) is retained.*

Terminal set

The terminal set X_f for the MPC problems in (4.6) is the maximal pos-
itively invariant set inside regions $X_{\Omega_3} \cup X_{\Omega_4}$ ($\bar{x}$-space of regions B and
C in Fig. 4.3). It can be computed based on the invariant control set
definition of the closed loop model $\bar{x}_{k+1} = (\bar{A}_2 + \bar{B}_2 K)\bar{x}_k + \bar{B}_2 w$ and the
system constraints.

For an arbitrary set Z, define the operator $\Phi(Z) = \left\{ \bar{x} \middle| (\bar{A}_2 + \bar{B}_2 K_2)\bar{x} + \bar{B}_2 w \in Z \right\}$. Let X_0 be a reasonably large compact polyhedron and the
sequence $\{X_i\}$ constructed such that

$$
X_0 \in \left\{ \bar{x} \middle| (\bar{x}, \bar{u}) \in \mathbb{X} \times \mathbb{U} \right\} \cap (X_{\Omega_3} \cup X_{\Omega_4}), \qquad (4.14)
$$

$$
X_i = \Phi(X_{i-1}) \cap X_{i-1}, \quad i = 1, 2, ..., \qquad (4.15)
$$

As proved in Lazar et al. [2006], this iterative procedure can be con-
verged in a finite number of steps and the resulted maximum robust
positive invariant set is $X_f = \lim_{i \to \infty} X_i$. A method to efficiently com-
pute this set has been formulated in Rakovic et al. [2005].

Observe that the problem (4.6) minimizes a convex value function
subject to a convex constraint set. The current state $\bar{x}_0$ can be considered
as a parameter for this problem. Interestingly, the state feedback gain
for $\bar{x}_0$ corresponds to velocity $v(k)$, position $x(k)$ and position integrating
$\theta(k)$, which is similar to a PID structure (except the feedforward part
because of the varying position reference and active constraints). Hence,
this is similar to a gain-scheduling feedforward PID where the decision
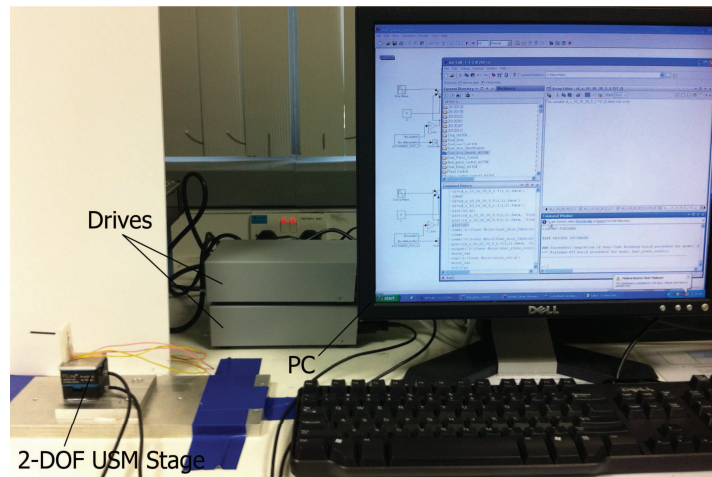
(a) Experiment setup of USM M-663 with DS1104.
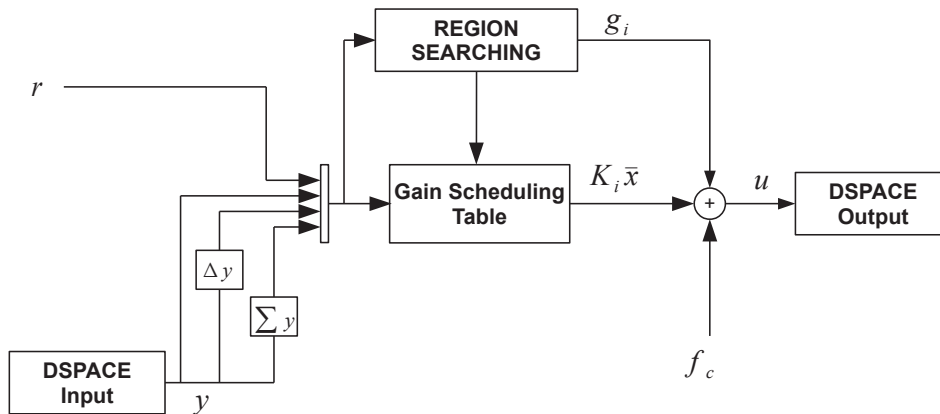
(b) Proposed PID gain scheduling structure implemented inside dSPACE.

Figure 4.6: Realtime control for a linear ultrasonic motor.

variable is the current state $\bar{x}_0$. Therefore, one practical way to design PID for constrained systems is designing a robust gain for its unconstrained region and applying these settings on the MPC formulation (4.6). Note that when $\bar{x}(k)$ reaches X_f, the system will be stabilized by the pure gain K_2.

4.4 Simulation Study and Experiment Results

The overall MPC controller design is simulated using multiparametric toolbox (MPT) Kvasnica et al. [2004] in MATLAB, which resulted in a simple gain-scheduling solution. Fig. 4.6 shows the controller structure.
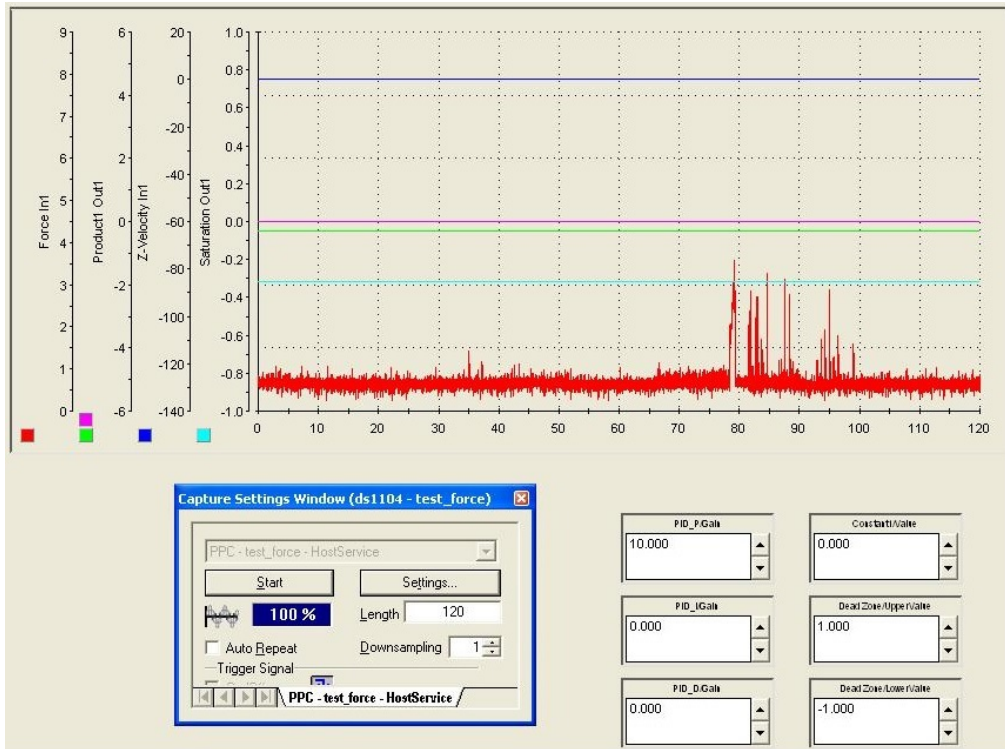
Figure 4.7: dSPACE ControlDesk Interface.

This control scheme is implemented in SIMULINK and then uploaded to dSPACE DS1104 Controller Board. The dSPACE control development and rapid prototyping system, in particular, the DS1104 board, is used, which integrates the development cycle into a single environment.

4.4.1 Simulation Studies

In this section, the previous theoretical development is applied to simulation examples. The purpose is to obtain a set of parameters to apply in the real experiment.

Firstly, MPC parameters are determined based on the nominal linear model $\{A_1, B_1\}$ without friction. The control horizon is chosen as $N = 10$ to cover the output transient response. Weighting matrices Q, R is tuned by the guideline in Nguyen et al. [2011] as $Q = diag\{10^4, 0.5, 0, 10^4\}, R = 0.001$. This choice gives a relative good performance for large changes of set point (Fig. 4.8). Notice that X_f falls inside the range $[v_n, v_p] = [-9, 9]\, mm/s$ due to the imposed conditions (4.14).

Parametric programming is used to solve the MPC problem for PWA

models to obtain a varible state-feedback gain over 23 subspace regions

$$\bar{u}_k = K_j \bar{x}_k + g_j \quad \text{if } \bar{x}_k \in CR_j \quad j = 1, \ldots, 23$$
$$\text{with} \quad K_j = \begin{bmatrix} K_{pj} & K_{dj} & K_{rj} & K_{ij} \end{bmatrix}, \tag{4.16}$$

a gain-scheduling form for feedforward PID. The output response is fast since $u(k) = u_{max} = 10\,V$ only powers up the actuator to a velocity $v(k) = 180\,mm/s$, smaller than $v_{max} = 400\,mm/s$.

In another study, the robust effective of the prosed control strategy is tested. To simulate a friction uncertainty, we assume that the ultrasonic motor has a similar linear model as the models identified from experiment data in Section 4.2, but a different friction form. The identified parameters are $f_{cp} = 2.5V$, $f_{cn} = -2.9\,V$ and

$$A_1 = \begin{bmatrix} 0.9968 & 6.289 \times 10^{-4} \\ -5.544 & 0.3623 \end{bmatrix}, \quad B_1 = \begin{bmatrix} 4.616 \times 10^{-3} \\ 3.493 \end{bmatrix}$$
$$A_2 = \begin{bmatrix} 0.9990 & 6.312 \times 10^{-4} \\ -1.658 & 0.3662 \end{bmatrix}, \quad B_2 = \begin{bmatrix} 2.033 \times 10^{-3} \\ 1.636 \end{bmatrix} \tag{4.17}$$

while the assumed real parameters are $f_{cp} = 2.4V$, $f_{cn} = -2.9\,V$, A_1, B_1 unchanged and

$$A_2 = \begin{bmatrix} 0.9990 & 6.312 \times 10^{-4} \\ -1.658 & 0.4000 \end{bmatrix}, \quad B_2 = \begin{bmatrix} 2.033 \times 10^{-3} \\ 1.636 \end{bmatrix} \tag{4.18}$$

An increase in $A_2(2,2)$ represents a steeper negative slope of F_{nl} (Fig. 4.3).

Two MPC schemes are compared: LQR MPC and the proposed controller with the additional robust design. Both MPCs are designed with the tuned parameters above. Fig. 4.9 shows the tracking errors, velocities and inputs after a step change in the reference. It can be seen that when friction mismatch presents, the output error with normal MPC strategy shows an oscillation around the set point. Through the H_∞ design, the oscillation magnitude is substantially reduced from 0.03 mm to 0.014 mm for the region near the setpoint $(y, v) = (0, 0)$. Hence, the effect of mitigating the friction model error is demonstrated by the proposed method.

4.4.2 Experiment

In this section, real-time experiments are carried out on an ultrasonic drive system to compare the performance of relay-PID and the suggested controller. The setup uses the PI M-663 with velocity limit 400 mm/s and travel range 19 mm. The sampling period for this test is chosen as 1 ms.

The commonly used relay-PID tuning is chosen to compare with the proposed method. In this experiment, the system model at $u = 3\,V$ is used for relay tuning to obtain a static PID gain

$$K_{pid} = \begin{bmatrix} 34.96 & 0.09674 & 1545.5 \end{bmatrix}. \tag{4.19}$$

While it may not offer the best PID tuning in all situations, relay-PID exhibits a large integrating factor to overcome the friction, thus achieving a fast rising time and zero-offset. These characteristics can be used to evaluate the performance of the MPC method Chen et al. [2009].

The gain-scheduling table from the simulation study is implemented intro dSPACE under a lookup table form with 23 regions where only matrix multiplication and comparison. This feasible form is computationally efficient for real-time implementation when compared to the traditional PID plus nonlinear feedforward. Additionally, in order to remove the error oscillation observed in the simulation studies, a dead band for the static friction force is imposed

$$f_c = \begin{cases} 0 & \text{if } |e| \leq \epsilon_1, \ |v| \leq \epsilon_2 \\ f_{cn} \text{ or } f_{cp} & \text{otherwise.} \end{cases} \tag{4.20}$$

The deadband could be implemented as a pre-condition prior to evaluating $u_k = \bar{u}_k + f_c$.

Tracking response of the two controllers for a square wave trajectory $f = 1\,Hz$, $A = 1\,mm$ is shown in Fig. 4.10. Fig. 4.10(a) shows that relay-PID creates an overshoot created about $0.5\,mm$ while the proposed controller produces no overshoot and achieves a settling time as short as the large-integrator PID. In Fig. 4.10(b) the actuator inputs are compared for the two cases. Relay-PID provides an excessive input higher than the actuator input threshold $[-9,9]$, while the new method has the input properly constrained. Next, we compare the low-speed compensation time in order to show the efficiency of adding modeling details of regions B and C. Both schemes depend on the PID setup to regulate the position

error at low speed. In the first controller, the input needs to overcome the unknown increasing friction force at low speed, so it takes some time to build up through the integral part. The fading-off signalizes the end of the compensation. In the opposite, the integrating part of the second controller only compensates for the small friction model mismatch, so it takes smaller time to overcome the friction with a pre-designed gain. Once $u \rightarrow 0$ ($f_c = 0$), the system state is in the deadband region which implies that the friction uncertainty around the stationary point has been compensated. This performance satisfies performance specification mentioned earlier in the Section 4.1. Finally, the saving on control effort per cycle is measured as $\frac{E_2}{E_1} = \frac{u_{MPC}^2}{u_{PID}^2} = 77.12\%$. Note that this measurement is only calculated from the setpoint change time to the end of low speed compensation. This is to ensure a fair comparison in case a deadband for PID input is also implemented.

4.5 Conclusion

This chapter has suggested a simplified scheme to deal with friction nonlinearity. A dual-stage linear model identification was used to describe the friction, thus easing the effort to choose which friction model to be applied. A robust MPC method was developed for compensation of friction, mitigating the model mismatch near zero speed. Simulation and experimental results have shown that the proposed compensation technique can overcome the limitations of the relay-PID tuning and keep the system under constraints, while attaining a simple real-time implementation.
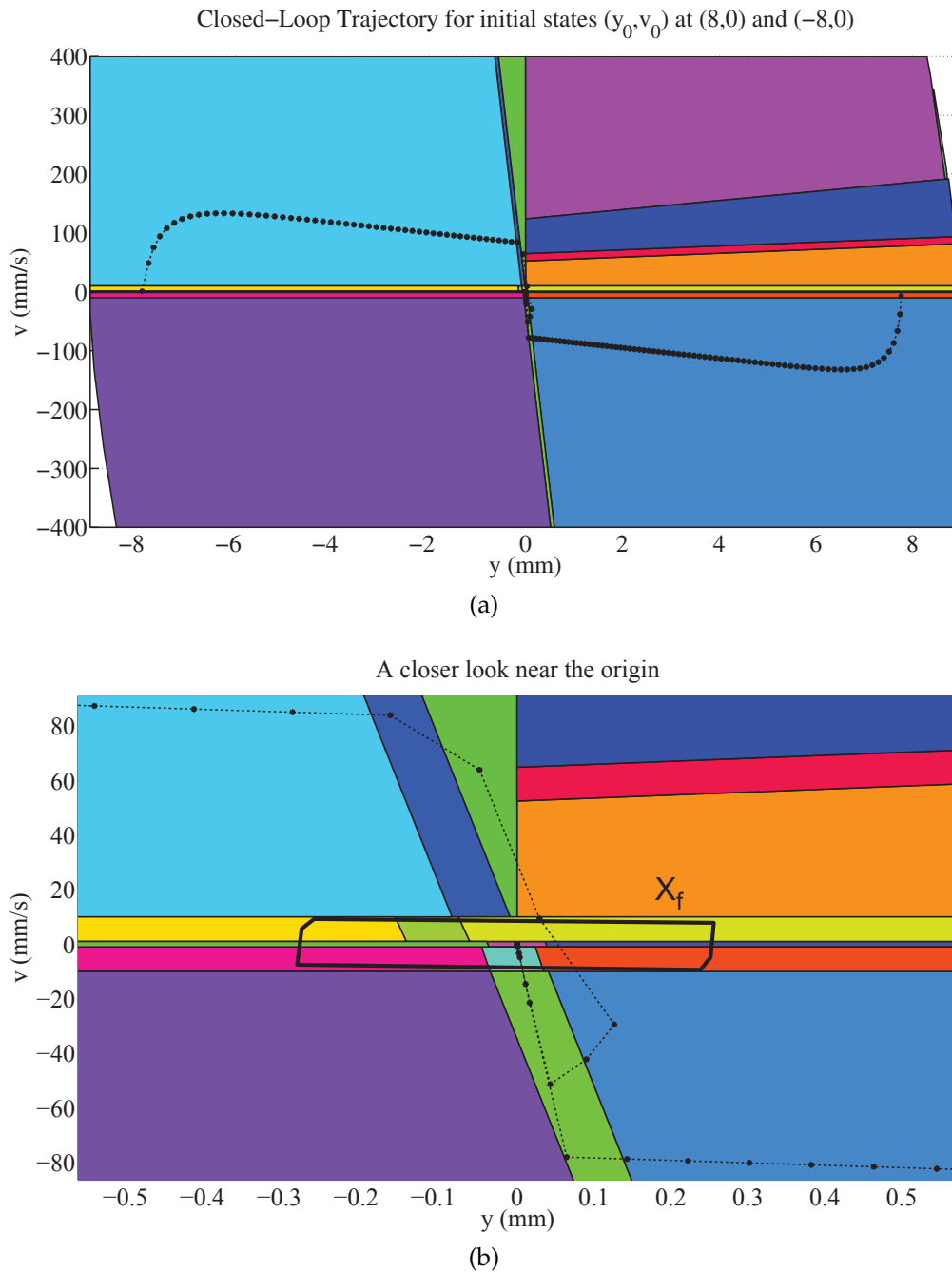
Figure 4.8: Tuning MPC weighting matrices by Nguyen et al. [2011] on the outer model $\{A_1, B_1\}$. Trajectory is projected on (y, v) space.
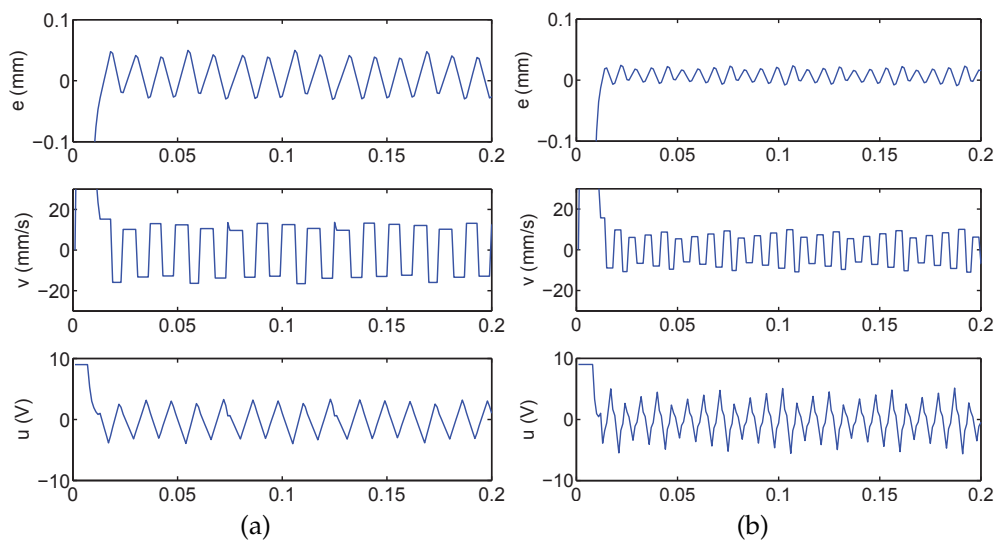
Figure 4.9: Simulated output errors with friction model mismatch for (a) LQR MPC design and (b) proposed robust MPC.
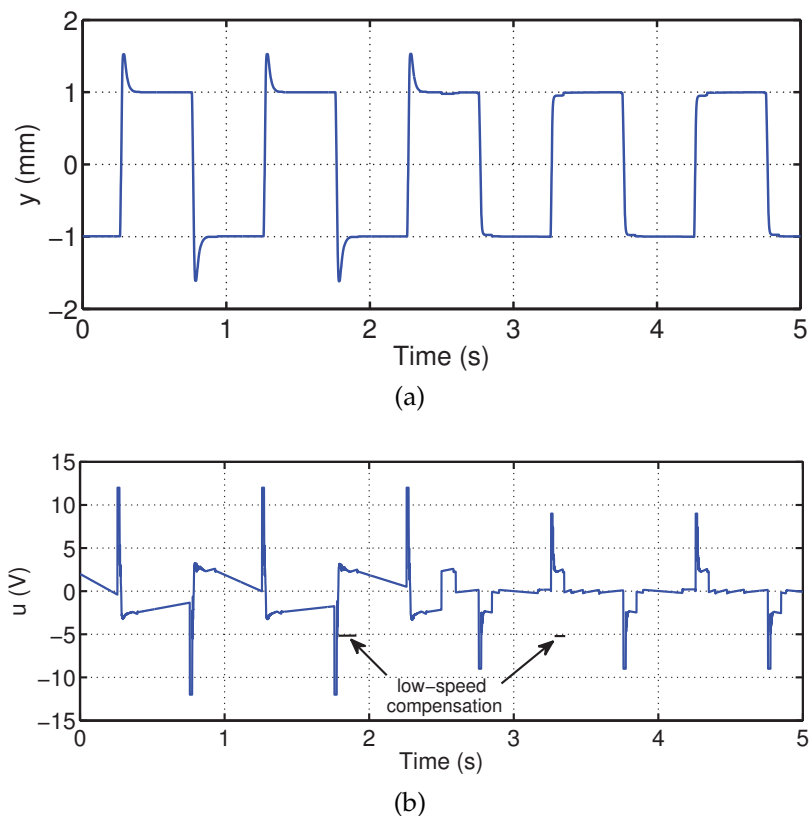
Figure 4.10: Experiment results when comparing relay-PID (before) and the proposed method (after). The transition is at $t = 2.5\,s$.

Chapter 5

Intelligent Control of In-vitro Fertilization Medical Systems

In-vitro fertilization (IVF) and related technologies are arguably the most challenging of all cell culture applications. This chapter introduces an integrated mechatronic solution for oocyte retrieval procedure before the oocytes are further put into laboratory processing during IVF treatment. It facilitates the surgery operation and addresses the temperature inaccuracy of follicular fluid during the transfer to the patients body. The mechanical design is implemented into a medical-standard conforming platform. An accurate temperature estimation and optimization scheme are proposed. Comparison before and after the introduction of the new prototype under various operating conditions reveals a significant improvement in performance. This yields a potential application for the medical/healthcare industry.

5.1 Introduction

In Vitro Fertilization (IVF) has gained much attention in the medical/healthcare industry as a major treatment for infertility in which one aims to produce an embryo capable of establishing a pregnancy eventually leading to a live birth. To obtain the initial oocytes from female bodies, doctors often flush follicular media before aspirating follicles, especially in the case of minimal stimulation IVF where the number of follicles is few [Hill and Levens, 2010; Lozano et al., 2008]. The retrieved oocytes are transferred to laboratories for fertilization and vitro culture. Surgery operation and laboratory processing during IVF treatment requires open ma-

nipulations of oocytes and embryos, which typically involves exposure to ambient conditions. While these cells can survive minor variations in culture conditions, they are very sensitive to changes in temperature. Protection from ambient conditions can reduce stress-induced cellular responses, thus promotes the success rate of IVF procedure [Sherbahn, 2010; Xie et al., 2008].

For laboratory cell processing, researchers has devised integrated, enclosed platforms to minimize the environment effect. A microrobotic cell convoying device was presented [Boukallel et al., 2007] to transfer cells between biomedical components. A method for controlling the culture environment of individual cells without is introduced [Kimura et al., 2009]. Recently, an isolator-based system for human embryos is reported in Hyslop et al. [2012] to increase a quarter the chance of IVF success.

For surgery operation i.e. the oocyte retrieval procedure, several commercial solutions are reported in Levens et al. [2009], Steiner [2011] to improve the viability of these essential cells. In Levens et al. [2009], the design is made by Cook Medical; they invent an oocyte retrieval system with on/off temperature control module. Another design is proposed in Steiner [2011] whereby the author suggested to use a syringe warmer, named the Steiner device, to maintain a constant desirable medium temperature. These existing designs feature unmodeled interactions between the heating bar, the medium and the environment, thus may reduce the overall egg retrieval success rate.

In this chapter, we propose the first integrated prototype for IVF egg retrieval systems. The control of IVF flushing and aspiration units are combined and consisted of two parts: the supervisory controller and the temperature optimizer. The supervisory controller directs the program flow with programmable logic control (PLC) to avoid undesirable human mistakes, and records flushing and aspiration rates. The temperature optimizer manipulates a heater to warm up the syringe during flushing process. This combined design provides a more convenient operation.

Solving the problem of medium temperature inaccuracy, caused by the unmodeled process and the operation in various conditions, is the second contribution. The thermal dynamics among the flushing fluid, the heating bar and air temperature is modeled, and an observer is built
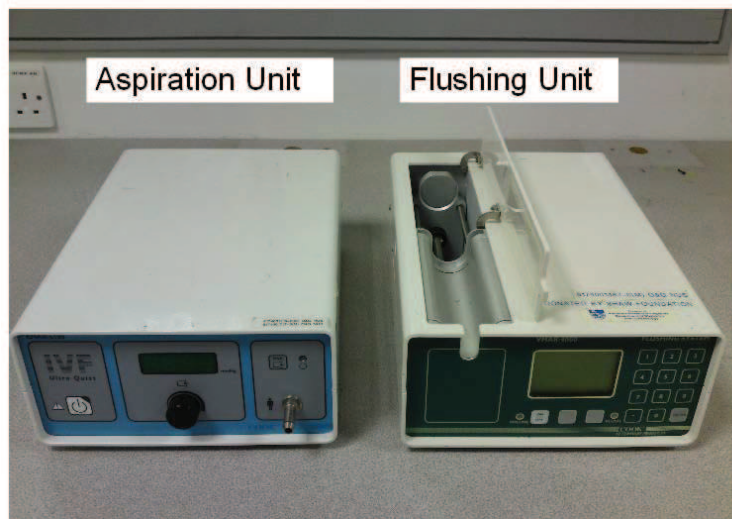
Figure 5.1: A former version of flushing and aspiration units.

to estimate the fluid temperature inside the syringe. Temperature drop
along the transfer tube is also estimated based on various operating con-
ditions (environment temperature and flushing speed) to compensate in
the optimizer. From the control aspect, model predictive control (MPC)
is suggested to replace the current on/off method. MPC is an advance
process control widely accepted in the academia and implemented in
many industrial areas [Froisy, 2006; Li et al., 2012; Qin and Badgwell,
2003]. Besides, robust predictive control has been proposed in supervi-
sory control frameworks [Wang, 2011; Zheng et al., 2011]. It provides a
more precise control of the medium temperature.

The following sections describe in greater details the design and test-
ing procedure. The existing problems of the current design are described
in section 5.2. The system architecture and thermal modeling for this
specific problem is then presented. Design of state estimation and the
MPC algorithm used in the temperature optimizer are introduced in Sec-
tion 5.4. Section V provides testing results where the new performance
is compared with that of an old design.

5.2   Problem Statements

The traditional design involves more human action during the IVF pro-
cess. By using two separate devices (Fig. 5.1), it gives unnecessary
inconvenience and prolongs the operation time on patients. Therefore
a compact, uniformed design is preferred to automate the IVF sequence.

This design must allow the control of procedure flow and avoid undesirable system states that are possibly caused by human errors.

Another pitfall of the current design is the inaccurate estimation and control of flushing fluid temperature. The flushing procedure contains two steps: heating and transferring. For that reason, the temperature of fluid inside the syringe must be heated to above $37\,^{\circ}C$ to account for the temperature drop along the transfer path. However, this temperature drop is dependent on the operating conditions: the air temperature and the transfer speed. By intuitively setting the heating bar temperature (e.g. $38\,^{\circ}C$) without the real-time information of fluid temperature, the fluid temperature error coming out from the needle can deviate $1\,to\,2\,^{\circ}C$ below the setpoint $37\,^{\circ}C$.

The uncertainty in operating conditions is the first cause of the above error. It is assumed that the fluid temperature has a similar dynamic with the metallic heating bar temperature, so only the holder temperature is measured and controlled with simple methods (on/off). This assumption has to be made because direct installation of a temperature sensor inside the syringe is impracticable. In reality, the syringe design exposes itself to the air and the dynamic of fluid temperature model is much slower than the metallic bar. In addition, the temperature drop along the transfer tube is also dependent on the air temperature. It relies on user experience to compensate for this offset, usually through adjusting the heating bar temperature in advance. Hence, thermal modeling involved key factors such as transfer speed and air temperature is required.

On another aspect, due to the on/off feature with modeled delay, the existing controller has two disadvantages. It trades off the accuracy with the settling time, causing ripples in the temperature output. The heater wear problem also persists from on/off constant cycling.

5.3 System Construction and Modeling

5.3.1 System Construction

The constructed IVF platform consists of five parts labeled with A, B, C, D and E shown in Fig. 5.2. The interface A displays the operating parameters specified by users and the system state. The stepper motor B, which has position and forward speed tracked by pulse signals, pushes

5. INTELLIGENT CONTROL OF IN-VITRO FERTILIZATION MEDICAL SYSTEMS
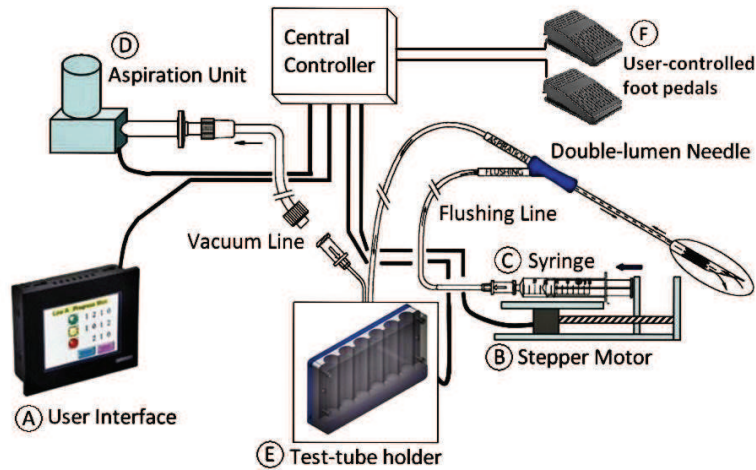
Figure 5.2: IVF integrated platform.

the syringe C and drives the medium into the flushing line and to the patient's body through a double-lumen needle. A heater pad is adhered on the syringe holder to control the temperature of flushing medium while feedback data is obtained by RTD PT100 sensors which meet industrial standards [Tan et al., 2008]. The aspiration pump D can work on variable speeds for egg retrieval and transfer eggs to test tubes E, which are maintained at $37\,^\circ C$. The user controls the start/stop of the flushing and aspiration by the two foot pedals F.

The flushing part is detailed in Fig. 5.3. Because the stepper motor is quite accurate, open-loop control is used to control the transfer speed. On the other hand, temperature control is done through the attached heater mat and feedback signals from PT100s. Since RTD-type PT100s output a nonlinear function

$$R_T = R_0(1 + aT + bT^2 + c(T - 100)T^3), \tag{5.1}$$

the analog conversion circuit in Fig. 5.3b is designed to linearize the output. The other I/O devices can directly interface with PLC through D/A channels.

Architecture of the integrated control design is shown in Fig. 5.4. A programmable logic controller (PLC) works in a low-level layer, directing the IVF oocyte retrieval procedure and automatically closing simple control loops (flushing rate, aspiration rate). It acquires system data and sends these information to a supervisory program. This program also receives inputs from users, and monitors the current system status. A
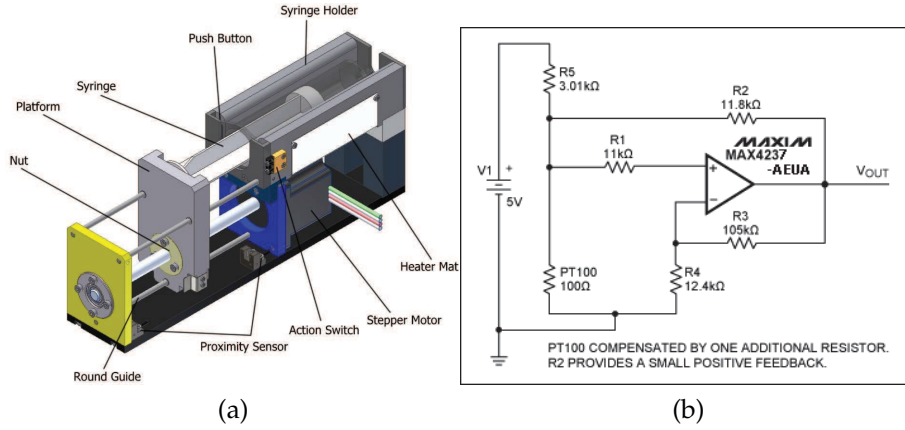
Figure 5.3: Mechatronic design. (a) The syringe holder design and (b) PT100 linearization circuit.

temperature control module collects the operating data from the supervisory system and uses MPC to provide an optimal input for the heater.

5.3.2 Temperature Modeling

In this section, fluid thermal model is studied from first-principles and the parameters are then derived from collected data. This model is dependent on ambient temperature and flushing velocity, thus information about these variables is important. In Fig. 5.5, the system is divided into heating segment and transfer segment. Temperature sensors I, II, III and IV are set up at the heating bar, inside syringe, in open air and at the end of the transfer tube, respectively.

Assumptions about the targeted thermal systems are made to simplify differential heat equations [Boglietti et al., 2008; Veluvolu and Soh, 2009]. Based on this assumption, lumped analysis on the thermal dynamic of individual objects can follow.

Assumption 2 *The temperature along the heating bar, the transfer tube and within fluid body inside the syringe are uniformly distributed.*

The heating system dynamics, analyzed at each time instant, can be captured as

$$
\begin{aligned}
\frac{dT_1}{dt} &= \frac{T_1 - T_2}{R_1} + \frac{T_1 - T_a}{R_{1a}} + bu(t - d) \\
\frac{dT_2}{dt} &= \frac{T_2 - T_1}{R_2} + \frac{T_2 - T_a}{R_{2a}},
\end{aligned}
\tag{5.2}
$$

5. INTELLIGENT CONTROL OF IN-VITRO FERTILIZATION MEDICAL SYSTEMS
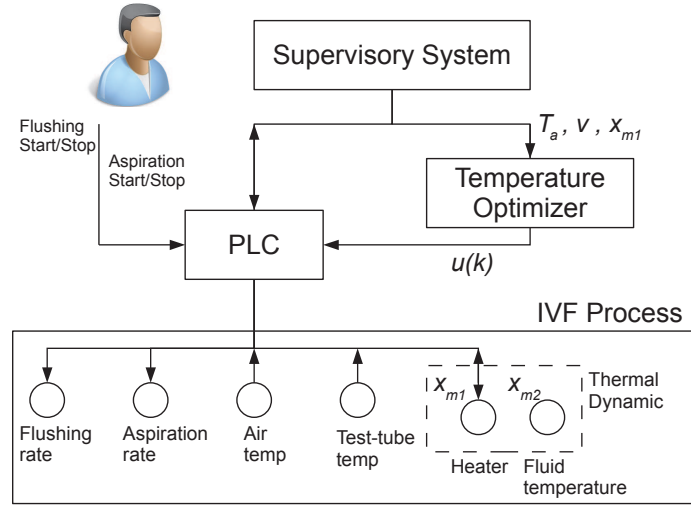
Figure 5.4: System control design.

where T_1, T_2, T_a are the heater, fluid and surrounding temperatures; R_1, R_2, R_{1a}, R_{2a} are thermal resistances between objects, u ($0 \leq u \leq 1$) represents the heater input with limited power (25W), d is the input delay.

For the transfer part, consider a small fluid portion f running through the tube of length L starting from $t_0 = 0$, such that $T_f(0) = T_2$, $T_f(L) = T_{end}$. The heat loss from internal energy of this portion at time t is

$$mc_p \frac{dT_f}{dt} = \frac{T_f - T_a}{R_e},$$

$$\int_{T_2 - T_a}^{T_{end} - T_a} \frac{d(T_f - T_a)}{T_f - T_a} = \frac{t_L}{mc_p R_e},$$

$$\frac{T_{end} - T_a}{T_2 - T_a} = e^{-\frac{L}{vmc_p R_e}} = \eta. \tag{5.3}$$

Here, the temperature loss rate $\eta < 1$ is a constant for any fixed transfer velocity v and constant environment temperature T_a.

Define the object temperatures *above* ambient air as state variables i.e. $x_{mi} = T_i - T_a$ $(i = 1, 2)$, $y_m = T_{end} - T_a$. A second-order state space model from equation (5.2),(5.3) is formed

$$x_m(k + 1) = A_m x_m(k) + B_m u(k - d)$$

$$y_m(k) = C_m x_m(k)$$

$$z_m(k) = \begin{bmatrix} 1 & 0 \end{bmatrix} x_m(k), \tag{5.4}$$

where y_m is the controlled fluid temperature at the end of the transfer
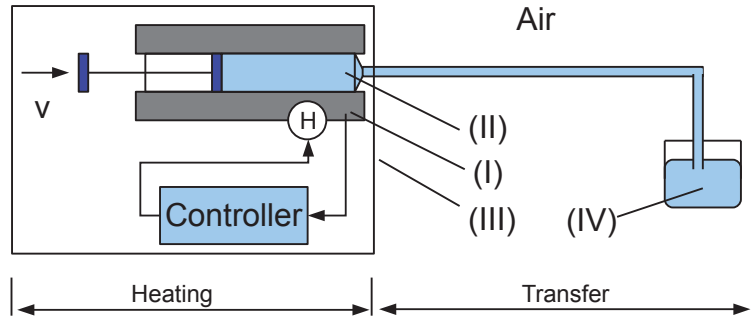
Figure 5.5: Flushing modeling.

tube, z_m is the heating bar temperature, A_m, B_m presents the transfer function from input to state, $C_m = [0 \quad \eta]$ shows the temperature drop ratio through the transfer tube ($\eta = \frac{y_m}{x_{m2}}$). From the heat flow equality, the system is thermally stable.

Parameters in model (5.4) are identified as time-invariant to avoid the nonlinear dependence of (5.2) on the syringe position. Two identification steps are performed for heating and transferring parts. In the former part, prediction error method (PEM) [Ljung, 2002], surveyed in Mercere and Bako [2011]; Reinelt et al. [2002], is used since it will give a good state prediction for MPC. The model is represented as a linear predictor of future output of the system $\hat{y}(k) = \theta^T \varphi(k)$ (θ: parameters, φ: past data). The data is collected from sensors I, II and III. The parameter θ is chosen such that the prediction error has as small variance as possible. In the latter part, temperature drop ratio is recorded by sensors II and IV, measured under different conditions (Table 5.1).

Remark 7 *Sensors II and IV are installed for modeling purpose. In real application, only sensors I and III are employed.*

The thermal models built here is to facilitate the temperature estimation and control in the next section.

5.4 Estimation and Control for Fluid Temperature

As mentioned in the introduction, aside from an innovative design for the IVF devices, this chapter seeks to accurately estimate and control the temperature of flushing medium. The main purpose is to ensure

the follicular fluid, after going through the transfer tube, emerges with a temperature of $37°\ C$ before it enters a human body. This is to avoid any temperature shock harmful to the follicles.

5.4.1 Temperature Estimation

Compared to the common used Kalman filter, sliding mode observers has the advantages of being insensitivity to external noise and having robustness to parameter uncertainty. It is also much simpler to implement and no knowledge of the noise statistics is required (room temperature, time-variant model).

A sliding mode observer (SMO) is used to estimate the state at the present time k from which the future state is subsequently predicted. These observers have attractive measurement noise resilience that is similar to a Kalman filter [Sabanovic, 2011; Veluvolu and Soh, 2009]. The goal is to design a high-gain state observer that estimates the state vector x_m using only information from the measurement $z_m = x_{m1}$ of sensor I.

Choose the switching function $\sigma = \hat{x}_{m1} - x_{m1}$. The sliding observer with a gain $L = \begin{bmatrix} -l_1 & l_2 \end{bmatrix}^T$ is formulated as

$$\hat{x}_m(k+1) = A_m\hat{x}_m(k) + B_mu(k-d) + Lsgn[\hat{x}_{m1}(k) - x_{m1}(k)], \quad (5.5)$$

then

$$e_m(k+1) = A_me_m(k) + Lsgn\ \sigma(k). \quad (5.6)$$

where $e_m = \hat{x}_m - x_m$ is the estimation error.

Reaching toward $\sigma = 0$ is assured in finite time since $sgn\ \sigma(k)$ is a discrete step. For the sliding along the surface, it requires to have

$$0 > \sigma(k+1)\sigma(k)$$
$$= [a_{11}e_{m1}(k) + a_{12}e_{m2}(k) - l_1sgn\ \sigma(k)]\ \sigma(k). \quad (5.7)$$

where a_{ij} are components of A_m. Assume the estimation error is bounded. Choose

$$l_1 > \|a_{11}e_{m1}(k) + a_{12}e_{m2}(k)\|_\infty, \quad (5.8)$$

so that the condition (5.7) satisfies.

Next, the asymptotic stability of e_{m2} must also be guaranteed. Note

that the sliding along $\sigma = 0$ means

$$\begin{cases} e_{m1}(k) = 0, \\ e_{m1}(k+1) = 0 \overset{(5.6)}{\Rightarrow} l_1 sgn\, \sigma(k) \overset{eqv}{=} a_{12}e_{m2}(k). \end{cases} \qquad (5.9)$$

Now, from (5.6)

$$\begin{aligned} e_{m2}(k+1) &= a_{22}e_{m2}(k) + l_2 sgn\, \sigma(k) \\ &\overset{eqv}{=} (a_{22} + (l_2/l_1)a_{12})e_{m2}(k) \end{aligned} \qquad (5.10)$$

Hence, l_2 must be chosen such that $|a_{22} + (l_2/l_1)a_{12}| < 1$.

In summary, the gain L is designed such that its amplitude *encompasses* the noise and model uncertainty, as well as ensure the convergence of (5.5) to the real state. An additional low pass filter (e.g. $\hat{x}_r = \frac{1}{2}\hat{x}_m(k+1) + \frac{1}{2}\hat{x}_m(k)$) can be implemented to avoid the chattering effect.

5.4.2 Stabilizing MPC

The specific methodology described in this chapter was inspired by Rawlings and Muske [1993]. It is shown that the infinite-horizon constrained optimal problem can be transformed to a finite-horizon receding control problem with a suitable terminal cost. Stability property is thus retained from the linear quadratic regulator (LQR) method.

Augment (5.4) under the velocity form [Ling et al., 2011] to include the integral of x_{m2}

$$\begin{aligned} x(k+1) &= Ax(k) + B\Delta u(k-d) \\ y(k) &= Cx(k), \end{aligned} \qquad (5.11)$$

where $A = \begin{bmatrix} A_m & 0 \\ [0\ 1]A_m & 1 \end{bmatrix}$, $B = \begin{bmatrix} B_m \\ [0\ 1]B_m \end{bmatrix}$, $C = \begin{bmatrix} 0 & 0 & 1 \end{bmatrix}$.

Assumption 3 *The control movements outside the control horizon is zero i.e.* $\Delta u(k+i) = 0$ *for* $i \geq N$.

For this application, the open-loop optimal problem that solves con-

5. INTELLIGENT CONTROL OF IN-VITRO FERTILIZATION MEDICAL SYSTEMS
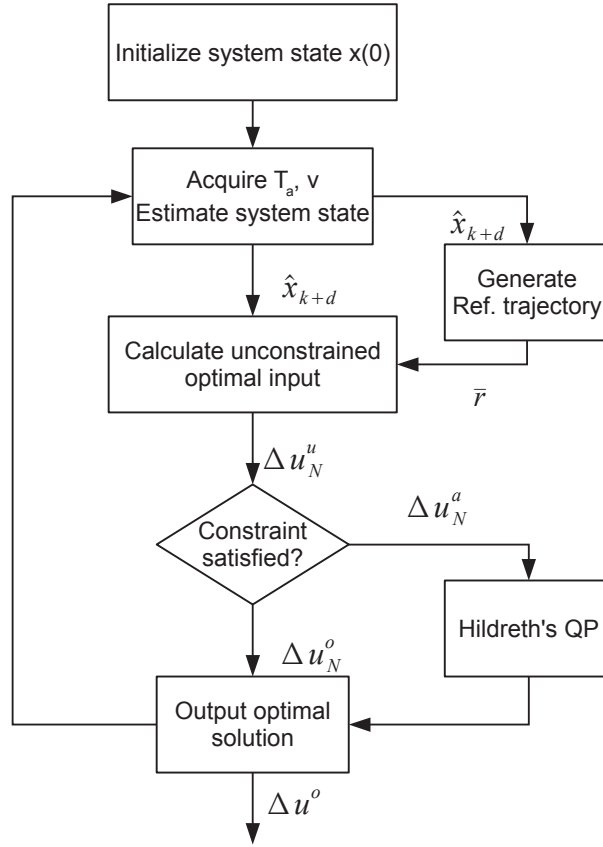
Figure 5.6: The algorithm of the temperature optimizer.

trol sequence $\Delta u_N = \{\Delta u(k+i)\}_{i=0}^{N-1}$ at every time step k is to minimize

$$J(\Delta u_N) = \sum_{i=0}^{\infty} \left[Qe(k+d+i)^2 \right] + \sum_{i=0}^{N-1} \left[R\Delta u(k+i)^2 \right]$$

subj. to (5.11) *holds*

$$M\Delta u_N \leq \gamma, \tag{5.12}$$

with P_0 the positive definite solution of the Riccati equation $P_0 = Q + A^T[P_0 - P_0B(B^TP_0B + R)^{-1}B^TP_0]A$ and the output error $e = r - y$. The first-order reference trajectory $\mathbf{r} = \{r_i\}_{i=k}^{\infty}$ is defined by

$$r(i) = \begin{cases} y(k), & \text{for } i = k \\ \alpha r_0 + (1 - \alpha)r(i-1), & \text{for } k < i < k + N \\ r(i-1), & \text{for } i \geq k + N. \end{cases} \tag{5.13}$$

Remark 8 *The reference must be feasible within N steps with the presence of input constraint. Firstly, $N = N_o$ is fixed to restrict calculation complexity. α_o*

is then chosen to satisfy Assumption 3 and maximize output response rate at all steps k.

The optimal control sequence Δu_N^o for problem (5.12) can be calculated in two steps, the unconstrained optimal control plus an active constraint adjustment [Wang, 2009]

$$\Delta u_N^o = \Delta u_N^u + \Delta u_N^a. \tag{5.14}$$

Unconstrained solution

Since A is stable, define $K = \sum_{j=0}^{\infty} A^{T^j} C^T Q C A^j$ and feedforward terms

$$\beta_i = \sum_{j=1}^{i} A^{T^{j-1}} C^T Q(r(k+N) - r(k+j))$$

$$for\ i = 1, \dots, N-1 \tag{5.15}$$

$$\beta = r(k+N) \sum_{j=0}^{\infty} A^{T^j} C^T Q. \tag{5.16}$$

Proposition 7 *The cost function J can be rewritten under a standard quadratic form as*

$$J(\Delta u_N) \ = \ \Delta u_N^T E_N \Delta u_N + \Delta u_N^T F_N \tag{5.17}$$

in which

$$E_N = \begin{bmatrix} B^T K B + R & \dots & B^T A^{T^{N-1}} K B \\ B^T K A B & \dots & B^T A^{T^{N-2}} K B \\ \vdots & \ddots & \vdots \\ B^T K A^{N-1} B & \dots & B^T K B + R \end{bmatrix}, \ F_N = B_N^T (G_N A x(k+d) - R_s)$$

where

$$B_N = \begin{bmatrix} B & \dots & 0 \\ \vdots & \ddots & \vdots \\ 0 & \dots & B \end{bmatrix}, G_N = \begin{bmatrix} K \\ \vdots \\ K A^{N-1} \end{bmatrix}, \ R_s = \begin{bmatrix} \beta - \beta_{N-1} & \dots & \beta \end{bmatrix}^T.$$

Proof 5 *Denoting the stacked output and input vectors $Y, \Delta u_N$ for equation*

5. INTELLIGENT CONTROL OF IN-VITRO FERTILIZATION MEDICAL SYSTEMS

(5.11) *over the prediction horizon N_p ($N_p \to \infty$), we have*

$$
Y = \begin{bmatrix} CA \\ \vdots \\ CA^{N_p} \end{bmatrix} x(k+d) + \begin{bmatrix} CB & \cdots & 0 \\ \vdots & \ddots & \vdots \\ CA^{N_p}B & \cdots & CA^{N_p-N}B \end{bmatrix} \Delta u_N
$$
$$
= M_1 x(k) + M_2 \Delta u_N. \tag{5.18}
$$

With $Q_{N_p} = diag(Q, ..., Q), R_N = diag(R, ..., R)$, the cost function J in (5.12) *becomes*

$$
\begin{aligned}
J &= (Y - \mathbf{r})^T Q_N (Y - \mathbf{r}) + \Delta u_N^T R_N \Delta u_N \\
&= \Delta u_N^T \left(M_2^T Q_N M_2 + R_N \right) \Delta u_N \\
&\quad + \Delta u_N^T M_2^T Q_N (M_1 x(k) - \mathbf{r})
\end{aligned} \tag{5.19}
$$

As defined in Proposition 7, E_N could be simplified by

$$
\begin{aligned}
E_N &= M_2^T Q_N M_2 + R_N \\
&= \begin{bmatrix} B^T K B + R & \cdots & B^T A^{T^{N-1}} K B \\ \vdots & \ddots & \vdots \\ B^T K A^{N-1} B & \cdots & B^T K B + R \end{bmatrix}.
\end{aligned} \tag{5.20}
$$

Similarly,

$$
\begin{aligned}
F_N &= M_2^T Q_N (M_1 x(k) - \mathbf{r}) \\
&= \begin{bmatrix} B^T C^T & \cdots & B^T (A^T)^{N_p} C^T \\ \vdots & \ddots & \vdots \\ 0 & \cdots & B^T (A^T)^{N_p - N} C^T \end{bmatrix} \cdot \begin{bmatrix} Q & & \\ & \ddots & \\ & & Q \end{bmatrix} \cdot \left(\begin{bmatrix} CA \\ \vdots \\ CA^{N_p} \end{bmatrix} - \begin{bmatrix} r(k+1) \\ \vdots \\ r(k+N_p) \end{bmatrix} \right) \\
&= B_N^T \left(\begin{bmatrix} KA \\ \vdots \\ KA^N \end{bmatrix} - \begin{bmatrix} \sum_{j=0}^{\infty} A^{T^j} C^T Q r(k+j+1) \\ \vdots \\ \sum_{j=0}^{\infty} A^{T^j} C^T Q r(k+j+N) \end{bmatrix} \right) \\
&= B_N^T \left(\begin{bmatrix} K \\ \vdots \\ KA^{N-1} \end{bmatrix} A - \begin{bmatrix} \beta - \beta_{N-1} \\ \vdots \\ \beta \end{bmatrix} \right) \\
&= B_N^T \left(G_N A - R_s \right). \tag{5.21}
\end{aligned}
$$

The results in Proposition 7 follows from (5.20) *and* (5.21).

The solution to the quadratic problem without constraints is easily determined by

$$\Delta u_N^u = -E_N^{-1} F_N. \tag{5.22}$$

Constraint handling

Suppose the knowledge of active constraints in Δu_N^u is unavailable. A simple way to impose the constraint (5.17) on Δu_N^u is given below.

Lemma 8 (Hildreth QP procedure) *For the QP problem* (5.12), *the optimal Lagrange multiplier vector λ^* would converge through an iterative update in a single component basis* $(i = 1, \ldots, dim(\gamma))$

$$\gamma_i^{m+1} = max(0, \omega_i^{m+1})$$
$$\omega_i^{m+1} = -\frac{1}{h_{ii}} \left[k_i + \sum_{j=1}^{i-1} h_{ij} \gamma_j^{m+1} + \sum_{j=i+1}^{i-1} h_{ij} \gamma_j^m \right], \tag{5.23}$$

where $H = M E_N^{-1} M^T$, $K = \gamma + M E_N^{-1} F_N$. The constrained complement for the optimal solution would be

$$\Delta u_N^a = -E_N^{-1} M^T \lambda^*. \tag{5.24}$$

Therefore the algorithm calculates Δu_N^u and verifies the constraints in (5.12). If necessary the Hildreth's algorithm can follow up to provide the constrained solution Δu_N^o.

Lastly, the receding horizon policy applies only the first input command from the optimal solution Δu_N^o, so $\Delta u^o(k) = \underbrace{[1 \ 0 \ \ldots \ 0]}_{N} \Delta u_N^o$.

The overall MPC control scheme is summarized in the block diagram of Fig. 5.6. To facilitate the implementation, the feedforward gain in (5.15) and the MPC gains in (5.22) are all determined *off-line*.

5.5 Experiments

The efficient design in Section 5.3-A is implemented in Fig. 5.7. The mechanical design of both flushing and aspirating operations are integrated into the prototype. The supervisory control and the temperature
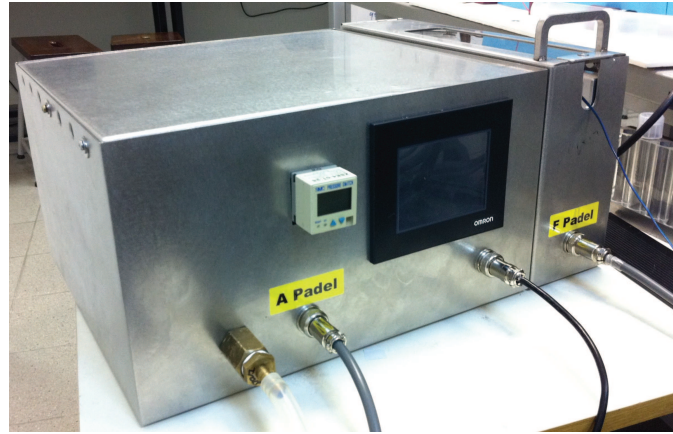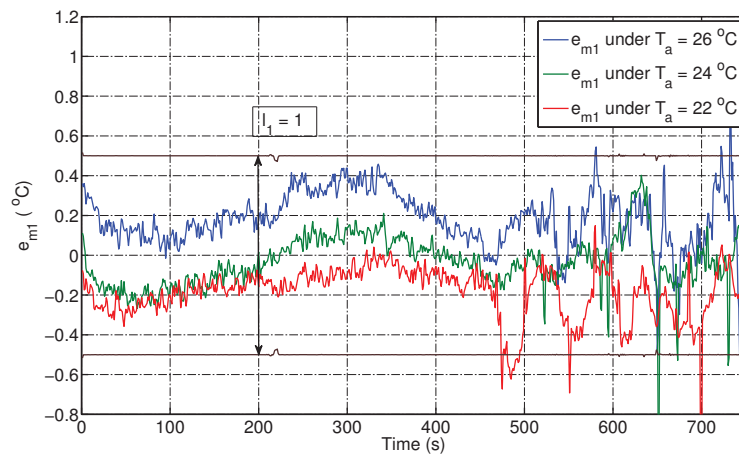
Figure 5.7: The proposed prototype.

(a)
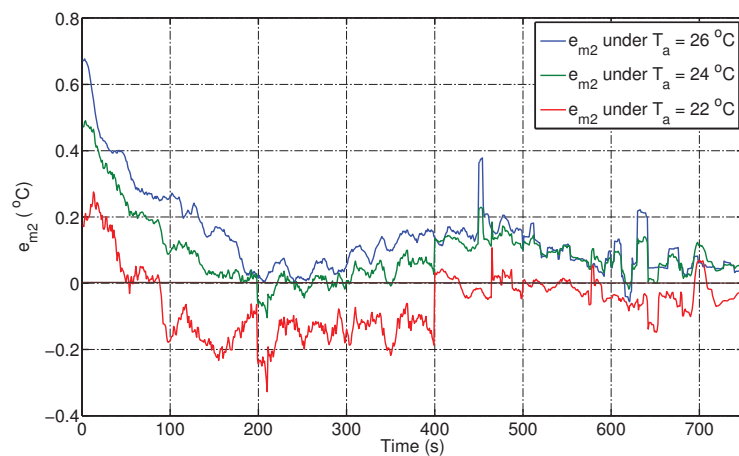
(b)

Figure 5.8: State estimation error of the SMO (a) e_{m1} and (b) e_{m2}.

optimizer are implemented on LABVIEW in a 3.4 GHz computer, which
interfaces with the PLC controller of the prototype through a NI DAQ

5. INTELLIGENT CONTROL OF IN-VITRO FERTILIZATION MEDICAL SYSTEMS

Table 5.1: Temperature drop ratio under different operating conditions

Temperature drop rate η	Transfer velocity (mL/s)				
	0.1	0.2	0.3	0.4	0.5
22	0.7952	0.8600	0.8920	0.9148	0.9308
Air temperature (°C) 24	0.8400	0.9028	0.9296	0.9540	0.9656
26	0.8560	0.9172	0.9552	0.9696	0.9788

card.

The discrete model of fluid temperature is based on the PEM identification method described in Ljung [2007]. High precision RTD PT100 (class A) sensors with accuracy $\pm 0.2° C$ are used at the locations I, II, IV, while an $\pm 0.5° C$ thermocouple sensor III measures the air temperature. From the collected data, the nominal parameters are identified as

$$A_m = \begin{bmatrix} 0.9981 & 0.00112 \\ 0.001148 & 0.99881 \end{bmatrix}, B_m = \begin{bmatrix} 0.049205 \\ 0 \end{bmatrix}, C_m = \begin{bmatrix} 0 & \eta \end{bmatrix},$$

with the temperature loss rate η recorded in Table 5.1 and the input delay $d = 12s$. The input constraint is $0 \leq u \leq 1$. A sampling time $t_s = 1s$ is chosen.

The estimation gain and the controller parameters follows from the analysis in Section 5.4. The sliding mode observer is designed with a gain $L = [-1\ 0.2]^T$. The MPC controller has a control horizon $N = 10$, reference factor $\alpha = 0.995$, weighting matrices $Q = I_{2\times2}, R = 0.015$. By using LABVIEW to check the real-time execution of the proposed controller, $t_{exe} \approx 0.012s$ satisfies the time constraints t_s.

Three experiments are carried out to test the performance of the proposed design.

In the first experiment, the accuracy of temperature estimation is examined, since it causes inaccurate temperature control. Within the heating dynamics, the only uncertainty affects the thermal model is the air temperature T_a. Hence, under different cases $T_a = 22, 24, 26° C$ the estimation accuracy is shown in Fig. 5.8. From the figure, it can be inferred that the estimation slides along the surface $e_{m1} = 0$ at all time (e_{m1} stays inside the tube), and the error e_{m2} converges asymptotically to zero once the sliding surface is reached.

The second experiment studies the performance of the following three designs under nominal condition: the commercial design with on/off
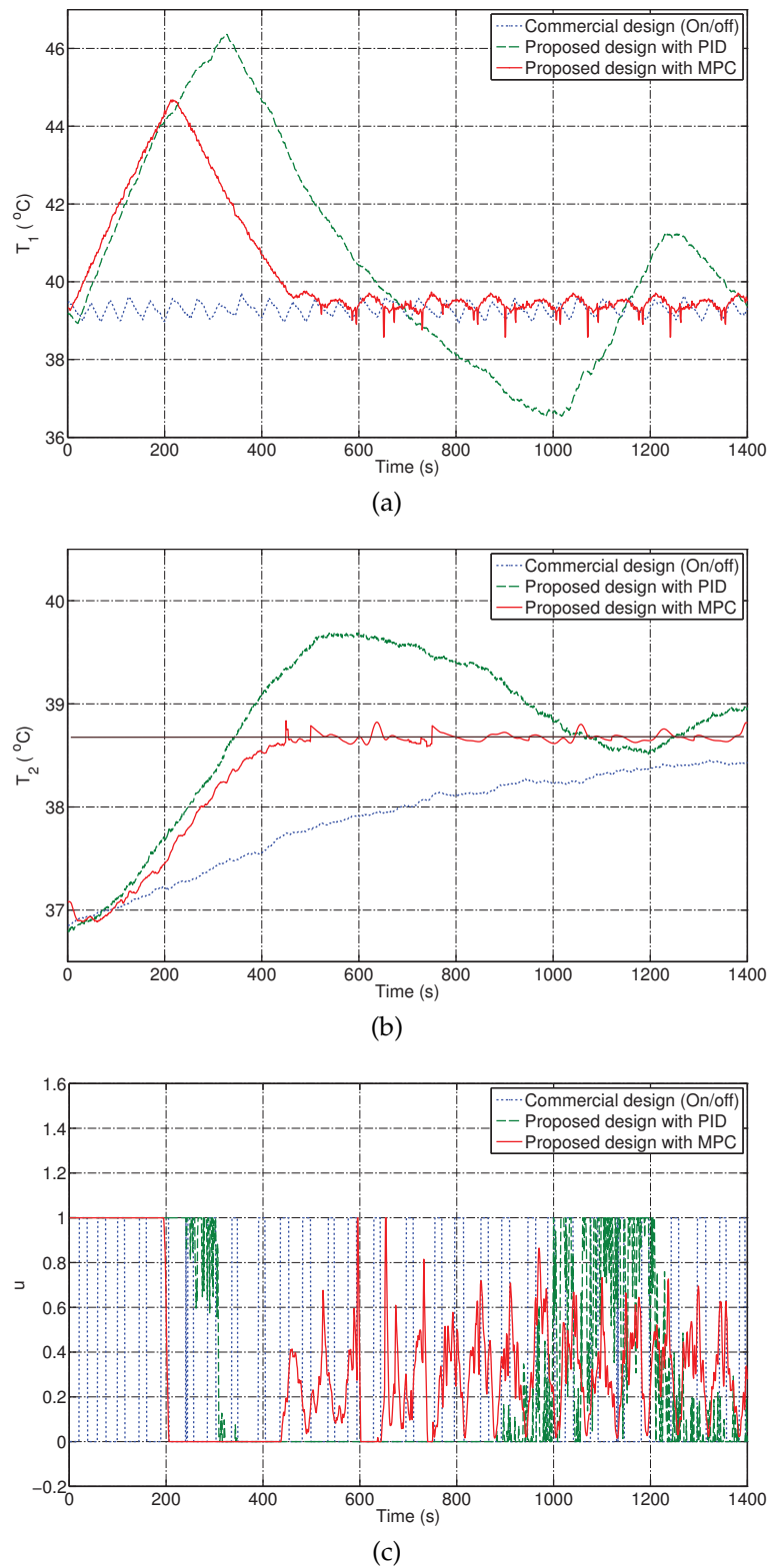
Figure 5.9: Comparison on state response and control input of the three
designs.

control, the proposed prototype with PID control and with a MPC controller. The objective is to prove that MPC performance is the right choice to replace on/off control. The fluid temperature inside syringe is shown in Fig. 5.9. For the commercial design, x_{m1} is maintained and x_{m2} converges to its setpoint $(37/\eta)°C$ in a very slow process because it targets the heating bar temperature. A PID controller with Smith predictor can be tuned in various ways. In order to give an effective comparison, a high gain tuning which produces a comparable response time to MPC is chosen. Due to the input constraint $u \geq 0$, the heater temperature at $t = 320s$ can not be decreased faster than a certain rate, resulting in a large overshoot for fluid temperature inside syringe. Compared with PID, MPC gives an early-stop input because of the first-order reference. Less oscillation and overshoot are observed. The settling time for fluid temperature of MPC is within $500s$, shorter than that of PID. Note that a low gain PID tuning could give a more accurate output, but it would give a slower settling time compared to MPC.

The third experiment shows that the proposed design can overcome the uncertainties in operating conditions. It tests the performance of on/off, PID and MPC controllers across various operating conditions which causes temperature inaccuracy in the commercial design.

Under the same environment temperature $T_a = 22 °C$, common settings of transfer speed are chosen $v = 0.1, 0.2, 0.3, 0.4, 0.5 \ (mL/s)$. It is shown in Fig. 5.11a that when the exposure time of the fluid to the external environment becomes shorter, the accuracy is improved for on/off and MPC methods because there is less uncertainty. On the other hand, shorter exposure time reduces the cooling effect on the overshoot of PID tuning and results in poor performance.

To observe the effect of environment temperature, we carried out $T_a = 22, 24, 26 °C$ on the three compared control methods with a fixed transfer velocity $v = 0.3 \ mL/s$. In this case, the air temperature affects not only the fluid transfer from syringe to the body, but also the heating model and consequently the observer. From Fig. 5.11b, on/off control is obviously most affected, since the response of x_{m2} would be slower if the air temperature is low. For PID control, the accuracy is better than on/off control, although its overshoot response is still affected by high air temperature. With MPC scheme, the performance is more robust and its accuracy is only limited by the lower bound of PT100 sensor accuracy.
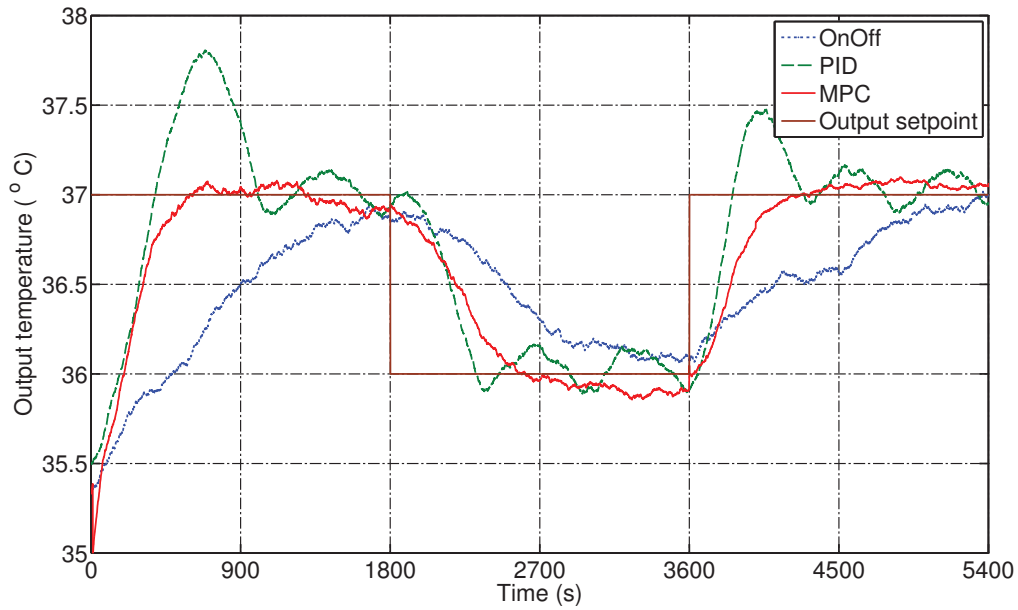
Figure 5.10: Fluid temperature output at the end of transfer tube, assuming that the transfer starts when the syringe is installed.
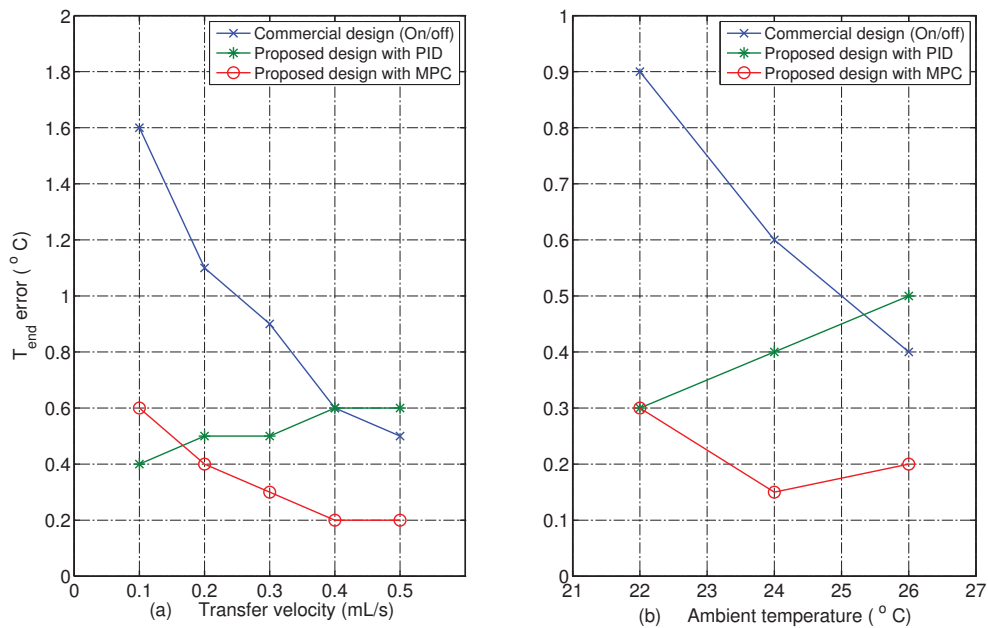
Figure 5.11: Steady-state errors (infinity norm) tested under (a) Different transfer velocities and (b) Different environment temperatures.

5.6 Conclusion

The chapter introduces a new control design for an IVF egg retrieval system. It integrates both the flushing and aspiration units, and provides a solution for the follicular medium temperature control. The objective

is to avoid any significant temperature shock in the female's ovary that can affect the viability of the collected oocytes. The design not only overcomes the temperature drop issue along the transfer tube, but also enhances the response time. The proposed design was tested with other options such as on/off and PID control under several operating conditions to show its effectiveness. This result can be beneficial to medical product manufacturing.

Chapter 6

Predictive Ratio Control in Interacting Processes

Ratio control for two interacting processes is proposed with a PID feed-forward design based on model predictive control (MPC) scheme. At each sampling instant, the MPC control action minimizes a state-dependent performance index associated with a PID-type state vector, thus yielding a PID-type control structure. Compared to the standard MPC formulations with separated single-variable control, such a control action allows one to take into account the non-uniformity of the two process outputs. After reformulating the MPC control law as a PID control law, we provide conditions for prediction horizon and weighting matrices so that the closed-loop control is asymptotically stable, and show the effectiveness of the approach with simulation and experiment results.

6.1 Introduction

Ratio control has become a demanding task in industrial processes involving combustion systems or blending operations. Ratio control methods are used to maintain the flow rate of one stream in the process at a specified proportion relative to that of another (the wild flow). Besides the traditional series and parallel control, an alternative architecture, called Blend station [Hagglund, 2001], was proposed as auto-tuning and later improved in Visioli [2005] for the choice of setpoint weighting. While ratio control of decoupled processes is well established, the problems become significantly complex for interacting processes. In this context, model predictive controllers (MPCs) have been recently applied to

deal with ratio control, such as engine airfuel and fuelgas ratio control [Giorgetti et al., 2006; Muske et al., 2008; Suzuki et al., 2009].

Among the various classes of MPCs, Generalized predictive control (GPC) is a potential method which overcome many pitfalls of other schemes when dealing with open loop unstable, nonminimum phase, or delayed systems [Clarke and Mohtadi, 1989; Normey-Rico and Camacho, 2007]. Moreover, GPC can be used with multivariable systems by an model-augmented modification, even when constraints are considered. These advantages have been reviewed in Bemporad et al. [2002]; Lee and Lee [2000]. Despite its efficiency, the computing burden discourages the widespread use of GPC compared to PID regulators in process industry. Compared with a true GPC method, PID control uses present and past data but not future information; moreover, its coefficients are limited to lower order polynomials than those of GPC law. To address GPC computational issues, several PID tuning procedures incorporating GPC were proposed so that they could achieve model-based control performance with a simpler structure. The idea of matching the GPC and PID control law structure was presented in Camacho et al. [2003]; Neshasteriz et al. [2010]; Sato [2010]. These chapters showed that, by using a first/second-order system model, it is possible to simplify the GPC law as PID control law. A PID predictive controller was proposed in Moradi [2003] where the author, rather than looking for the match of GPC and PID laws, considered a number of parallel PID controllers corresponding to the prediction horizon of GPC. In another context, the work in Tan et al. [2000] developed a GPC-based PID controller by bringing PID error state into GPC performance index.

To bring these predictive PID design closer to the original ratio control problem, a previous work from Tan et al. [2009] achieved composition control by changing setpoint when the output ratio is out of a predetermined threshold, without considering time delays. However, this setpoint variation method modifies control input through feedforward term outside MPC, so it easily upsets the input constraint. In addition, when the dead-time factor is included, especially different dead-times for individual processes, the information of future output ratio is demanded and the solution becomes more complicated. Thus the question is how to deal with a normal delayed process, as in Hagglund [2001]; Visioli [2005].

In this chapter, a PID feed-forward design based on predictive control concept is presented. It can be used for ratio control of two-input two-output (TITO) with inconsistent input delays. The solution for the delay case is solved by using equivalent control in MPC formula. Moreover, it incorporates ratio control into the performance index of GPC, so that no setpoint variation is required. The control law is still obtained as a feed-forward PID structure, with time-varying gains during the initial time-delay period and with constant gains thereafter. Proportion control is also taken care by a structural tuning. As a consequence, a feasible approach for proportion control is delivered.

The chapter is presented as follows. First, the state-space approach for TITO systems with dead-time is presented so that it includes the PID state vector (Section 6.2). Second, the GPC control law is formulated in the given context, which allows us to recast GPC into feed-forward PID structure and criteria for choosing weighting matrices for the derived method are given so that the closed-loop system is asymptotically stable (Sections 6.3). In Section 6.4, the enhancement for ratio control through modification of the performance index is presented. Section 6.5 delivers simulation studies for the wafer thermal uniformity control example. Finally, experiment results are shown in Section 6.6 and the main principles of this chapter is concluded in Section 6.7.

Notation

For the examined system, h denotes the input delay. The subscript i ($i = 1, 2$) is to address the two channels of TITO systems. Besides, r is the output setpoint, while $\tilde{r}$ is auxiliary reference and $\tilde{R}$ is the future auxiliary reference across prediction horizon. We also denote the system state as X and PID state as $\tilde{X}$ in which θ is the integral term over output error e. Open-loop and closed-loop gains are indicated by F and $\bar{F}$. The notation $Q > 0$ ($Q \geq 0$) denotes positive (semi) definiteness.

6.2 State-space Representation of TITO System

Consider the problem of regulating a process modeled by the typical FOPDT transfer functions:

$$
\begin{aligned}
y_1(z) &= \frac{b_{11}z^{-h_1}}{z + a_{11}}u_1(z) + \frac{b_{12}z^{-h_2}}{z + a_{12}}u_2(z) \\
y_2(z) &= \frac{b_{21}z^{-h_1}}{z + a_{21}}u_1(z) + \frac{b_{22}z^{-h_2}}{z + a_{22}}u_2(z)
\end{aligned}
\tag{6.1}
$$

where $h_1 \leq h_2$ ($h_1, h_2 \in \mathbb{R}^+$) are input delays of the system. The output ratio between y_1 and y_2 is to be maintained at the desired value of $\alpha = \frac{r_2}{r_1}$ (r_1, r_2 are the output setpoints).

In order to deal with inconsistent input delays, we define the equivalent control as

$$
U(k - h) = \begin{bmatrix} u_1(k - h_1) & u_2(k - h_2) \end{bmatrix}^T,
\tag{6.2}
$$

used as a convenient notation for the derivation of MPC control law in Section 6.3.

Rearrange (6.1) intro the difference equation and define special state definition $X(k)$ for TITO system (refer to Tan et al. [2009] for details). By describing the PID state vector as $\tilde{X}_k = \begin{bmatrix} e_1(k) & e_1(k-1) & \theta_1(k) & e_2(k) & e_2(k-1) & \theta_2(k) \end{bmatrix}^T$, we have a complete state space equation

$$
X(k + 1) = FX(k) + GU(k - h) + E\tilde{r}(k),
\tag{6.3}
$$

with

$$
X(k) = M\tilde{X}(k) + NU(k - 1 - h).
\tag{6.4}
$$

These system matrices F, G, E, M, N are given as

$$
F = \begin{bmatrix}
-a_{11}+a_{12} & 1 & 0 & 0 & 0 & 0 \\
-a_{11}a_{12} & 0 & 0 & 0 & 0 & 0 \\
1 & 0 & 1 & 0 & 0 & 0 \\
0 & 0 & 0 & -a_{21}+a_{22} & 1 & 0 \\
0 & 0 & 0 & -a_{21}a_{22} & 0 & 0 \\
0 & 0 & 0 & 1 & 0 & 1
\end{bmatrix}, \;
G = \begin{bmatrix}
-b_{11} & -b_{12} \\
-b_{11}a_{12} & -b_{12}a_{11} \\
0 & 0 \\
-b_{21} & -b_{22} \\
-b_{21}a_{22} & -b_{22}a_{21} \\
0 & 0
\end{bmatrix},
$$

$$
E = \begin{bmatrix}
1 & 0 \\
0 & 0 \\
0 & 0 \\
0 & 1 \\
0 & 0 \\
0 & 0
\end{bmatrix}, \;
F = \begin{bmatrix}
1 & 0 & 0 & 0 & 0 & 0 \\
0 & -a_{11}a_{12} & 0 & 0 & 0 & 0 \\
0 & 0 & 1 & 0 & 0 & 0 \\
0 & 0 & 0 & 1 & 0 & 0 \\
0 & 0 & 0 & 0 & -a_{21}a_{22} & 0 \\
0 & 0 & 0 & 0 & 0 & 1
\end{bmatrix}, \;
N = \begin{bmatrix}
0 & 0 \\
-b_{11}a_{12} & -b_{12}a_{11} \\
0 & 0 \\
0 & 0 \\
-b_{21}a_{22} & -b_{22}a_{21} \\
0 & 0
\end{bmatrix}.
$$

6.3 Predictive PID controller

6.3.1 GPC Control Law

The system model is written as

$$X(k+1) = FX(k) + GU(k-h) + E\tilde{r}(k) \tag{6.5}$$

where $X \in \mathbb{R}^n$, $U \in \mathbb{R}^m$ ($n = 6, m = 2$). With this model, the following problem is posed: given the current state $X(k)$, find the equivalent N-step control sequence $\bar{U} = \{U(k-h), U(k-h+1), ..., U(k-h+N-1)\}$ that minimizes the performance index:

$$J = \sum_{j=k}^{k+N-1} [X(j+1)^T Q_j X(j+1) + U(j-h+1)^T R_j U(j-h+1)]. \tag{6.6}$$

In (6.6), N is the prediction horizon; $Q_j \geq 0$, $R_j > 0$ are the state and control weighting matrices.

Now define stacked vectors $\bar{X} = \begin{bmatrix} X(k+1) & ... & X(k+N) \end{bmatrix}^T$, $\tilde{R}(k) = [\tilde{r}(k) \ldots \tilde{r}(k+N-1)]^T$. Then (6.5) can be written as

$$\bar{X} = HFX(k) + P\bar{U} + \bar{E}\tilde{R}(k), \tag{6.7}$$

where

$$H = \begin{bmatrix} I \\ F \\ ... \\ F^{l-1} \end{bmatrix}, P = \begin{bmatrix} G & 0 & ... & 0 \\ FG & G & ... & 0 \\ ... & ... & ... & ... \\ F^{l-1}G & F^{l-2}G & ... & G \end{bmatrix}, \bar{E} = \begin{bmatrix} E & 0 & ... & 0 \\ FE & E & ... & 0 \\ ... & ... & ... & ... \\ F^{l-1}E & F^{l-2}E & ... & E \end{bmatrix}.$$

The performance index (6.6) can be expressed as

$$J = \bar{X}^T Q \bar{X} + \bar{U}^T R \bar{U}. \tag{6.8}$$

The corresponding optimal control law is determined by taking the gradient $\partial J / \partial \bar{U}$ to be zero, so that

$$\bar{U} = -(P^T Q P + R)^{-1} P^T Q (HFX(k) + \bar{E}\tilde{R}(k)). \tag{6.9}$$

Apply the receding horizon control concept, the first-step input is

$$U(k - h) = -D(P^T Q P + R)^{-1} P^T Q (HFX(k) + \bar{E}\tilde{R}(k)) \tag{6.10}$$

$$= K_{GPC} X(k) + K_{ref}\tilde{R}(k), \tag{6.11}$$

where $D = \begin{bmatrix} 1 & 0 & ... & 0 \end{bmatrix}$, $K_{GPC} = -D(P^T Q P + R)^{-1} P^T Q HF = \begin{bmatrix} K_{1GPC} & K_{2GPC} \end{bmatrix}^T$ and $K_{ref} = D(P^T Q P + R)^{-1} P^T Q \bar{E} = \begin{bmatrix} K_{1ref} & K_{2ref} \end{bmatrix}^T$. The second term in (6.11) can be considered as a feed-forward part of the controller design, assuming that the future setpoint sequence is known. It follows from the equivalent control definition in (6.2) that

$$u_1(k) = K_{1GPC} X(k + h_1) + K_{1ref}\tilde{R}(k + h_1)$$
$$u_2(k) = K_{2GPC} X(k + h_2) + K_{2ref}\tilde{R}(k + h_2). \tag{6.12}$$

6.3.2 Future State Prediction

From (6.12), it can be seen that in order to minimize J, the control at the current instant depends on the fixed gains K_{GPC} and a future state at time $k + h_1$ and $k + h_2$.

For $k > h_2$:

Let $\bar{F} = F + GK_{GPC}$. In order to predict the future states, a closed-loop

equation is formed by combining (6.3) and (6.11):

$$X(k+1) = \bar{F}X(k) + GK_{ref}\tilde{R}(k) + E\tilde{r}(k). \tag{6.13}$$

From the one-step prediction above, the future states $X(k+h_1)$, $X(k+h_2)$ are determined iteratively by

$$\begin{aligned}
X(k+h_1) &= \bar{F}^{h_1}X(k) + \bar{F}^{h_1-1}[GK_{ref}\tilde{R}(k) + E\tilde{r}(k)] + \dots \\
&\quad + [GK_{ref}\tilde{R}(k+h_1-1) + E\tilde{r}(k+h_1-1)], \quad (6.14) \\
X(k+h_2) &= \bar{F}^{h_2}X(k) + \bar{F}^{h_2-1}[GK_{ref}\tilde{R}(k) + E\tilde{r}(k)] + \dots \\
&\quad + [GK_{ref}\tilde{R}(k+h_2-1) + E\tilde{r}(k+h_2-1)]. \quad (6.15)
\end{aligned}$$

As seen from (6.14), (6.15), the coefficient of $X(k)$ in these formula is independent of time k for $k > h_2$. In the next case, we will see that the state prediction during time-delay period has the k-dependent gains.

For $1 \le k \le h_2$:

Denote $\bar{F}^1 = F + G \begin{bmatrix} K_{1GPC} & 0 \end{bmatrix}^T$, $K_{ref}^1 = \begin{bmatrix} K_{1ref} & 0 \end{bmatrix}^T$, with the superscript $(.)^1$ indicating the region $min\{h_1, h_2\} < k < max\{h_1, h_2\}$. Depending on the existence of the optimal input in (6.11), the system in (6.5) can become

$$X(l+1) = \begin{cases} \bar{F}^1 X(l) + K_{ref}^1 \tilde{R}(k) + E\tilde{r}(k) & \text{if } h_1 \le l \le h_2 \\ \bar{F}X(l) + GK_{ref}\tilde{R}(k) + E\tilde{r}(k) & \text{if } l \ge h_2. \end{cases} \tag{6.16}$$

Now l can be substituted by $k+h_1$ or $k+h_2$ to get the future states.

6.3.3 Predictive PID Control Law

Substituting the predicted states obtained in (6.14), (6.15) into the control law (6.12)

$$\begin{aligned}
u_1(k) &= K_{1GPC}\bar{F}_1 X(k) + S_1(k) \\
u_2(k) &= K_{2GPC}\bar{F}_2 X(k) + S_2(k), \tag{6.17}
\end{aligned}$$

where $\bar{F}_1, \bar{F}_2$ are the coefficients associated with $X(k)$ and $S_1(k), S_2(k)$ are the terms that involve future reference. $S_1(k), S_2(k)$ can be updated at every step, as in the Algorithm 1 below.

The control law in (6.17) can be incorporated within the PID structure by using (6.4):

$$u_1(k) = K_{1PID}\tilde{X}(k) + K_{1u}U(k-1-h) + S_1(k)$$
$$u_2(k) = K_{2PID}\tilde{X}(k) + K_{2u}U(k-1-h) + S_2(k), \qquad (6.18)$$

where $K_{1PID} = K_{1GPC}\bar{F}_1 M$, $K_{2PID} = K_{2GPC}\bar{F}_2 M$ and $K_{1u} = K_{1GPC}\bar{F}_1 N$, $K_{2u} = K_{2GPC}\bar{F}_2 N$.

Remark 9 *In Eq.* (6.18) *each of the control inputs is navigated by the outputs of two PIDs (as $\tilde{X} \in \mathbb{R}^6$) and a feed-forward term that consists of the rest of the formula.*

As one observes, the MPC law based on future output prediction in (6.12), which is open-loop in nature, has been reformed to a closed-loop control law as in (6.18). The closed-loop stability would be guaranteed later on Section 6.3.4. It is also worth mentioning that because of the future state prediction during time-delay period $max\{h_1, h_2\} = h_2$, this PID formulation has time-varying gains during initial stage . Beyond this period, the PID controller resumes constant gains. In general, the state feedback control law (6.18) refers to the optimal lookup table for the PID gains, and a closed-form solution is created.

The predictive PID algorithm can be summarized in the following:

6.3.4 Stability

As the system has time delays incorporated in its transfer functions, the stability criterion becomes more complex than the one suggested in the work of Tan et al. [2009]. The closed-loop stability created by the proposed feedback is analyzed in long-term situation where the PID controllers have already passed the initial stage of delay and converged to the fixed gain region ($k > h_2$). Without loss of generality, all reference values are assumed to be zero, and the dead-time $h_2 \geq h_1$. From (6.17),

$$
\begin{aligned}
U(k-h) &= \begin{bmatrix} u_1(k-h_1) \\ u_2(k-h_2) \end{bmatrix} = \begin{bmatrix} K_{1GPC}\bar{F}^{h_1}X(k-h_1) \\ K_{2GPC}\bar{F}^{h_2}X(k-h_2) \end{bmatrix} \\
&= \begin{bmatrix} K_{1GPC} \\ 0 \end{bmatrix} \bar{F}^{h_1}X(k-h_1) + \begin{bmatrix} 0 \\ K_{2GPC} \end{bmatrix} \bar{F}^{h_2}X(k-h_2) \\
&= K_{GPC}^1 \bar{F}^{h_1}X(k-h_1) + K_{GPC}^2 \bar{F}^{h_2}X(k-h_2), \qquad (6.19)
\end{aligned}
$$

Algorithm 1: Computation of predictive PID gains.

Data: k, $\tilde{r}$, X

Result: K_{1PID}, K_{2PID}, K_{1u}, K_{2u}

initialize $\tilde{R}(k)$, $\tilde{R}(k+h_1)$, $\tilde{R}(k+h_2)$ by definition in (6.7). Determine K_{GPC} and K_{ref} offline from (6.11). **if** $k \le h_2$ **then**

    $S \leftarrow 0, F_b \leftarrow I, \tilde{R} \leftarrow \tilde{R}(k)$;

    for $i \leftarrow k + h_2 - 1$ **do**

        update $\tilde{R}$ by removing $\tilde{r}(i)$ and adding $\tilde{r}(i+N)$ to the queue;

        $\tilde{r} \leftarrow \tilde{r}(i+1)$;

        Assign

            $S \leftarrow FS + E\tilde{r}, F_b \leftarrow FF_b$ if $i \le h_1$;

            $S \leftarrow \bar{F}^1 S + GK_{ref}^1 \tilde{R} + E\tilde{r}, F_b \leftarrow \bar{F}^1 F_b$ if $h_1 \le i \le h_2$

            $S \leftarrow \bar{F}S + GK_{ref}\tilde{R} + E\tilde{r}, F_b \leftarrow \bar{F}F_b$ if $i \ge h_2$;

        if $i == k + h_1 - 1$ **then**

            $S_1 \leftarrow K_{1GPC}S + K_{1ref}\tilde{R}(k+h_1)$;

            $\bar{F}_1 \leftarrow F_b$;

        end

    end

    $S_2 \leftarrow K_{2GPC}S + K_{2ref}\tilde{R}(k+h_2)$;

    $\bar{F}_2 \leftarrow F_b$;

    evaluate the gains K_{1PID}, K_{2PID}, K_{1u}, K_{2u} from (6.18);

else

    Fix K_{1PID}, K_{2PID}, K_{1u}, K_{2u} from here on;

end

---

where $K_{GPC}^1 = \begin{bmatrix} K_{1GPC} & 0 \end{bmatrix}^T$, $K_{GPC}^2 = \begin{bmatrix} 0 & K_{2GPC} \end{bmatrix}^T$. Substituting (6.19) into (6.3), we obtain

$$X(k+1) = FX(k) + GK_{GPC}^1 \bar{F}^{h_1} X(k-h_1) + GK_{GPC}^2 \bar{F}^{h_2} X(k-h_2). \quad (6.20)$$

Now, the stability condition of the closed-loop system (6.20) is presented through Theorem 1.

Theorem 9 *The system* (6.20) *will be stable if and only if all the roots λ of the following determinant equation*

$$det[\lambda^{h_2+1}I - F\lambda^{h_2} - GK_{GPC}^1 \bar{F}^{h_1}\lambda^{h2-h1} - GK_{GPC}^2 \bar{F}^{h_2}] = 0, \quad (6.21)$$

satisfy $|\lambda| < 1$, assuming that $h_2 \ge h_1$.

Proof 6 *From (6.20), a new state space equation is constructed as*

$$
\begin{bmatrix} X(k-h_2+1) \\ \vdots \\ X(k) \\ X(k+1) \end{bmatrix} = \begin{bmatrix} 0 & I & \cdots & & 0 \\ & & \ddots & & \\ \vdots & \vdots & & I & \vdots \\ & & & & \ddots \\ 0 & 0 & \cdots & & I \\ GK^2_{GPC}\bar{F}^{h_2} & 0 & \cdots & GK^1_{GPC}\bar{F}^{h_1} & \cdots & F \end{bmatrix} \cdot \begin{bmatrix} X(k-h_2) \\ \cdots \\ X(k-1) \\ X(k) \end{bmatrix}
$$
(6.22)

This is the canonical controllable block form, in which the characteristic equation is obtained easily. The proof is directly followed by a block elimination which leads to lower triangular block form, as in the singular form. Thus the above system has eigenvalues which are obtained by solving the equation

$$
det[\lambda^{h_2+1}I - F\lambda^{h_2} - GK^1_{GPC}\bar{F}^{h_1}\lambda^{h2-h1} - GK^2_{GPC}\bar{F}^{h_2}] = 0.
$$

Therefore, this system will be asymptotically stable if all the eigenvalues are within the unit circle, or the condition of (6.21) to be satisfied. Note that the size of the matrix $[\lambda^{h_2+1}I - F\lambda^{h_2} - GK^1_{GPC}\bar{F}^{h_1}\lambda^{h2-h1} - GK^2_{GPC}\bar{F}^{h_2}]$ is equal to 6×6. Interested readers are referred to Sain [1966] for further detail on determinant equation which helps to reduce the size of the matrix when larger systems are concerned.

Corollary 10 *The condition in (6.21) implies a necessary condition that all eigenvalues of the matrix $\bar{F} = F + GK_{GPC}$ is within the unit circle.*

Proof 7 *Indeed, note that $K^1_{GPC} + K^2_{GPC} = K_{GPC}$ and $\bar{F} = F + GK_{GPC}$, so*

$$
\lambda^{h_2+1}I - F\lambda^{h_2} - GK^1_{GPC}\bar{F}\lambda^{h_1}\lambda^{h_2-h_1} - GK^2_{GPC}\bar{F}^{h_2}
$$
$$
= \lambda^{h_2+1}I - [\bar{F} - G(K_1 + K_2)]\lambda^{h_2} - GK^1_{GPC}\bar{F}^{h_1}\lambda^{h_2-h_1} - GK^2_{GPC}\bar{F}^{h_2}
$$
$$
= (\lambda^{h_2+1}I - \bar{F}\lambda^{h_2}) + GK^1_{GPC}\lambda^{h_2-h_1}(\lambda^{h_1}I - \bar{F}^{h_1}) + GK^2_{GPC}(\lambda^{h_2}I - \bar{F}^{h_2})
$$
$$
= [\lambda^{h_2} + GK_GPC^1(\lambda^{h_2-1}I + \bar{F}\lambda^{h_2-2} + \ldots + \bar{F}^{h_1-1}\lambda^{h_2-h_1})
$$
$$
+ GK_GPC^2(\lambda^{h_2-1}I + \bar{F}\lambda^{h_2-2} + \ldots + \bar{F}^{h_2-1})](\lambda I - \bar{F}).
$$
(6.23)

Thus, the eigenvalues of $\bar{F}$ must be within unit circle in order to satisfy (6.21). A typical eigenvalue map for the system (6.20) is presented in Fig. 6.1.
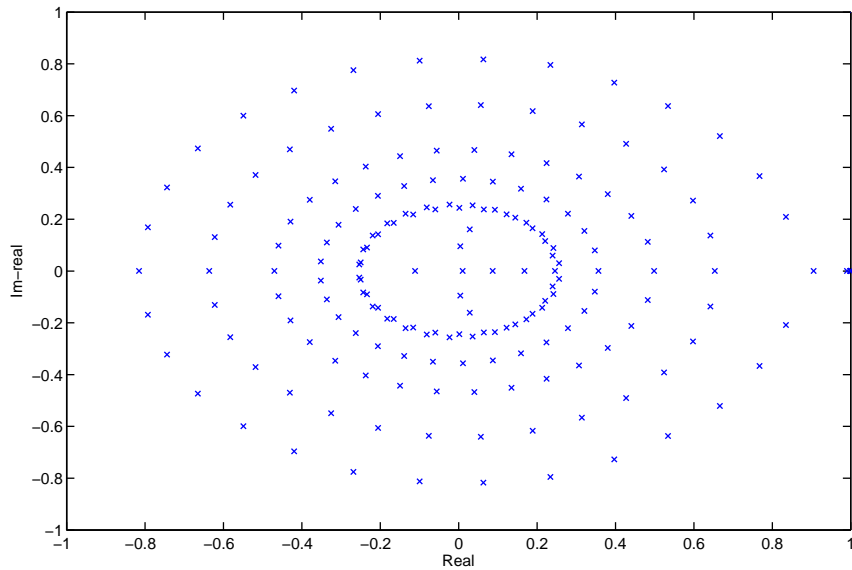
Figure 6.1: A typical eigenvalue map of the closed-loop system using the proposed method.

6.4 Tightening ratio control

6.4.1 Ratio control design

Ratio control, traditionally, is implemented either via a series configuration with $r_2 = \alpha y_1$ or a parallel one with $r_2 = \alpha r_1$. The parallel configuration proves to be better than series configuration in removing or reducing lag phenomenon of slave variable. However, it incurs a different disadvantage, an open-loop design, in which a significant upset to the ratio of the variables can follow when a large or fast load disturbance occurs, which cannot be tolerated in certain applications such as the wafer temperature uniformity control. Hence, the setpoint variation scheme was proposed in Hagglund [2001]. The dynamic information of ratio error was reflected in setpoint and it adjusts the optimal control law in (6.18) through feed-forward calculation. This can only be applied for systems with no delay, since threshold decision and ratio error in future time after the delay may be difficult to predict.

A new ratio control scheme is proposed, which can also improve the transient performance and disturbance rejection. The first advantage over setpoint variation is that the prediction of future ratio error is avoided. Moreover, this scheme is imposed directly into the perfor-

mance index, thus achieving optimal control through PID gains instead of feedforward control. This is implemented by introducing the error ratio into the performance index J.

Let us fraction Q into $Q_1 + \beta Q_2 + \gamma Q_3$ ($\beta, \gamma \in \mathbb{R}^+$) where β, γ are weighting factors. For simplicity, define Q_1 as an identity matrix; this matrix would be used as a normal gain for output tracking. Besides, define $Q_2 = M_2^T M_2$ and $Q_3 = M_3^T M_3$ such that

$$M_2 = \begin{bmatrix} 1 & 0 & 0 - \frac{1}{\alpha} & 0 & 0 \end{bmatrix}$$
$$M_3 = \begin{bmatrix} 0 & 0 & 1 & 0 & 0 & -\frac{1}{\alpha} \end{bmatrix} \tag{6.24}$$

With the definition of the system state $X(k)$ in Section 6.2, it follows that

$$\|X(k)\|_{Q_2}^2 = [M_2 X(k)]^T.[M_2 X(k)] = (e_1(k) - \frac{1}{\alpha} e_2(k))^2,$$
$$\|X(k)\|_{Q_3}^2 = [M_3 X(k)]^T.[M_3 X(k)] = (\theta_1(k) - \frac{1}{\alpha} \theta_2(k))^2, \tag{6.25}$$

and these two terms could be used to optimize the output ratio effectively.

The role of Q_2 is to control the output errors $e_1 = r_1 - y_1$, $e_2 = r_2 - y_2$ to follow the desired output ratio α. Normally, the term Q_1 commands the two processes outputs $y_1(k)$ and $y_2(k)$ to the setpoints r_1, r_2 without taking care of the ratio y_2/y_1 during the transient stage. Since one knows the information $r_2/r_1 = \alpha$, controlling the error ratio e_2/e_1 towards α can be an advantage in assuring the desired output ratio. The attractive point is that this feature still works when the initial output ratio is different from the desired output ratio, or, the ratio setpoint α is varying.

If one considers Q_2 as the proportional gain for ratio error, then Q_3 plays the role of integral gain. It helps to shape the response rates of the two processes to be closer to each other, instead of force the faster flow to following the slower one. In other words, the output ratio returns to the desired value faster and is prevented from possible offset. This can be illustrated in Fig. 6.2.

As a whole, the new performance index would be changed to

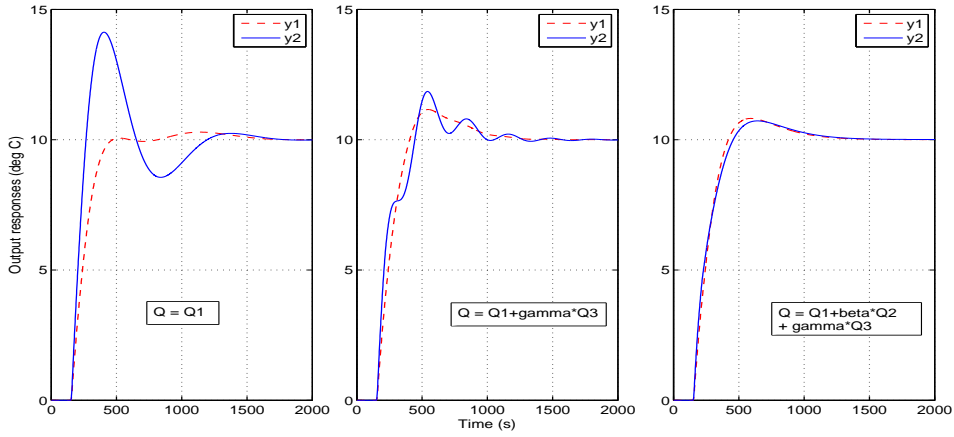$$J = \sum_{k=t+i}^{t+N} (\|X(k)\|_{Q_1+\beta Q_2+\gamma Q_3}^2 + \|U(k-h)\|_R^2), \tag{6.26}$$

Figure 6.2: Tuning for weighting parameters β and γ.

dependent on the balance of Q_1 (output error), Q_2 (ratio error) and Q_3 (ratio error integrator). A tuning method for β, γ will be discussed more in the next section.

Again, since the ratio dynamic information is used as feedback within the performance index, disadvantages such as lag phenomenon and open-loop problem, caused by the traditional designs, could be reduced for the most part.

Remark 10 *This systematic tuning for Q in (6.19) is more adequate than the arbitrary tuning in (6.6). As this algorithm focuses on reduces the ratio error while driving outputs to the setpoints, weighting factors are put among Q_1 (output error), Q_2 (ratio error) and Q_3 (ratio error integrator) to balance the priority of these goals. It is also easier for practical users to decide the positive real values of β and γ rather than the original matrix Q, which is usually chosen in diagonal form.*

6.4.2 Tuning weighting matrices

A formal tuning procedure for the new ratio controller proposed in Section 6.4.1 must satisfy the stability condition in Section 6.3.4. In this part, an simple, practical tuning method is presented.

Firstly, define the weighting matrices Q_1, R_1 as

$$Q_1 = diag(P_1, 0, I_1, P_2, 0, I_2), \ R_1 = \epsilon I \tag{6.27}$$

where I is an identity matrix. The ultimate gains and periods for the

two processes have to be identified as K_{u1}, T_{u1} and K_{u2}, T_{u2}. Let $I_1 = I_2 = 0$, fix the proportional gains P_1, P_2 in the Q_1 form above and decrease the value of ϵ until one achieves $\epsilon = min\{\epsilon \in \mathbb{R}^+ : u_1, u_2 \in \mathbb{U}, no\ overshoot\}$, where $P_1/P_2 = (K_{u1}/K_{u2})^2$ and $\mathbb{U}$ is the input constraint set. This is also to ensure that one achieve the stability at low gain.

Increase I_1, I_2 for faster output response and desirable overshoot degree, while maintaining the ratio $I_1/I_2 = (\frac{K_{u1}}{T_{u1}}.\frac{T_{u2}}{K_{u2}})^2$. By doing this, one actually tunes Q_1, R_1 according to Ziegler-Nichols formula, but with different coefficients.

In order to tune ratio weighting parameters β, γ, it depends on the emphasis of either maximum ratio error, or fast convergence of ratio error. In general, one would increase β to correct the response rates of the two processes, then increase γ to possibly eliminate the remaining ratio error. This is illustrated in Fig. 6.2.

6.5 Simulation Studies

6.5.1 Example 1

To demonstrate the principles of the GPC-based PID scheme discussed on the previous sections, the controller is applied to maintain a ratio between two bake plate temperatures $y_1(t)$, $y_2(t)$ of the thermal system as in [15] with input delays, represented by the process:

$$Y_1(s) = \frac{2.67e^{-60s}}{323.58s + 1}U_1(s) + \frac{1.039e^{-80s}}{759.2s + 1}U_2(s)$$
$$Y_2(s) = \frac{1.039e^{-60s}}{759.2s + 1}U_1(s) + \frac{1.5595e^{-80s}}{524.5s + 1}U_2(s), \qquad (6.28)$$

where $u_1(t)$, $u_2(t)$ are the control inputs with delay $h_1 = 60s$, $h_2 = 80s$. In this example, a sampling time $t = 1s$ is used. Two zone temperature changes y_1, y_2 have zero initial values, and the setpoints are $10.00° C$. The ratio between two process variables $y_1(t)$ and $y_2(t)$ is kept at a tight ratio $\alpha = y_2/y_1 = 1.000$.

The GPC control law is designed using prediction horizon $N = 10$. Three different methods aiding ratio control to GPC-based PID are compared. The first method is the normal predictive ratio control where $r_2 = \alpha r_1$, without any ratio-tightening scheme. The second method is
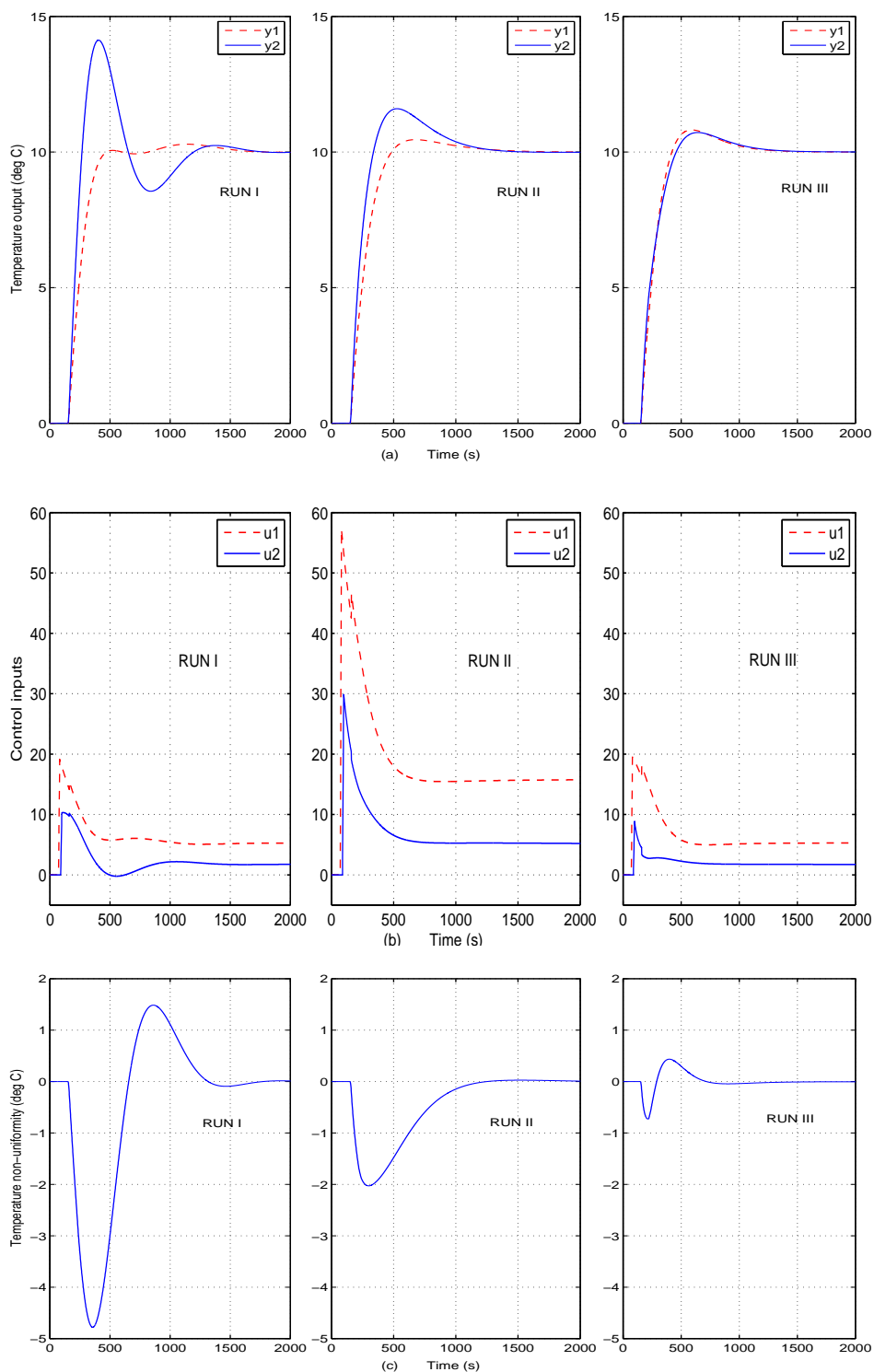
Figure 6.3: Comparison of (a) output response, (b) control effort and (c) temperature non-uniformity between Run I (normal predictive ratio control), Run II (setpoint variation) and Run III (ratio error cost) in the presence of a set-point change at $t = 150s$.
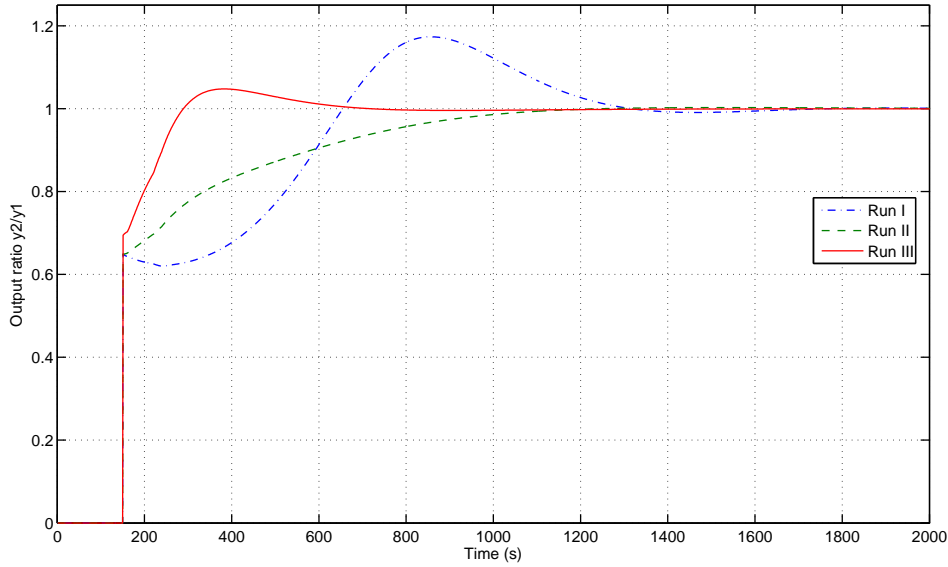
Figure 6.4: IVF integrated platform.

set-point variation scheme proposed in [15] with threshold $\alpha_b = 0.001$ and the gain $K = 120$. The proposed method, on the other hand, considers error-ratio cost residing in performance index. The weighting parameters are chosen by the tuning procedure in Section 6.4.1. Here we have $Q = diag(10, 0, 0.007, 50, 0, 0.1)$, $R = 0.6I$ and $\beta = 10$, $\gamma = 0.1$. The prediction horizon N is rather dependent on the calculation power, so it is chosen as $N = 5$ here.

Define the output non-uniformity as $e_m = \alpha y_1 - y_2$. Fig. 6.3 shows the performance of three mentioned methods. From the output responses, one can notice that the control inputs actually react in advance to the future error which only incurs at $t = 150s$. It has been also observed that the normal predictive ratio control (Run I) yields unsatisfactory results with the maximum non-uniformity of $4.81° C$, as expected. The same method with setpoint variation approach (Run II) gives a relative good performance, as the uniformity is below $2.05° C$. However, this improvement requires a very high input effort to achieve due to the different amount of process delays. For the proposed ratio error cost (Run III), the uniformity performance is better above all, and smaller control inputs are required.

In order to illustrate clearly the effect of the new ratio error minimization method, the actual ratio between two process variables y_2/y_1

in Example 1 is shown in Fig. 6.4. The ratio produced by the proposed
method has the small deviation from the desired ratio and fast response.

6.5.2 Example 2

In real situations, it is very difficult to identify a plant model with ac-
curate parameters, not mentioning that the plant model may be a time-
varying or non-linear system. Hence, in order to demonstrate the robust-
ness of the suggested control scheme, parametric errors are introduced
so that the real model of (6.29) is given by

$$Y_1(s) = \frac{2.67xe^{-60s}}{323.58xs + 1}U_1(s) + \frac{(1.039/x)e^{-80s}}{(759.2/x)s + 1}U_2(s)$$

$$Y_2(s) = \frac{(1.039/x)e^{-60s}}{(759.2/x)s + 1}U_1(s) + \frac{1.5595xe^{-80s}}{524.5xs + 1}U_2(s), \qquad (6.29)$$

with $x = 1.4$ (model error up to 40%).

According to the adaptive Blend station procedure, the setpoint weight-
ing is chosen as $\gamma' = 0.32$ through a series of setpoint change tests,
and PI controllers are tuned by Ziegler-Nichols formula as $(k_{p1}, k_{i1}) =
(1.514, 0.016)$, $(k_{p2}, k_{i2}) = (3.205, 0.026)$. Meanwhile, the proposed con-
troller is the same as in Example 1.

Fig. 6.5a and 6.5b shows the output responses of the Blend station
architecture in Hagglund [2001] and proposed method under model er-
rors. Fig. 6.5c illustrates the degree of robustness of these two schemes.
The former configuration without predictive control is not able to resolve
the model error and results in long recovery of ratio control. Meanwhile,
the latter method recovers output non-uniformity to 0 after enduring the
model mismatch. In fact, the integral cost of error ratio control suggested
enables this flexibility as it is merged into the performance index. This
may not be a proof for robust stability of the system, but it ensures
that with significant model error, the proposed method still maintains
its good performance.

6.6 Experimental Results

Fig. 6.6 presents the setup of a desktop thermal chamber, mounted on
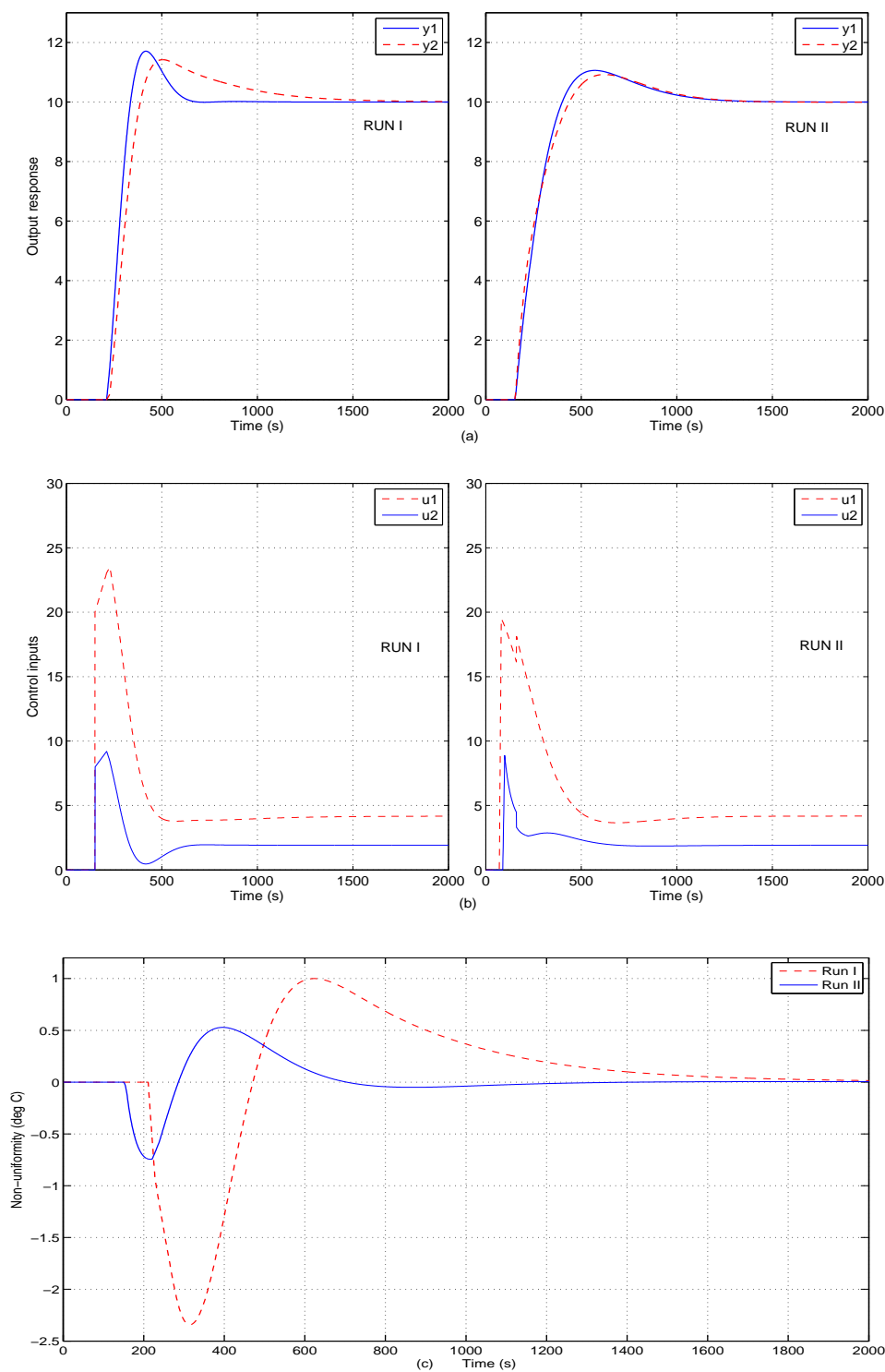a National Instrument (NI) SC-2345 platform with configurable connec-

Figure 6.5: System response for a model perturbation in case of: (a) blend station configuration, (b) proposed method and (c) comparison in temperature non-uniformity.
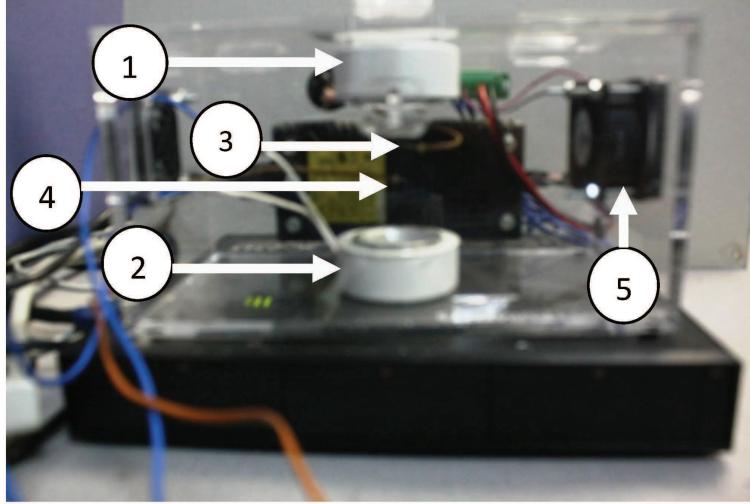
Figure 6.6: Setup of the thermal chamber system with (1, 2) J-Type thermocouples, (3,4) halogen lights and (5) cooling fan.

tors. In this real-time experiment, the air temperature can be controlled by adjusting the power of the lights and the fan. The variables of interest are the air temperatures y_1, y_2 sensed by SCC-TC02 J-type thermocouples at two different height locations. These outputs are manipulated through the upper and lower halogen bulbs in an interactive process. Different delays h_1, h_2 are contained in the two input channels. Besides, the cooling fan fulfills the role of disturbance source. NI LABVIEW is used to develop a controller for this system.

One can reasonably assume the above system as a nonlinear process, due to the advection of air. In this experiment, simple system identification through step responses is exploited in a particular operating point to estimate and formulate a first-order system with delays, as follows:

$$Y_1(s) = \frac{35e^{-2s}}{51s+1}U_1(s) + \frac{25.5e^{-6s}}{99s+1}U_2(s)$$
$$Y_2(s) = \frac{19e^{-2s}}{108s+1}U_1(s) + \frac{31.5e^{-6s}}{68s+1}U_2(s), \tag{6.30}$$

Initial values of the two outputs are $y_{1o} = y_{2o} = 26°\,C$. A setpoint change of $5°\,C$ is given for the first output y_1, and the ratio $alpha = y_2/y_1 = 1.000$ is to be maintained during the process. In addition, notice that the input constraint is present here, whereby $0 \leq u_1, u_2 \leq 1$. The sampling rate is 0.1s.

The objective of this experiment is to show how the MPC implementation with ratio control can cope with this interactive system when

Table 6.1: Non-uniformity statistics for output ratio control in the thermal interaction experiment.

Controller	Abs. Peak	Mean	RMS
Parallel PID	1.1918	0.0764	0.549
Predictive PID	0.2693	0.0065	0.102

compared with a fixed PID regulator. In this experiment, besides the potential model error, there is also a disturbance to test the performance of these two methods. Again the fixed PID regulator was chosen as Blend station design tuned to provide good ratio control of the given process with fast response and no excessive overshoot: $\gamma' = 0.75$ and $(k_{p1}, k_{i1}) = (0.31, 0.045)$, $(k_p2, k_i2) = (0.07, 0.0036)$. The parameters of predictive PID ratio control were adjusted through the tuning procedure provided. The prediction horizon is given as $N = 5$. $Q = diag(1, 0, 0.001, 1, 0, 0.001)$, $R = 5I$ and $\beta = 5$, $\alpha = 0.15$.

Fig. 6.7a shows the behavior of a fixed PID regulator, giving a reasonable but rather non-uniform control and so, a poor ratio performance. Due to the interacting feature in the processes, the response rates are different. The control inputs u_1, u_2 only respond to the output errors individually. The same situation happens in the event of an unpredicted step disturbance $d = 1$.

The simulation results using the proposed MPC ratio control with variable PID gains are shown in Fig. 6.7b. The rates, as well as the shapes, of output response are closely followed. Moreover, recovery after disturbance is also faster, along with the uniformity of the outputs. This can be attributed to the corporation between the control inputs during the course of transient response. Performance statistics are shown in Table 6.1, with the absolute peak, mean and root-mean-square of the ratio non-uniformity are considered. The proposed method helps improve the performance from five to ten times, according to the data.

6.7 Conclusion

This chapter presents a predictive feed-forward and PID control scheme based on MPC that copes with ratio control for interacting delayed processes. Compared to the standard parallel configuration, the proposed method allows one to take into account the ratio error cost, thus tight-
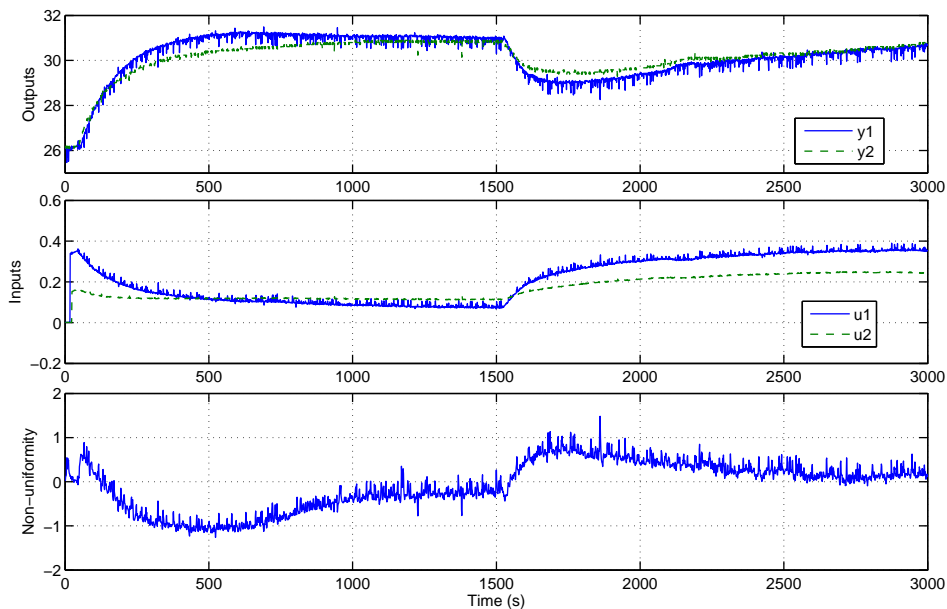
(a)
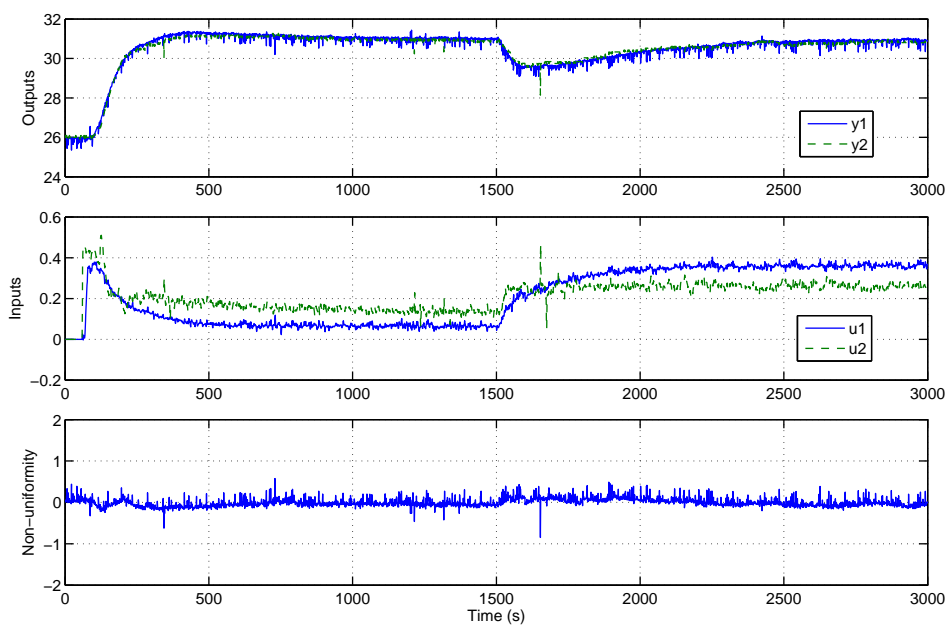
(b)

Figure 6.7: Performance of (a) the Blend station PID and (b) the predictive PID controller.

ening the output ratio towards desired value. In addition, this method is more efficient than the mentioned approaches as the dynamic ratio error information improves the optimal control input through PID gains instead of feed-forward calculation. With the new ratio control scheme, a better performance in output ratio control is achieved with smaller control effort.

Chapter 7

Conclusions

This thesis presents a framework for the future development and improvement of linear model predictive control technology for control applications. In the domain of theory contribution, it builds a bridge between the design of an offset-free model predictive control and a robust control design to be incorporated at the core of MPC. From the implementation perspective, it transforms high-level optimization into PID control design, thus closing the gap between these two control layers. By bringing together concepts and results from control and optimization theory, this document serves as another deep thought on the formulation of model-based control optimization towards real-world applications.

Robust and offset-free control are two important and desirable properties to be implanted in an industrial controller such as MPC. Chapter 2 elaborated a unified MPC framework under which these characteristics can be efficiently delivered in the control performance. The key to the union of these two mature fields is the use of a PID-augmented model which removes the need for a disturbance estimation approach and facilitates the role of established robust control in the core terminal region of the MPC. The framework opens the access of offset-free MPC to robust and nonlinear control, and contributes to both analysis and applications of MPC. A systematic design flow for practical application of the proposed methodology has been formulated, and potential areas which can benefit from the framework were discussed in the chapter.

Chapter 3 further developed the ideas proposed in Chapter 2 into practical designs for MPC - PID. The linear controller is modified for offset-free tracking. The resultant control architecture is a PID gain scheduling network with a feedforward part to deal with state and input constraints. A simple test for setpoint tracking feasibility is also discussed.

Finally, the example results show that robustness stability against distur-
bances of the proposed method is inherent within the PI/PID structure.

Chapter 4 is the first example in this thesis to formulate an optimiza-
tion problem in a real problem-solving case. A robust MPC method has
been developed for compensation of friction arising in linear ultrasonic
motors. The objective of the control scheme is to achieve good static
tracking performance in the presence of the uncertain friction model-
ing. This is obtained by incorporating linear friction inside the hybrid
plant model and designing a robust terminal gain for MPC. Simulation
and experimental results have shown that the proposed compensation
technique can overcome the limitations of the relay-PID tuning while
attaining a simple real-time implementation.

Chapter 5, again using the developed framework in Chapter 2 and
3, introduces a new control design for an IVF egg retrieval system -
a mechatronics system. It integrates both the flushing and aspiration
units, and provides a solution for the follicular medium temperature
control. The objective is to avoid any significant temperature shock in
the female's ovary that can affect the viability of the collected oocytes.
The design not only overcomes the temperature drop issue along the
transfer tube, but also enhances the response time. The proposed design
was tested with other options such as on/off and PID control under
several operating conditions to show its effectiveness. This result can
be beneficial to medical product manufacturing.

Chapter 6 presents a predictive feed-forward and PID control scheme
based on MPC that copes with ratio control for interacting delayed pro-
cesses. Compared to the standard parallel configuration, the proposed
method allows one to take into account the ratio error cost, thus tight-
ening the output ratio towards desired value. In addition, this method
is more efficient than the mentioned approaches as the dynamic ratio
error information improves the optimal control input through PID gains
instead of feed-forward calculation. With the new ratio control scheme,
a better performance in output ratio control is achieved with smaller
control effort.

All these chapters have formed a broad look on control optimization.
It is not simply using the mathematical tools to solve problems, but
instead formulating the problems to be solved efficiently with available
tools. Model predictive control acts as an anchor throughout the context.

Future works include investigating distributed MPC to separate the region searching of parametric solution into manageable subspaces. This will speed up the critical region searching of parametric MPC and allow scalable implementation of this method.

Another outlook for this thesis is imposing a pure optimal PID control by relatively optimal control: a PID gain network control without feedforward part.

Author's Publications

Journal Papers

K.K. Tan, S. Huang, M. H-T Nguyen, W. Liang and S.C. Ng. An innovative design for In-vitro Fertilization oocyte retrieval systems. *IEEE Transactions on Industrial Informatics*, PP(99), p.1, 2013.

M. H-T Nguyen, K.K. Tan and S. Huang. Enhanced predictive ratio control of interacting systems. *Journal of Process Control*, 21(7), p.1115-1125, 2011.

Conference Papers

M. H-T Nguyen, K.K. Tan and C.S. Teo. PID Tuning by Robust Model Predictive Control. *IEEE/ASME International Conference on Advanced Intelligent Mechatronics*, p. 944-948, Australia, Jul. 2013.

K.K. Tan, M. H-T Nguyen, W. Liang and C.S. Teo. Robust precision positioning control on linear ultrasonic motor. *IEEE/ASME International Conference on Advanced Intelligent Mechatronics*, p. 170-175, Australia, Jul. 2013.

M. H-T Nguyen, S. Huang and K.K. Tan. Robust control for optimal operation of a reproductive assisting platform. *4th International Conference on Communications and Electronics*, p.495-499, Vietnam, 2012.

Under review

M. H-T Nguyen, K.K. Tan, Liang, W. and Teo, C.S. Improving identification and compensation of friction in linear ultrasonic motors. *Submitted to IEEE Transactions on Control Systems Technology*.

M. H-T Nguyen and K.K. Tan. From parametric model-based optimization to robust PID gain scheduling network. *Submitted to IEEE Transactions on Automatic Control*.

M. H-T Nguyen, K.K. Tan, Liang, W. Model predictive control of precise actuators. *Modeling and Control of Precise Actuators*, invited book chapter.

References

A. Alessio, A. Bemporad, M. Lazar, and W.P.M.H. Heemels. Convex polyhedral invariant sets for closed-loop linear mpc systems. In *Decision and Control, 2006 45th IEEE Conference on*, pages 4532 –4537, dec. 2006. 18, 34

I. Alvarado, D. Limon, T. Alamo, and E.F. Camacho. Output feedback robust tube based mpc for tracking of piece-wise constant references. In *Decision and Control, 2007 46th IEEE Conference on*, pages 2175 –2180, dec. 2008. 28

D. Angeli, A. Casavola, and E. Mosca. Predictive pi-control of linear plants under positional and incremental input saturations. *Automatica*, 36(10):1505 – 1516, 2000. ISSN 0005-1098. 13

B. Armstrong and B. Amin. Pid control in the presence of static friction: A comparison of algebraic and describing function analysis. *Automatica*, 32(5):679 – 692, 1996. ISSN 0005-1098. 46

F. Arousi, U. Schmitz, R. Bars, and R. Haber. Robust predictive pi controller based on first-order dead time model. In *IFAC World Congress*, 2008. 29

V.L. Bageshwar and F. Borrelli. On a property of a class of offset-free model predictive controllers. *Automatic Control, IEEE Transactions on*, 54(3):663 –669, march 2009. ISSN 0018-9286. 5, 12

M. Baotic. An efficient algorithm for multiparametric quadratic programming. Technical report, ETH, April 2002. 37

G.I. Bara and M. Boutayeb. Static output feedback stabilization with h-infinity performance for linear discrete-time systems. *Automatic*

Control, IEEE Transactions on, 50(2):250–254, 2005. ISSN 0018-9286. 20, 35

A.. Bemporad, M.. Morari, V.. Dua, and E.N. Pistikopoulos. The explicit linear quadratic regulator for constrained systems. *Automatica*, 38(1):3 – 20, 2002. ISSN 0005-1098. 28, 37, 39, 85

A. Bemporad, F. Borrelli, and M. Morari. Min-max control of constrained uncertain discrete-time linear systems. *Automatic Control, IEEE Transactions on*, 48(9):1600 – 1606, sept. 2003. ISSN 0018-9286. 20, 28

F. Blanchini. Set invariance in control. *Automatica*, 35(11):1747 – 1767, 1999. ISSN 0005-1098. 18, 34

F. Blanchini. The gain scheduling and the robust state feedback stabilization problems. *Automatic Control, IEEE Transactions on*, 45(11): 2061 – 2070, nov 2000. ISSN 0018-9286. 42

F. Blanchini and F.A. Pellegrino. Relatively optimal control: a static piecewise-affine solution. In *Decision and Control, 2007 46th IEEE Conference on*, pages 807 –812, dec. 2007. 42

A. Boglietti, A. Cavagnino, and D. Staton. Determination of critical parameters in electrical machine thermal models. *IEEE Transactions on Industry Applications*, 44(4):1150–1159, 2008. 68

M.. Boukallel, M.. Gauthier, M.. Dauge, E.. Piat, and J.. Abadie. Smart microrobots for mechanical cell characterization and cell convoying. *Biomedical Engineering, IEEE Transactions on*, 54(8):1536 –1540, aug. 2007. ISSN 0018-9294. 64

E.F. Camacho, C Bordons, and J.E. Normey-Rico. *Model predictive control*, volume 13. Springer Verlag, 2003. 29, 85

B.M. Chen. *Robust and H-infinity Control.* Communications and Control Engineering. Springer, 2000. ISBN 9781852332556. 16, 54

Si-Lu Chen, Kok-Kiong Tan, and Sunan Huang. Friction modeling and compensation of servomechanical systems with dual-relay feedback approach. *Control Systems Technology, IEEE Transactions on*, 17(6):1295–1305, 2009. ISSN 1063-6536. doi: 10.1109/TCST.2008.2006905. 59

D. Chmielewski and V. Manousiouthakis. On constrained infinite-time linear quadratic optimal control. *Systems and Control Letters*, 29(3):121 – 129, 1996. ISSN 0167-6911. 34

D.W. Clarke and C. Mohtadi. Properties of generalized predictive control. *Automatica*, 25(6):859 – 875, 1989. ISSN 0005-1098. 85

D.W. Cutler, A. Morshedi, and J. Haydel. An industrial perspective on advanced control. In *AIChE Annual Meeting*, 1983. 3

Francesco Alessandro Cuzzola and Manfred Morari. An lmi approach for hinf analysis and control of discrete-time piecewise affine systems. *International Journal of Control*, 75(16-17):1293–1301, 2002. doi: 10.1080/ 0020717021000023726. 52

D.Q. Dang, Y. Wang, and W. Cai. Offset-free predictive control for variable speed wind turbines. *Sustainable Energy, IEEE Transactions on*, PP(99):1 –9, 2012. ISSN 1949-3029. 5

S. Di Cairano and A. Bemporad. Model predictive control tuning by controller matching. *Automatic Control, IEEE Transactions on*, 55(1):185 –190, 2010. ISSN 0018-9286. 29

P.B. Dickinson and A.T. Shenton. A parameter space approach to constrained variance PID controller design. *Automatica*, 45(3):830 – 835, 2009. ISSN 0005-1098. 36

J. Dong and G.H. Yang. Static output feedback control synthesis for linear systems with time-invariant parametric uncertainties. *Automatic Control, IEEE Transactions on*, 52(10):1930 –1936, 2007. ISSN 0018-9286. 35

J.C. Doyle, K. Glover, P.P. Khargonekar, and B.A. Francis. State-space solutions to standard h2 and h infin; control problems. *Automatic Control, IEEE Transactions on*, 34(8):831 –847, aug 1989. ISSN 0018-9286. 16

P. Dupont, V. Hayward, B. Armstrong, and F. Altpeter. Single state elastoplastic friction models. *Automatic Control, IEEE Transactions on*, 47(5):787 –792, may 2002. ISSN 0018-9286. 47

J.B. Froisy. Model predictive control - building a bridge between theory and practice. *Computers and Chemical Engineering*, 30:1426–1435, 2006. 3, 5, 12, 28, 65

H. Fujioka, C.Y. Kao, S. Almer, and U. Jonsson. Robust tracking with performance for pwm systems. *Automatica*, 45(8):1808 – 1818, 2009. ISSN 0005-1098. 13

C.E. Garcia and A.M. Morshedi. Quadratic programming solution of dynamic matrix control (qdmc). *Chemical Engineering Communications*, 46:73–87, 1986. 3

C.E. Garcia, D.M. Prett, and M. Morari. Model predictive control: theory and practice - a survey. *Automatica*, 25(3):335–348, 1989. 1

G. Garcia, B. Pradin, S. Tarbouriech, and F. Zeng. Robust stabilization and guaranteed cost control for discrete-time linear systems by static output feedback. *Automatica*, 39(9):1635 – 1641, 2003. ISSN 0005-1098. 20, 35

E.G. Gilbert and K.T. Tan. Linear systems with state and control constraints: the theory and application of maximal output admissible sets. *Automatic Control, IEEE Transactions on*, 36(9):1008 –1020, sep 1991. ISSN 0018-9286. 18

N. Giorgetti, G. Ripaccioli, A. Bemporad, I.V. Kolmanovsky, and D. Hrovat. Hybrid model predictive control of direct injection stratified charge engines. *Mechatronics, IEEE/ASME Transactions on*, 11(5):499–506, 2006. ISSN 1083-4435. 85

A. Grancharova, T. A. Johansen, and J. Kocijan. Explicit model predictive control of gas and liquid separation plant via orthogonal search tree partitioning. *Computers and Chemical Engineering*, 28(12):2481 – 2491, 2004. ISSN 0098-1354. 13

P. Grieder and M. Morari. Complexity reduction of receding horizon control. In *Decision and Control, 2003. Proceedings. 42nd IEEE Conference on*, volume 3, pages 3179 – 3190 Vol.3, dec. 2003. 28

P. Grieder, M. Kvasnica, M. Baoti, and M. Morari. Stabilizing low complexity feedback control of constrained piecewise affine systems. *Automatica*, 41(10):1683 – 1694, 2005. ISSN 0005-1098. 18, 34

T. Hagglund. The blend station - a new ratio control structure. *Control Engineering Practice*, 9(11):1215 – 1220, 2001. ISSN 0967-0661. 84, 85, 94, 100

V. Hayward, B.S.R. Armstrong, F. Altpeter, and P.E. Dupont. Discrete-time elasto-plastic friction estimation. *Control Systems Technology, IEEE Transactions on*, 17(3):688 –696, may 2009. ISSN 1063-6536. 47, 48

Y. He, M. Wu, Liu. G.P., and J.H. She. Output feedback stabilization for a discrete-time system with a time-varying delay. *Automatic Control, IEEE Transactions on*, 53(10):2372 –2377, 2008. ISSN 0018-9286. 35

M. Herceg, M. Kvasnica, and M. Fikar. Minimum-time predictive control of a servo engine with deadzone. *Control Engineering Practice*, 17(11): 1349 – 1357, 2009. ISSN 0967-0661. 47

M.J. Hill and E.D. Levens. Is there a benefit in follicular flushing in assisted reproductive technology? *Curr Opin Obstet Gynecol*, 22(3): 208–212, 2010. 63

L. Hyslop, N. Prathalingam, L. Nowak, J. Fenwick, S. Harbottle, S. Byerley, J. Rhodes, B. Watson, R. Henderson, A. Murdoch, and M. Herbert. A novel isolator-based system promotes viability of human embryos during laboratory processing. *PLoS ONE*, 7(2)(2): e31010, 02 2012. 64

Z.P. Jiang and I. Marcels. Robust nonlinear integral control. *Automatic Control, IEEE Transactions on*, 46(8):1336 –1342, aug 2001. ISSN 0018-9286. 13

E.C. Kerrigan and J.M. Maciejowski. Robustly stable feedback min-max model predictive control. In *American Control Conference, 2003. Proceedings of the 2003*, volume 4, pages 3490 – 3495 vol.4, june 2003. 6

H. Kimura, H. Nakamura, T. Akai, T. Yamamoto, H. Hattori, Y. Sakai, and T. Fujii. On-chip single embryo coculture with microporous-membrane-supported endometrial cells. *NanoBioscience, IEEE Transactions on*, 8(4):318 –324, dec. 2009. ISSN 1536-1241. 64

M. Kvasnica, P. Grieder, and M. Baoti. Multi-parametric toolbox (MPT), 2004. 40, 56

W. Langson, I. Chryssochoos, S.V. Rakovi, and D.Q. Mayne. Robust model predictive control using tubes. *Automatica*, 40(1):125 – 133, 2004. ISSN 0005-1098. 6

M. Lazar, W.P.M.H. Heemels, S. Weiland, and A. Bemporad. Stabilizing model predictive control of hybrid systems. *Automatic Control, IEEE Transactions on*, 51(11):1813 –1818, nov. 2006. ISSN 0018-9286. 47, 52, 55

K.S. Lee and J.H. Lee. Convergence of constrained model-based predictive control for batch processes. *Automatic Control, IEEE Transactions on*, 45(10):1928–1932, 2000. ISSN 0018-9286. 85

Y. Lee II and B. Kouvaritakis. Robust receding horizon predictive control for systems with uncertain dynamics and input saturation. *Automatica*, 36(10):1497 – 1504, 2000. ISSN 0005-1098. 6

E.D. Levens, B.W. Whitcomb, M.D. Payson, and F.W. Larsen. Ovarian follicular flushing among low-responding patients undergoing assisted reproductive technology. *Fertility and Sterility*, 91(4, Supplement):1381 – 1384, 2009. ISSN 0015-0282. 64

B. Li, L.S. Xuefang, B. Allard, and J.M. Retif. A digital dual-state-variable predictive controller for high switching frequency buck converter with improved sigma delta dpwm. *IEEE Trans. on Industrial Informatics*, 8(3): 472–481, Aug 2012. 65

K.V. Ling, W.K. Ho, Y. Feng, and B. Wu. Integral-square-error performance of multiplexed model predictive control. *IEEE Transactions on Industrial Informatics*, 7(2):196 –203, may 2011. ISSN 1551-3203. 72

L. Ljung. Prediction error estimation methods. *Circuits, Systems, and Signal Processing*, 21:11–21, 2002. ISSN 0278-081X. 70

L. Ljung. *System Identification Toolbox for use with MATLAB*. Natick, MA: The MathWorks Inc., 7th edition, 2007. 78

C. Lovaas, M.M. Seron, and G.C. Goodwin. Robust output-feedback mpc with integral action. *Automatic Control, IEEE Transactions on*, 55(7):1531 –1543, july 2010. ISSN 0018-9286. 13

D.H.M. Lozano, J.B. Scheffer, N. Frydman, S. Fay, R. Fanchin, and R. Frydman. Optimal reproductive competence of oocytes retrieved through follicular flushing in minimal stimulation ivf. *Reproductive BioMedicine Online*, 16(1):119–123, 2008. 63

U. Maeder and M. Morari. Offset-free reference tracking with model predictive control. *Automatica*, 46(9):1469 – 1476, 2010. ISSN 0005-1098. 3, 12, 19

U. Maeder, F. Borrelli, and M. Morari. Linear offset-free model predictive control. *Automatica*, 45(10):2214 – 2222, 2009. ISSN 0005-1098. 5, 12, 31

L. Magni, G. De Nicolao, R. Scattolini, and F. Allgwer. Robust model predictive control for nonlinear discrete-time systems. *International Journal of Robust and Nonlinear Control*, 13(3-4):229–246, 2003. ISSN 1099-1239. 5

C. Mark, B. Kouvaritakis, S.V. Rakovic, and Q. Cheng. Stochastic tubes in model predictive control with probabilistic constraints. *IEEE Transactions on Automatic Control*, 56:194–199, 2011. 6, 21, 28

P. Marquis and J. P. Broustail. Smoc, a bridge between state space and model predictive controllers: application to the automation of a hydrotreating unit. In *IFAC workshop on model based process control*, 1998. 3

J.M. Martin, P. Vega, and S. Revollar. Set-point optimization for enhancing the mpc control of the n-removal process in wwtp's. In *World Automation Congress (WAC), 2012*, pages 1 –6, june 2012. 5

D.Q. Mayne, J.B. Rawlings, C.V. Rao, and P.O.M. Scokaert. Constrained model predictive control: Stability and optimality. *Automatica*, 36:789–814, 2000. 2, 18, 28, 33

D.Q. Mayne, M.M. Seron, and S.V. Rakovic. Robust model predictive control of constrained linear systems with bounded disturbances. *Automatica*, 41(2):219 – 224, 2005. ISSN 0005-1098. 6

G. Mercere and L. Bako. Parameterization and identification of multivariable state-space systems: A canonical approach. *Automatica*, 47(8):1547 – 1555, 2011. ISSN 0005-1098. 70

M.H. Moradi. State space representation of MIMO predictive PID controller. In *Proceedings of 2003 IEEE Conference on Control Applications*, volume 1, pages 452–457, 2003. 29, 85

M. Morari and U. Maeder. Nonlinear offset-free model predictive control. *Automatica*, 48(9):2059 – 2067, 2012. ISSN 0005-1098. 5, 12, 13

K.R. Muske and T.A. Badgwell. Disturbance modeling for offset-free linear model predictive control. *Journal of Process Control*, 12(5):617–632, 2002. ISSN 0959-1524. 5, 12, 19, 22

K.R. Muske and J.B. Rawlings. Model predictive control with linear models. *AIChE Journal*, 39(2):262–287, 1993. ISSN 1547-5905. 5, 11, 15, 18

K.R. Muske, J.C.P. Jones, and E.M. Franceschi. Adaptive analytical model-based control for si engine air-fuel ratio. *Control Systems Technology, IEEE Transactions on*, 16(4):763–768, 2008. ISSN 1063-6536. 85

Z.K. Nagy and R.D. Braatz. Robust nonlinear model predictive control of batch processes. *AIChE Journal*, 49(7):1776–1786, 2003. ISSN 1547-5905. 6

Z.K. Nagy and R.D. Braatz. Open-loop and closed-loop robust optimal control of batch processes using distributional and worst-case analysis. *Journal of Process Control*, 14(4):411 – 422, 2004. ISSN 0959-1524. 28

A.R. Neshasteriz, A.K. Sedigh, and H. Sadjadian. Generalized predictive control and tuning of industrial processes with second order plus dead time models. *Journal of Process Control*, 20(1):63 – 72, 2010. ISSN 0959-1524. 85

Minh H-T Nguyen, K.K. Tan, and S. Huang. Enhanced predictive ratio control of interacting systems. *Journal of Process Control*, 21(7):1115 – 1125, 2011. ISSN 0959-1524. xv, 40, 57, 61

J.E. Normey-Rico and E.F. Camacho. *Control of Dead-time Processes*. Advanced Textbooks in Control and Signal Processing. Springer, 2007. ISBN 9781846288289. 85

M. C. De Oliveira, J. C. Geromel, and J. Bernussou. Extended h2 and hinf norm characterizations and controller parametrizations for discrete-time systems. *International Journal of Control*, 75(9):666–679, 2002. 54, 55

G. Pannocchia and J.B. Rawlings. Disturbance models for offset-free model-predictive control. *AIChE Journal*, 49(2):426–437, 2003. ISSN 1547-5905. 5, 12, 13, 22

G. Pannocchia, J.B. Rawlings, and S.J. Wright. Fast, large-scale model predictive control by partial enumeration. *Automatica*, 43(5):852 – 860, 2007. ISSN 0005-1098. 3

U. Parlitz, A. Hornstein, D. Engster, F. Al-Bender, V. Lampaert, T. Tjahjowidodo, S.D. Fassois, D. Rizos, C.X. Wong, K. Worden, and G. Manson. Identification of pre-sliding friction dynamics. *Chaos*, 14(2):420–430, 2004. 47

Y.-F. Peng and C.-M. Lin. Intelligent motion control of linear ultrasonic motor with h infin; tracking performance. *Control Theory Applications, IET*, 1(1):9 –17, january 2007. ISSN 1751-8644. 47

J.A. Primbs and C.H. Sung. Stochastic receding horizon control of constrained linear systems with state and control multiplicative noise. *Automatic Control, IEEE Transactions on*, 54(2):221 –230, feb. 2009. ISSN 0018-9286. 6

S.J. Qin and T.A. Badgwell. A survey of industrial model predictive control technology. *Control Engineering Practice*, 11:733–764, 2003. xiv, 3, 4, 11, 20, 28, 65

G.V. Raffo, M.G. Ortega, and F.R. Rubio. An integral pre-dictive/nonlinear control structure for a quadrotor helicopter. *Automatica*, 46(1):29 – 39, 2010. ISSN 0005-1098. 14, 17

S.V. Rakovic, E.C. Kerrigan, K.I. Kouramas, and D.Q. Mayne. Invariant approximations of the minimal robust positively invariant set. *Automatic Control, IEEE Transactions on*, 50(3):406 – 410, march 2005. ISSN 0018-9286. 6, 55

J. B. Rawlings. Tutorial overview of model predictive control. *IEEE Control Systems Magazine*, Special section - Industrial Process Control: 38–52, 2000. 52

J.B. Rawlings and D.Q. Mayne. *Model Predictive Control: Theory and Design*. Nob Hill Publishing, 2009. ISBN 9780975937709. 12, 13, 21, 33

J.B. Rawlings and K.R. Muske. Stability of constrained receding horizon control. *IEEE Transactions on Automatic Control*, 38(10):1512–1516, 1993. 72

J.B. Rawlings, D. Bonne, J.B. Jorgensen, A.N. Venkat, and S.B. Jorgensen. Unreachable setpoints in model predictive control. *Automatic Control, IEEE Transactions on*, 53(9):2209 –2215, oct. 2008. ISSN 0018-9286. 18

W. Reinelt, A. Garulli, and L. Ljung. Comparing different approaches to model error modeling in robust identification. *Automatica*, 38(5):787 – 803, 2002. ISSN 0005-1098. 70

J. Richalet, A. Rault, J.L. Testud, and J. Papon. Model predictive heuristic control: Applications to industrial processes. *Automatica*, 14(5):413 – 428, 1978. ISSN 0005-1098. 2

A. Sabanovic. Variable structure systems with sliding modes in motion control - a survey. *IEEE Transactions on Industrial Informatics*, 7(2):212 –223, may 2011. ISSN 1551-3203. 71

D.R. Saffer-II and F.J. Doyle-III. Analysis of linear programming in model predictive control. *Computers & Chemical Engineering*, 28 (12):2749 – 2763, 2004. ISSN 0098-1354. 17

M. Sain. On the control applications of a determinant equality related to eigenvalue computation. *Automatic Control, IEEE Transactions on*, 11 (1):109 – 111, jan 1966. ISSN 0018-9286. 93

V. Sakizlis, N.M.P. Kakalis, V. Dua, J.D. Perkins, and E.N. Pistikopoulos. Design of robust model-based controllers via parametric programming. *Automatica*, 40(2):189 – 201, 2004. ISSN 0005-1098. 13, 17

T. Sato. Design of a gpc-based pid controller for controlling a weigh feeder. *Control Engineering Practice*, 18(2):105 – 113, 2010. ISSN 0967-0661. Special Issue of the 3rd International Symposium on Advanced Control of Industrial Processes. 85

T. Sato. Predictive control approaches for PID control design and its extension to multirate system. *Advances in Industrial Control,*, 4:553–595, 2012. 29

P.O.M. Scokaert and D.Q. Mayne. Min-max feedback model predictive control for constrained linear systems. *Automatic Control, IEEE Transactions on*, 43(8):1136 –1142, aug 1998. ISSN 0018-9286. 5, 6

P.O.M. Scokaert and J.B. Rawlings. Constrained linear quadratic regulation. *Automatic Control, IEEE Transactions on*, 43(8):1163 –1169, 1998. ISSN 0018-9286. 34

S. Seshagiri and H.K. Khalil. Robust output feedback regulation of minimum-phase nonlinear systems using conditional integrators. *Automatica*, 41(1):43 – 54, 2005. ISSN 0005-1098. 13

R. Sherbahn. Assessment of effect of follicular fluid temperature at egg retrieval on blastocyst development, implantation and live birth rates. *Fertility and Sterility*, 94(4):S68–S69, 2010. 64

F.G. Shinskey. *Feedback controllers for the process industries*. McGraw-Hill, 1994. ISBN 9780070569058. 15

M.T. Soylemez, N. Munro, and H. Baki. Fast calculation of stabilizing pid controllers. *Automatica*, 39(1):121–126, 2003. ISSN 0005-1098. 36

H.-P. Steiner. *Optimizing Technique in Follicular Aspiration and Flushing*. Textbook of Minimal Stimulation Ivf: Milder, Mildest Or Back to Nature. JP Medical Pub, 2011. ISBN 9789350250143. 64

K. Suzuki, T. Shen, J. Kako, and S. Yoshida. Individual a/f estimation and control with the fuel-gas ratio for multicylinder ic engines. *Vehicular Technology, IEEE Transactions on*, 58(9):4757–4768, 2009. ISSN 0018-9545. 85

K.K. Tan, S.N. Huang, and T.H. Lee. Development of a gpc-based pid controller for unstable systems with deadtime. *ISA Transactions*, 39(1): 57 – 70, 2000. ISSN 0019-0578. 13, 85

K.K. Tan, A. Tay, Z. Shao, S. Huang, and T.H. Lee. Predictive ratio control for interacting processes. *Industrial and Engineering Chemistry Research*, 48(23):10515–10521, 2009. 85, 87, 91

W.W. Tan, R.F.Y. Li, A.P. Loh, and W.H. Ho. Rtd response time estimation in the presence of temperature variations and its application to semiconductor manufacturing. *IEEE Transactions on Instrumentation and Measurement*, 57(2):406–412, 2008. 67

P. Tatjewski. Advanced control and on-line process optimization in multilayer structures. *Annual Reviews in Control*, 32(1):71–85, 2008. ISSN 1367-5788. 27

P. Tondel, T. A. Johansen, and A. Bemporad. An algorithm for multi-parametric quadratic programming and explicit MPC solutions. *Automatica*, 39(3):489 – 497, 2003. ISSN 0005-1098. 37

R. Toscano and P. Lyonnet. Robust PID controller tuning based on the heuristic Kalman algorithm. *Automatica*, 45(9):2099 – 2106, 2009. ISSN 0005-1098. 36

D.H. van Hessem and O.H. Bosgra. A conic reformulation of model predictive control including bounded and stochastic disturbances under state and input constraints. In *Decision and Control, 2002, Proceedings of the 41st IEEE Conference on*, volume 4, pages 4643 – 4648 vol.4, dec. 2002. 6

M. Vasak, M. Baotic, I. Petrovic, and N. Peric. Hybrid theory-based time-optimal control of an electronic throttle. *Industrial Electronics, IEEE Transactions on*, 54(3):1483 –1494, june 2007. ISSN 0278-0046. 47

K.C. Veluvolu and Y.C. Soh. High-gain observers with sliding mode for state and unknown input estimations. *IEEE Transactions on Industrial Electronics*, 56(9):3386 –3393, sept. 2009. ISSN 0278-0046. 68, 71

A. Visioli. Design and tuning of a ratio controller. *Control Engineering Practice*, 13(4):485 – 497, 2005. ISSN 0967-0661. 84, 85

M. Wallace, B. Das, P. Mhaskar, J. House, and T. Salsbury. Offset-free model predictive controller for vapor compression cycle. In *American Control Conference (ACC), 2012*, pages 398 –403, june 2012. 5

D. Wang.   Robust data-driven modeling approach for real-time final product quality prediction in batch process operation. *IEEE Transactions on Industrial Informatics*, 7(2):371 –377, may 2011. ISSN 1551-3203. 65

L. Wang. *Model Predictive Control System Design and Implementation Using MATLAB*. Advances in Industrial Control. Springer, 2009. 74

Y. Xie, J. Liu, S. Proteasa, G. Proteasa, W. Zhong, Y. Wang, F. Wang, E.E. Puscheck, and D.A. Rappolee.   Transient stress and stress enzyme responses have practical impacts on parameters of embryo development, from ivf to directed differentiation of stem cells. *Molecular reproduction and development*, 75(4):689697, 2008. 64

C. Yousfi and R. Tournier.   Steady state optimization inside model predictive control. In *American Control Conference, 1991*, pages 1866 –1870, june 1991. 3

Y. Zhang, L.-S. Shieh, and A.C. Dunn. Pid controller design for disturbed multivariable systems. *Control Theory and Applications, IEE Proceedings -*, 151(5):567 – 576, sept. 2004. ISSN 1350-2379. 13

F. Zheng, Q.G. Wang, and T.H. Lee. On the design of multivariable PID controllers via LMI approach. *Automatica*, 38(3):517–526, 2002. ISSN 0005-1098. 34

Y. Zheng, S. Li, and X. Wang. Horizon-varying model predictive control for accelerated and controlled cooling process. *IEEE Transactions on Industrial Electronics*, 58(1):329 –336, jan. 2011. ISSN 0278-0046. 65

K. Zhou and J.C. Doyle. *Essentials of Robust Control*. Prentice Hall, 1998. ISBN 9780135258330. 13